Unequally spaced knot techniques for the numerical solution of partial differential equations.

WISHER, Stephen J.

UNEQUALLY SPACED KNOT TECHNIQUES FOR THE NUMERICAL SOLUTION OF PARTIAL DIFFERENTIAL EQUATIONS

Being a thesis submitted
in partial fulfilment of the degree of

Doctor of Philosophy

at

Sheffield City Polytechnic

by

STEPHEN JOHN WISHER

August, 1983

ACKNOWLEDGEMENTS

I wish to express my sincere thanks to my Director of Studies, Dr G F Raggett, for his general support, constructive criticism and continual encouragement during my work on this thesis.

I would also like to thank numerous members of the Department of Mathematics, Statistics and Operational Research at Sheffield City Polytechnic for many helpful discussions; particular thanks are due to Dr A C Allen, Dr R McLaughlin, Mr R Ward and, my second supervisor, Dr J A R Stone.

I wish to acknowledge a very helpful discussion which took place between myself, Dr Raggett and certain members of the Division of Numerical Analysis and Computer Science at the National Physical Laboratory. Particularly, I wish to thank Dr M G Cox for bringing to my attention the variable knot point results for approximation on which two of the methods of this thesis are based.

My thanks are also due to Mrs Renee Hayes for her expert typing of this thesis.

ABSTRACT OF THE THESIS

"Unequally Spaced Knot Techniques for the Numerical Solution of Partial Differential Equations"

by

S J WISHER

Cubic spline approximations to time dependent partial differential equations, having both constant and variable coefficients, are developed in which the knot points may be chosen to be unequally spaced. Four methods are presented for obtaining 'optimal' knot positions, these being chosen so at to produce an increase in accuracy compared with methods based on equally spaced knots. Three of the procedures described produce knot partitions which are fixed throughout time. The fourth procedure yields differently placed 'optimal' knots on each time line, thus enabling us to better approximate the varying time nature characteristic of many partial differential equations. Truncation errors and stability criteria are derived and full numerical implementation procedures are given. Five case studies are presented to enable comparisons to be drawn between the knot placement methods and results found using equally spaced knots. Possible extensions of the work of this thesis are given.

CONTENTS

CHAPTER 1

Introduction

1.1 Finite Difference Solution of Partial Differential Equations

The most well-known early work on the use of finite differences was that of Richardson (1910), although the paper by Courant, Friedrichs and Lewy (1928) is usually considered as the birthplace of modern numerical methods for solving partial differential equations. In that work Courant, Friedrichs and Lewy also showed that the convergence of simple difference approximations depends on the mesh ratio satisfying certain conditions. Such conditions were also derived using Fourier techniques for a wide variety of problems by von Neumann during the Second World War. A detailed discussion of von Neumann's work is given in O'Brien, Hyman and Kaplan (1951).

Since the work of von Neumann many finite difference schemes have been proposed, perhaps the most well-known being that of Crank and Nicolson (1947). A thorough description of methods available is given in Richtmyer and Morton (1967). The computational aspects and the application of finite difference methods to partial differential equations with variable coefficients and generalised boundary conditions is discussed in, for example, Ames (1977), Mitchell (1969) and Mitchell and Griffiths (1980).

The majority of finite difference schemes derived for the solution of time dependent partial differential equations use rectangular grids which have constant step lengths in both the space and time directions. There are, however, certain instances in which unequally spaced mesh points in the space direction are beneficial. For example, situations frequently arise in which the solution of a partial differential equation varies very rapidly over a small part of the domain but changes slowly over the rest of the domain. The problem in using non-uniform grids in such situations is that, in general, an order of accuracy is lost by employing unequally spaced mesh point schemes. It is therefore important to position the mesh points so that optimal numerical performance is achieved. Pearson (1968) proposed an iterative scheme for the solution of boundary layer problems in which additional mesh points are added where the variation in solution values exceeds some predetermined level. Woodford (1975) extended this idea and produced a scheme which used graded meshes in which the mesh points are systematically chosen according to the natural structure of the problem. The use of such transformation techniques has also been considered by various authors (see, for example, Jones and Thompson (1980) and references therein) in determining the position of mesh

points for the solution of fluid flow problems.

An additional area where non-uniform grids have been used is in the numerical solution of moving boundary problems in heat flow. Murray and Landis (1959) solved such so-called Stefan problems by employing a uniform grid on the solid side of the boundary and a different uniform grid on the liquid side. A change in the size of the step lengths therefore occurs from one side of the boundary to the other. These moving boundary problems were also considered by Douglas and Gallie (1955). They used a scheme with a variable time step length which is chosen so that the boundary always moves from one line of the space grid to the neighbouring line in a single time step. More recently, Crank and Gupta (1972_b),proposed a method for solving Stefan problems which employed cubic splines to interpolate solution values.

1.2 Development of Spline Techniques

The term 'spline function' was first used by Schoenberg (1946) in a paper describing the use of generalised splines and other piecewise polynomials to approximate smooth functions of one variable. Although Schoenberg's early paper was an important contribution to the use of spline techniques, it was not until the 1960's that further work in the field was published.

Since that time, spline functions have been used extensively as methods of interpolation and approximation, see for example, Birkhoff and de Boor (1967), Greville (1969), Schumaker (1969), Curtis (1970), Hayes and Halliday (1974) and Cox (1975). An excellent summary of spline techniques is given in Ahlberg, Nilson and Walsh (1967).

Due to the benefit gained by employing splines in approximation problems, numerous authors have adapted spline techniques to obtain solutions to various problems in numerical analysis. For example, Loscalzo and Talbot (1967), Loscalzo (1969), Micula (1973) and Patricio (1978) considered the solution of initial value problems, whilst methods for solving two-point boundary value problems were presented by Bickley (1968), Albasiny and Hoskins (1969), Fyfe (1969) and Khalifa and Eilbeck (1982).

In addition, El Tom (1974 and 1976) has used spline techniques in the solution of Volterra integral equations.

The development of spline techniques for obtaining numerical solutions to partial differential equations began with Papamichael and Whiteman (1973). In that work the authors presented a method for solving the simple one-dimensional heat conduction equation in which use was made of a cubic

spline approximation in the space direction together with a finite difference approximation in the time direction. A similar technique was used by Raggett and Wilson (1974) in obtaining numerical solutions to the one-dimensional wave equation.

Spline function approximations have since been applied to more general partial differential equations. For example, Raggett, Stone and Wisher (1976) considered the solution of practical problems modelled by hyperbolic partial differential equations of the form

$$\frac{\partial^2 u}{\partial t^2} = \frac{\partial}{\partial x}\left[a(x,t) \frac{\partial u}{\partial x} \right] + b(x,t) \frac{\partial u}{\partial x} + c(x,t)u. \quad (1.2.1)$$

In addition, Rubin and Graves (1975) and Rubin and Khosla (1976) presented spline techniques for solving problems in fluid mechanics. In particular, their work developed the use of spline techniques in the solution of non-linear equations. The application of spline function approximations to partial differential equations in two space dimensions was considered by Jain and Holla (1978). They proposed a high accuracy formula, using a technique similar to that of McKee (1973), for the spline solution of wave equations of

the form

$$\frac{\partial^2 u}{\partial t^2} = a(x,y,t)\,\frac{\partial^2 u}{\partial x^2} + b(x,y,t)\,\frac{\partial^2 u}{\partial y^2} \quad . \qquad (1.2.2)$$

Jain and Aziz (1981) have also recently applied parametric spline techniques to a variety of differential equations and have found that they compare favourably with the more usual cubic spline approximations. In addition, papers by Sastry (1976) and Pala and Spano (1978) have also proposed methods for obtaining spline solutions to parabolic partial differential equations.

1.3 Motivation for Present Work

As mentioned earlier, the use of cubic splines for the numerical solution of the one-dimensional wave equation has been considered by Raggett and Wilson (1974). An indication of how that work could be generalised to the solution of more general one-dimensional, constant coefficient, hyperbolic partial differential equations was shown by Raggett (1974). The completion of that work was carried out by Wisher (1977), who indicated that the use of spline techniques gave increased accuracy over comparative finite difference approximations. The schemes used on

hyperbolic equations by Wisher (1977) are illustrated in Chapter 3 of this thesis. The extension of that work to include parabolic partial differential equations is also given in Chapter 3.

Most of the previously mentioned works on the application of spline techniques to the solution of partial differential equations have produced methods in which the knots were chosen to be equally spaced. An exception here is that of Wisher (1977) who used unequally spaced knots in solving the simple wave equation. In that work, the knots were positioned in an ad-hoc manner and no improvement in accuracy was observed over the use of uniform knot partitions. Further, some experimentation on choosing the knot points to be the zeros or extrema of the shifted Chebyshev polynomial

$$T_n^*(x) = \mathrm{Cos}(n\mathrm{Cos}^{-1}(2x-1)) \qquad (1.2.3)$$

was undertaken in Wisher (1977). Again no improvement in accuracy over constant knot spacing was observed.

In this thesis we employ spline techniques with unequally spaced knots for the numerical solution of both hyperbolic and parabolic partial differential equations. Further, we present methods for the optimal positioning of these knots.

The derivation of schemes allowing the non-uniform partitioning of knot points is given in Chapter 4.

The problem of determining optimal positions of knots has been shown to be a difficult one and has only to-date been applied to approximation problems.

In the earlier works on approximating functions (see for example, Curtis and Powell (1967)) equally spaced knots were employed with additional knots being inserted when the error in the approximation was larger than some prescribed magnitude. Since that time various authors have attempted to choose the positions of the knots, in some optimal sense, given knowledge about the function f being approximated. De Boor and Rice (1968) described an algorithm for solving the least-squares cubic spline approximation problem. Their idea was to vary one knot at a time so as to reduce the error of best approximation. Similarly, Esch and Eastman (1969) proposed a method for a best discrete Chebyshev approximation by splines. Both these algorithms are computationally expensive and de Boor (1973) has since proposed an alternative method which chooses the knot partition from the given function f. This method is applied to the solution of partial differential equations

in Chapter 5 by taking the function f to be the given initial condition. Two additional methods for optimally positioning the knots are also derived in Chapter 5.

In Chapter 6 of this thesis, a number of case studies are considered and solutions derived using knot partitions resulting from each of the methods given in Chapter 5. Comparisons are also made with results produced using equally spaced knots.

The results of Chapter 6 suggest that improvement on the methods for locating the knot points given in Chapter 5 would be desirable. An improved algorithm is thus presented in Chapter 7, which chooses optimal partitions of knots on each time line. The suitability of this method is examined in Chapter 8, where the earlier case studies are again considered.

Throughout this thesis, no particular reference to the associated characteristics has been made for hyperbolic problems. However, it should be realised that due account has been taken in the satisfaction of the Courant Friedrichs Lewy condition (see Mitchell and Griffiths (1980)) for all the problems cited.

CHAPTER 2

Review of Cubic Spline Theory

2.1 Definition of a Cubic Spline

Let f(x) be a function with continuous derivatives in the range $a \leq x \leq b$. To approximate f(x) using cubic spline techniques we may subdivide the interval $a \leq x \leq b$ into N sub-intervals by inserting knots x_i such that

$$a = x_0 < x_1 < \ldots < x_N = b. \tag{2.1.1}$$

S(x) is a cubic spline interpolating to the function f(x) at the knots $x_0, x_1, \ldots, x_N$ if

(i) in each sub-interval $x_{i-1} \leq x \leq x_i$ (i=1,2,...,N), S(x) is a cubic polynomial,

(ii) $S'(x)$ and $S''(x)$ are continuous everywhere in $[a,b]$,

(iii) $S(x_i) = f(x_i)$ (i=0,1,...,N).

A cubic spline thus consists of a set of cubic polynomial arcs which are joined smoothly end to end with continuous first and second derivatives. In general, the third derivative will have a discontinuity at each of the knots $x_1, x_2, \ldots, x_{N-1}$.

2.2 Cubic Spline Functions

From Ahlberg, Nilson and Walsh (1967), in the interval $[x_{i-1}, x_i]$ we define $S''(x)$ as

$$S''(x) = M_{i-1}\left(\frac{x_i - x}{h_i}\right) + M_i\left(\frac{x - x_{i-1}}{h_i}\right) \tag{2.2.1}$$

where $h_i = x_i - x_{i-1}$ $(i = 1,2,\ldots,N)$ (2.2.2)

and $M_i = S''(x_i)$. Integrating twice gives the cubic spline function $S(x)$ on $\left[x_{i-1}, x_i \right]$ as

$$S(x) = M_{i-1} \frac{(x_i - x)^3}{6h_i} + M_i \frac{(x - x_{i-1})^3}{6h_i} + \left(f(x_{i-1}) - \frac{h_i^2}{6} M_{i-1} \right) \frac{(x_i - x)}{h_i} + \left(f(x_i) - \frac{h_i^2}{6} M_i \right) \frac{(x - x_{i-1})}{h_i} \quad (i=1,2,\ldots,N) \tag{2.2.3}$$

the constants of integration being evaluated from $S(x_i) = f(x_i)$ and $S(x_{i-1}) = f(x_{i-1})$. From (2.2.3) the following one-sided limits of the derivatives of $S'(x)$ are derived

$$S'(x_i-) = \frac{h_i}{6} M_{i-1} + \frac{h_i}{3} M_i + \frac{f(x_i) - f(x_{i-1})}{h_i} \quad (i=1,2,\ldots,N) \tag{2.2.4}$$

$$S'(x_i+) = -\frac{h_{i+1}}{3} M_i - \frac{h_{i+1}}{6} M_{i+1} + \frac{f(x_{i+1}) - f(x_i)}{h_{i+1}} \quad (i=0,1,\ldots(N-1)) \tag{2.2.5}$$

The unknowns $M_i (i=0,2,\ldots,N)$ are obtained by equating these one-sided limits, thus giving

$$\frac{h_i}{6} M_{i-1} + \frac{h_i + h_{i+1}}{3} M_i + \frac{h_{i+1}}{6} M_{i+1} = \frac{h_i f(x_{i+1}) - (h_i + h_{i+1}) f(x_i) + h_{i+1} f(x_{i-1})}{h_i h_{i+1}} \quad (i=1,2,\ldots,(N-1)) \tag{2.2.6}$$

Equation (2.2.6) is a tri-diagonal system of (N-1) equations in (N+1) unknowns. To solve this system various choices of conditions are available at the end points, x_0 and x_N, of the interval to produce a consistent set of (N+1) equations

(i) $S''(x_i) = 0 \quad (i=0,N)$ (2.2.7)

(ii) $S'(x_i) = f'(x_i) \quad (i=0,N)$ (2.2.8)

(III) $S''(x_i) = f''(x_i) \quad (i=0,N)$ (2.2.9)

As suggested by Behforooz and Papamichael (1979), the choice of these extra conditions plays an important role on the quality of the spline approximation. It is well-known that the best order of approximation which can be achieved by an interpolatory cubic spline is

$$|| S - f || = O(h^4)$$

where $|| \cdot ||$ denotes the uniform norm on $[a,b]$ and $h = \max(h_i)$. This order of accuracy is obtained if either (ii) or (iii) are used as the extra conditions. As stated by Kershaw (1973) an $O(h^4)$ accuracy is not obtained if condition (i) is applied. However, the conditions (ii) and (iii) require knowledge of the derivatives of the function f(x). This knowledge is not generally available from any imposed boundary conditions of partial differential equations and we thus use (i) as the extra conditions in

this thesis, S(x) and (i) being known as a 'natural' cubic spline. Papamichael and Worsey (1981) have recently derived improved extra conditions for spline approximation which could result in increased accuracy to the results of case studies considered later.

Having decided on the choice of 'end conditions', substitution of these into (2.2.6) gives a system of (N-1) equations which are linearly independent, tri-diagonal and diagonally dominant. They can therefore easily be solved for M_i (i=1,2,...,(N-1)), the satisfaction of the end conditions then giving M_0 and M_N. The spline function S(x) can then be obtained from (2.2.3).

CHAPTER 3

Initial Value Partial Differential Equations with Equally Spaced Knots.

(i) Hyperbolic Partial Differential Equations

3.1 Constants Coefficients

Suppose that $u(x,t)$ satisfies the second order linear hyperbolic partial differential equation

$$\frac{\partial^2 u}{\partial t^2} = a\frac{\partial^2 u}{\partial x^2} + b\frac{\partial u}{dx} + cu \quad (0 \leq x \leq 1,\ t > 0) \tag{3.1.1}$$

where the coefficients a, b, c are constants ($a > 0$).

Assume further that (3.1.1) is subject to the function value boundary conditions

$$u(0,t) = f_1(t) \quad , \quad u(1,t) = f_2(t) \tag{3.1.2}$$

and the initial conditions

$$u(x,0) = g_1(x) \quad , \quad \frac{\partial u(x,0)}{\partial t} = g_2(x) \tag{3.1.3}$$

where $f_1(t)$, $f_2(t)$, $g_1(x)$ and $g_2(x)$ are known functions.

To obtain solutions to (3.1.1) using spline techniques we here consider the knots

$$0 = x_0 < x_1 < \ldots . < x_N = 1 \tag{3.1.4}$$

to be equally spaced where the distance between successive knots is h, so that $x_i = ih$ $(i=0,1,\ldots.,N)$. We now replace the time derivative in (3.1.1) by a finite difference approximation and the space derivatives by a cubic spline, thus obtaining at the point (ih,jk) the implicit relationship (see Wisher (1977))

$$\frac{u_{i,j-1}-2u_{i,j}+u_{i,j+1}}{k^2} = a\left\{\theta M_{i,j-1}+(1-2\theta)M_{i,j}+\theta M_{i,j+1}\right\}$$
$$+ b\left\{\theta L_{i,j-1}+(1-2\theta)L_{i,j}+\theta L_{i,j+1}\right\}$$
$$+ c\left\{\theta u_{i,j-1}+(1-2\theta)u_{i,j}+\theta u_{i,j+1}\right\} \qquad (3.1.5)$$

$(i=0,1,\ldots,N;\ j=1,2,\ldots;\ Nh=1\ ;\ \theta \geq 0)$

where $L_{i,j} = S_j'(x_i)$, $M_{i,j} = S_j''(x_i)$; $S_j(x)$ denoting the cubic spline interpolating the values $u_{i,j}$ on the j^{th} time line, this being given by

$$S_j(x) = M_{i-1,j}\frac{(x_i-x)^3}{6h} + M_{i,j}\frac{(x-x_{i-1})^3}{6h} + \left(u_{i-1,j}-\frac{h^2}{6}M_{i-1,j}\right)\frac{(x_i-x)}{h}$$
$$+ \left(u_{i,j}-\frac{h^2}{6}M_{i,j}\right)\frac{(x-x_{i-1})}{h} \qquad (i=1,2,\ldots,N) \quad (3.1.6)$$

As shown in section 2.2, the continuity of the first derivatives of the spline function yields

$$\frac{1}{6}M_{i-1,j} + \frac{2}{3}M_{i,j} + \frac{1}{6}M_{i+1,j} = \frac{u_{i-1,j}-2u_{i,j}+u_{i+1,j}}{h^2} \qquad (3.1.7)$$
$$(i=1,2,\ldots,(N-1))$$

This relationship also holds on the $(j-1)^{th}$ and $(j+1)^{th}$ time lines, giving respectively

$$\frac{1}{6}M_{i-1,j-1} + \frac{2}{3}M_{i,j-1} + \frac{1}{6}M_{i+1,j-1} = \frac{u_{i-1,j-1}-2u_{i,j-1}+u_{i+1,j-1}}{h^2}$$
$$(i=1,2,\ldots,(N-1)) \qquad (3.1.8)$$

and

$$\frac{1}{6}M_{i-1,j+1} + \frac{2}{3}M_{i,j+1} + \frac{1}{6}M_{i+1,j+1} = \frac{u_{i-1,j+1}-2u_{i,j+1}+u_{i+1,j+1}}{h^2}$$
$$(i=1,2,\ldots,(N-1)) \qquad (3.1.9)$$

We now require an expression similar to (3.1.7) which incorporates the $L_{i,j}$ values. On the j^{th} time line (2.2.4) and (2.2.5) respectively become

$$L_{i,j} = S_j'(x_i-) = \frac{hM}{6}_{i-1,j} + \frac{hM}{3}_{i,j} + \frac{u_{i,j} - u_{i-1,j}}{h} \qquad (3.1.10)$$

$$(i=1,2,\ldots,N)$$

and

$$L_{i,j} = S_j'(x_i+) = \frac{-hM}{3}_{i,j} \frac{-hM}{6}_{i+1,j} + \frac{u_{i+1,j} - u_{i,j}}{h} \qquad (3.1.11)$$

$$(i=0,1,\ldots,(N-1))$$

From (3.1.10) we have

$$L_{i+1,j} = \frac{hM}{6}_{i,j} + \frac{hM}{3}_{i+1,j} + \frac{u_{i+1,j} - u_{i,j}}{h} \qquad (3.1.12)$$

$$(i=0,1,\ldots,(N-1))$$

and from (3.1.11)

$$L_{i-1,j} = \frac{-hM}{3}_{i-1,j} - \frac{hM}{6}_{i,j} + \frac{u_{i,j} - u_{i-1,j}}{h} \qquad (3.1.13)$$

$$(i=1,2,\ldots,N)$$

A relationship is now obtained by adding (3.1.10) and (3.1.11), the result being added to half the sum of (3.1.12) and (3.1.13). Thus on the j^{th} time line

$$\frac{1L}{6}_{i-1,j} + \frac{2L}{3}_{i,j} + \frac{1L}{6}_{i+1,j} = \frac{u_{i+1,j} - u_{i-1,j}}{2h} \qquad (3.1.14)$$

$$(i=1,2,\ldots,(N-1))$$

Again (3.1.14) holds on the $(j-1)^{th}$ and $(j+1)^{th}$ time lines giving

$$\frac{1L}{6}_{i-1,j-1} + \frac{2L}{3}_{i,j-1} + \frac{1L}{6}_{i+1,j-1} = \frac{u_{i+1,j-1} - u_{i-1,j-1}}{2h} \qquad (3.1.15)$$

$$(i=1,2,\ldots,(N-1))$$

and

$$\frac{1}{6}L_{i-1,j+1} + \frac{2}{3}L_{i,j+1} + \frac{1}{6}L_{i+1,j+1} = \frac{u_{i+1,j+1} - u_{i-1,j+1}}{2h} \qquad (3.1.16)$$

$$(i=1,2,\ldots,(N-1))$$

As shown in Wisher (1977) the required scheme incorporating splines is obtained by performing the following operations:

(i) multiply (3.1.7) by $a(1-2\theta)$;

(ii) add (3.1.8) and (3.1.9), multiply the result by $a\theta$;

(iii) multiply (3.1.14) by $b(1-2\theta)$;

(iv) add (3.1.15) and (3.1.16), multiply the result by $b\theta$;

(v) add the expressions produced in (i) - (iv) together;

(vi) use (3.1.5) to eliminate the $M_{i,j}$ and $L_{i,j}$ values, thus giving the following three time level scheme

$$(1-\beta_1\theta)u_{i-1,j+1} + 4(1+\beta_2\theta)u_{i,j+1} + (1-\beta_3\theta)u_{i+1,j+1}$$

$$=\{2+\beta_1(1-2\theta)\}\, u_{i-1,j} + 4\,\{2-\beta_2(1-2\theta)\}\, u_{i,j} + \{2+\beta_3(1-2\theta)\}\, u_{i+1,j}$$

$$-(1-\beta_1\theta)u_{i-1,j-1} - 4(1+\beta_2\theta)u_{i,j-1} - (1-\beta_3\theta)u_{i+1,j-1} \qquad (3.1.17)$$

$$(i=1,2,\ldots,(N-1))$$

where $\beta_1 = 6ar^2-3brk+ck^2$; $\beta_2=3ar^2-ck^2$; $\beta_3=6ar^2+3brk+ck^2$ and the mesh ratio $r=k/h$.

The truncation error for (3.1.17) is obtained by expanding each term of the scheme about the mesh point (ih,jk) using Taylor series approximations. After appropriate rearrangements (see Wisher (1977)) the following expression, to fourth order, is obtained

$$k^2h^2\left[c^2r^2f(\theta)u + 2bcr^2f(\theta)\frac{\partial u}{\partial x}\right.$$

$$+\left\{r^2(2ac + b^2)f(\theta) - \frac{1}{6}c^2k^2\theta\right\}\frac{\partial^2 u}{\partial x^2}$$

$$+\left\{2abr^2f(\theta) - \frac{1}{6}bck^2\theta\right\}\frac{\partial^3 u}{\partial x^3}$$

$$\left.+\left\{a^2r^2f(\theta) + \frac{1}{12}a - \frac{1}{72}ch^2 - \frac{1}{6}ack^2\theta\right\}\frac{\partial^4 u}{\partial x^4}\right] \qquad (3.1.18)$$

where $$f(\theta) = \frac{1}{12}(1 - ck^2\theta) - \theta. \qquad (3.1.19)$$

This truncation error may be considerably simplified by choosing $f(\theta) = 0$, in which case the parameter θ is chosen such that

$$\theta = \frac{1}{12 + ck^2} \qquad (3.1.20)$$

Thus, in the special case where fourth and higher order derivatives are small, the truncation error is reduced in magnitude from $O(k^2h^2)$ to $O(k^4h^2)$. The technique of optimally choosing the parameter θ has been considered in detail by Wisher (1977). For example, when obtaining solutions to the wave equation ((3.1.1) with a=1, b=c=0) the truncation error (3.1.18) can be reduced to $O(k^2h^4+k^6)$ by choosing

$$\theta = \frac{1}{12r^2}(1+r^2) \qquad (3.1.21)$$

and, in fact, to $O(k^2h^6+k^8)$ by suitable choice of both θ and r.

To examine the stability of the scheme (3.1.17) we use the well known von Neumann method (see Mitchell (1969)) in which a harmonic decomposition is made of the error at mesh points (see Wisher (1977) for full details). The following stability conditions are obtained

(a) if $\theta \geq \frac{1}{4}$, it is unconditionally stable

(b) if $\theta < \frac{1}{4}$, it is stable when

$$r \leq \{3a(1-4\theta)\}^{-1/2} . \qquad (3.1.22)$$

3.2 Variable Coefficients.

Here we require solutions to the hyperbolic partial differential equation

$$\frac{\partial^2 u}{\partial t^2} = \frac{\partial}{\partial x}\left[a(x,t) \frac{\partial u}{\partial x}\right] + b(x,t) \frac{\partial u}{\partial x} + c(x,t)u \qquad (3.2.1)$$

where a(x,t), b(x,t) and c(x,t) are variable coefficients and $a(x,t) > 0$ at all points in the solution domain. Again we consider the knots to be equally spaced and perform an analysis identical to that of the previous section. Though complicated by the variable coefficients the following scheme, similar to (3.1.17), is derived at (ih,jk)

$$(\phi_{i-1,j+1} - \theta\psi_{i,j+1})u_{i-1,j+1} + 4(\phi_{i,j+1} + 3\gamma_{i,j+1})u_{i,j+1}$$

$$+(\phi_{i+1,j+1} - \theta\chi_{i,j+1})u_{i+1,j+1}$$

$$=\{2\phi_{i-1,j} + k^2 c_{i-1,j} + (1-2\theta)\psi_{i,j}\}\, u_{i-1,j} + 4\{2\phi_{i,j} + k^2 c_{i,j}$$

$$-3(1-2\theta)\gamma_{i,j}\}\, u_{ij} + \{2\phi_{i+1,j} + k^2 c_{i+1,j} + (1-2\theta)\chi_{i,j}\}\, u_{i+1,j}$$

$$- (\phi_{i-1,j-1} - \theta\psi_{i,j-1})u_{i-1,j-1} - 4(\phi_{i,j-1} + 3\gamma_{i,j-1})u_{i,j-1}$$

$$-(\phi_{i+1,j-1} - \theta\chi_{i,j-1})u_{i+1,j-1} \quad (i=1,2,\ldots,(N-1)) \qquad (3.2.2)$$

where

$$\phi_{i,j} = 1-k^2\theta c_{i,j}\ ,\ \gamma_{i,j} = r^2 a_{i,j}\ ,\ \psi_{i,j} = 6\gamma_{i,j} - \beta_{i,j}\ ,$$

$$\chi_{i,j} = 6\gamma_{i,j} + \beta_{i,j}\ ,\ \beta_{i,j} = 3rk(a'_{i,j} + b_{i,j})\ ,$$

the prime denoting differentiation with respect to x.

The truncation error for (3.2.2) is again obtained using Taylor series expansions. It is found that the error is $O(k^2h^2)$, although in this case the expression is much more complex, involving derivatives of the variable coefficients and odd order derivatives of u with respect to t. The full expression for this truncation error is given in Wisher (1977).

The stability condition for (3.2.2) is obtained by applying the von Neumann method locally, since the method is only applicable to difference schemes with constant coefficients.

As suggested by Widlund (1966) and Mitchell (1969) we therefore perform the analysis by considering the coefficients to be constant and assume that the scheme with variable coefficients will be stable provided the condition obtained is satisfied at every point of the solution domain. The scheme (3.2.2) then has the following stability condition

(a) if $\theta \geq \frac{1}{4}$, it is unconditionally stable;

(b) if $\theta < \frac{1}{4}$, it is stable whenever

$$r \leq \{3a(x,t)(1-4\theta)\}^{-1/2} \qquad (3.2.3)$$

is satisfied independently at each point of the solution domain.

Equations of the form (3.2.1) have been considered in detail by Raggett, Stone and Wisher (1975) and (1976).

(ii) Parabolic Partial Differential Equations

3.3 Constant Coefficients

The cubic spline solution of the simple heat conduction equation has been considered by Papamichael and Whiteman(1973) and by Sastry (1976). In this section we extend the technique to the more general parabolic partial differential equation

$$\frac{\partial u}{\partial t} = a \frac{\partial^2 u}{\partial x^2} + b \frac{\partial u}{\partial x} + cu \quad (0 \leq x \leq 1,\ t > 0) \qquad (3.3.1)$$

where a, b, c are constants ($a > 0$). We here assume that (3.3.1) is subject to the initial condition

$$u(x,0) = g(x) \tag{3.3.2}$$

and the function value boundary conditions

$$u(0,t) = f_1(t) \quad , \quad u(1,t) = f_2(t) \tag{3.3.3}$$

where $f_1(t)$, $f_2(t)$ and $g(x)$ are known functions. If the knot partition (3.1.4) is again chosen to be equally spaced, then by similarly replacing the time derivative in (3.3.1) by a finite difference approximation and the space derivatives by a cubic spline we have at (ih, jk)

$$\begin{aligned} \frac{u_{i,j+1} - u_{i,j}}{k} &= a\{\theta M_{i,j+1} + (1-\theta)M_{i,j}\} \\ &\quad + b\{\theta L_{i,j+1} + (1-\theta)L_{i,j}\} \\ &\quad + c\{\theta u_{i,j+1} + (1-\theta)u_{i,j}\} \end{aligned} \tag{3.3.4}$$

$(i=0,1,\ldots,N \; ; \; j=1,2,\ldots \; ; \; Nh=1 \; ; \; \theta \geq 0)$

where $L_{i,j}$ and $M_{i,j}$ are as previously defined. A scheme similar in nature to (3.1.17) is obtained by performing the following operations:

(i) multiply (3.1.7) by $a(1-\theta)$;

(ii) multiply (3.1.9) by $a\theta$;

(iii) multiply (3.1.14) by $b(1-\theta)$;

(iv) multiply (3.1.16) by $b\theta$;

(v) add the expressions produced in (i)-(iv) above together;

(vi) use (3.3.4) to eliminate the $M_{i,j}$ and $L_{i,j}$ values.

The following scheme incorporating splines thus results

$$(1-\beta_1\theta)u_{i-1,j+1} + 4(1+\beta_2\theta)u_{i,j+1} + (1-\beta_3\theta)u_{i+1,j+1}$$

$$= \{1+\beta_1(1-\theta)\}u_{i-1,j} + 4\{1-\beta_2(1-\theta)\}u_{i,j} + \{1+\beta_3(1-\theta)\}u_{i+1,j} \quad (3.3.5)$$

$$(i=1,2,\ldots,(N-1))$$

where $\beta_1 = 6ar - 3brh + kc$; $\beta_2 = 3ar - ck$; $\beta_3 = 6ar + 3brh + kc$ and the mesh ratio $r = k/h^2$.

The scheme (3.3.5) reduces to that of Papamichael and Whiteman (1973) for a=1, b=c=0 and is analogous to (3.1.17) for hyperbolic equations. In fact, if a=1, b=c=0, suitable choices of the parameter θ lead to other well-known finite difference schemes. For example, by choosing $\theta = \frac{1}{6r}$ the scheme (3.3.5) reduces to the simple explicit representation; $\theta = \frac{1}{2} + \frac{1}{6r}$ gives rise to the Crank-Nicolson formula and $\theta = \frac{1}{2} + \frac{1}{12r}$ yields the high accuracy formula of Douglas (1956).

The truncation error associated with the scheme (3.3.5) is again obtained using Taylor series expansions. Fuller details are given here (compared to the hyperbolic case) since this truncation error has not been derived elsewhere. Thus, expanding (3.3.5) about the mesh point (ih, jk) we have

$$
\begin{aligned}
&(1-\beta_1\theta)\Bigg[u_{i,j} + k\left(\frac{\partial u}{\partial t}\right)_{i,j} + \frac{k^2}{2!}\left(\frac{\partial^2 u}{\partial t^2}\right)_{i,j} + \frac{k^3}{3!}\left(\frac{\partial^3 u}{\partial t^3}\right)_{i,j} + \frac{k^4}{4!}\left(\frac{\partial^4 u}{\partial t^4}\right)_{i,j} \\
&\quad -h\left\{\left(\frac{\partial u}{\partial x}\right)_{i,j} + k\left(\frac{\partial^2 u}{\partial x \partial t}\right)_{i,j} + \frac{k^2}{2!}\left(\frac{\partial^3 u}{\partial x \partial t^2}\right)_{i,j} + \frac{k^3}{3!}\left(\frac{\partial^4 u}{\partial x \partial t^3}\right)_{i,j}\right\} \\
&\quad + \frac{h^2}{2!}\left\{\left(\frac{\partial^2 u}{\partial x^2}\right)_{i,j} + k\left(\frac{\partial^3 u}{\partial x^2 \partial t}\right)_{i,j} + \frac{k^2}{2!}\left(\frac{\partial^4 u}{\partial x^2 \partial t^2}\right)_{i,j}\right\} \\
&\quad - \frac{h^3}{3!}\left\{\left(\frac{\partial^3 u}{\partial x^3}\right)_{i,j} + k\left(\frac{\partial^4 u}{\partial x^3 \partial t}\right)_{i,j}\right\} + \frac{h^4}{4!}\left(\frac{\partial^4 u}{\partial x^4}\right)_{i,j}\Bigg] \\
&+ 4(1-\beta_2\theta)\Bigg[u_{i,j} + k\left(\frac{\partial u}{\partial t}\right)_{i,j} + \frac{k^2}{2!}\left(\frac{\partial^2 u}{\partial t^2}\right)_{i,j} + \frac{k^3}{3!}\left(\frac{\partial^3 u}{\partial t^3}\right)_{i,j} + \frac{k^4}{4!}\left(\frac{\partial^4 u}{\partial t^4}\right)_{i,j}\Bigg] \\
&+(1-\beta_3\theta)\Bigg[u_{i,j} + k\left(\frac{\partial u}{\partial t}\right)_{i,j} + \frac{k^2}{2!}\left(\frac{\partial^2 u}{\partial t^2}\right)_{i,j} + \frac{k^3}{3!}\left(\frac{\partial^3 u}{\partial t^3}\right)_{i,j} + \frac{k^4}{4!}\left(\frac{\partial^4 u}{\partial t^4}\right)_{i,j} \\
&\quad +h\left\{\left(\frac{\partial u}{\partial x}\right)_{i,j} + k\left(\frac{\partial^2 u}{\partial x \partial t}\right)_{i,j} + \frac{k^2}{2!}\left(\frac{\partial^3 u}{\partial x \partial t^2}\right)_{i,j} + \frac{k^3}{3!}\left(\frac{\partial^4 u}{\partial x \partial t^3}\right)_{i,j}\right\} \\
&\quad +\frac{h^2}{2!}\left\{\left(\frac{\partial^2 u}{\partial x^2}\right)_{i,j} + k\left(\frac{\partial^3 u}{\partial x^2 \partial t}\right)_{i,j} + \frac{k^2}{2!}\left(\frac{\partial^4 u}{\partial x^2 \partial t^2}\right)_{i,j}\right\} \\
&\quad +\frac{h^3}{3!}\left\{\left(\frac{\partial^3 u}{\partial x^3}\right)_{i,j} + k\left(\frac{\partial^4 u}{\partial x^3 \partial t}\right)_{i,j}\right\} + \frac{h^4}{4!}\left(\frac{\partial^4 u}{\partial x^4}\right)_{i,j}\Bigg]
\end{aligned}
$$

$$= \{1+\beta_1(1-\theta)\}\left[u_{i,j} - h\left(\frac{\partial u}{\partial x}\right)_{i,j} + \frac{h^2}{2!}\left(\frac{\partial^2 u}{\partial x^2}\right)_{i,j} - \frac{h^3}{3!}\left(\frac{\partial^3 u}{\partial x^3}\right)_{i,j} + \frac{h^4}{4!}\left(\frac{\partial^4 u}{\partial x^4}\right)_{i,j}\right]$$

$$+ 4\{1-\beta_2(1-\theta)\}u_{i,j}$$

$$+ \{1+\beta_3(1-\theta)\}\left[u_{i,j} + h\left(\frac{\partial u}{\partial x}\right)_{i,j} + \frac{h^2}{2!}\left(\frac{\partial^2 u}{\partial x^2}\right)_{i,j} + \frac{h^3}{3!}\left(\frac{\partial^3 u}{\partial x^3}\right)_{i,j} + \frac{h^4}{4!}\left(\frac{\partial^4 u}{\partial x^4}\right)_{i.j}\right]$$

(3.3.6)

Using the expressions for β_1, β_2, β_3 given earlier and rearranging we obtain the following truncation error to fourth order

$$(-ck^2\theta)\frac{\partial u}{\partial t} + \frac{1}{2}(k^2 - ck^3\theta)\frac{\partial^2 u}{\partial t^2} + \frac{1}{6}(k^3 - ck^4\theta)\frac{\partial^3 u}{\partial t^3}$$

$$+ \frac{1}{24}(k^4 - ck^5\theta)\frac{\partial^4 u}{\partial t^4} + (-bk^2\theta)\frac{\partial^2 u}{\partial x \partial t} + (-\frac{1}{2}bk^3\theta)\frac{\partial^3 u}{\partial x \partial t^2}$$

$$+ (-\frac{1}{6}bk^4\theta)\frac{\partial^4 u}{\partial x \partial t^3} + (-\frac{1}{6}ckh^2)\frac{\partial^2 u}{\partial x^2} + \frac{1}{6}(kh^2 - 6ak^2\theta - ck^2h^2\theta)\frac{\partial^4 u}{\partial x^2 \partial t^2}$$

$$+ \frac{1}{6}(\frac{k^2h^2}{12} - 3ak^3\theta - \frac{ck^3h^2}{2}\theta)\frac{\partial^4 u}{\partial x^2 \partial t^2} + (-\frac{1}{6}bkh^2)\frac{\partial^3 u}{\partial x^3}$$

$$+ (-\frac{1}{6}bk^2h^2\theta)\frac{\partial^4 u}{\partial x^3 \partial t} + \frac{1}{12}\left(-akh^2 - \frac{ckh^4}{6}\right)\frac{\partial^4 u}{\partial x^4} \qquad (3.3.7)$$

The time and mixed derivatives in (3.3.7) can now be replaced by space derivatives by employing (3.3.1).

For example

$$\frac{\partial^2 u}{\partial t^2} = a^2\frac{\partial^4 u}{\partial x^4} + 2ab\frac{\partial^3 u}{\partial x^3} + (2ac + b^2)\frac{\partial^2 u}{\partial x^2} + 2bc\frac{\partial u}{\partial x} + c^2 u,$$

$$\frac{\partial^2 u}{\partial x \partial t} = a\frac{\partial^3 u}{\partial x^3} + b\frac{\partial^2 u}{\partial x^2} + c\frac{\partial u}{\partial x}.$$

The following expression for the truncation error involving space derivatives only, is thus obtained

$$
\begin{aligned}
k^2\Bigg\{ & \left[c^2\left(\frac{1}{2}(1-2\theta) + \frac{ck}{6}(1-3\theta) + \frac{c^2k^2}{24}(1 - 4\theta - ck\theta) \right)\right] u \\
& + \left[bc \left(1-2\theta + \frac{ck}{2}(1-3\theta) + \frac{c^2k^2}{6}(1 - 4\theta - ck\theta) \right)\right] \frac{\partial u}{\partial x} \\
& + \Bigg[ac \left(1-2\theta + \frac{ck}{2}(1-3\theta) + \frac{c^2k^2}{6}(1 - 3\theta - ck\theta) \right) \\
& \quad + b^2 \left(\frac{1}{2}(1-2\theta) + \frac{ck}{2}(1-3\theta) + \frac{c^2k^4}{4}(1 - 4\theta - ck\theta) \right) \\
& \quad + \frac{c^2h^2}{72}(1 - 12\theta - ck\theta) \Bigg] \frac{\partial^2 u}{\partial x^2} \\
& + \Bigg[ab \left(1-2\theta + ck(1-3\theta) + \frac{c^2k^2}{2}(1 - 3\theta - ck\theta) \right) \\
& \quad + b^3 \left(\frac{ck^2}{6}(1 - 4\theta - ck\theta) + \frac{k}{6}(1 -3\theta) \right) \\
& \quad + \frac{bch^2}{36}(1 - 12\theta - 6ck\theta) \Bigg] \frac{\partial^3 u}{\partial x^3} \\
& + \Bigg[a^2 \left(\frac{1}{2}(1-2\theta) + \frac{ck}{2}(1-3\theta) + \frac{c^2k^2}{4}(1-2\theta - ck\theta) \right) \\
& + ab^2 \left(\frac{k}{2}(1-3\theta) + \frac{ck^2}{2}(1 - 3\theta - ck\theta) \right) \\
& + \frac{ach^2}{36}(1 - 6\theta - 6ck\theta) + \frac{b^2h^2}{72}(1 - 12\theta - 6ck\theta) \\
& + \frac{b^4k^2}{24}(1 - 4\theta - ck\theta) + \frac{a}{12r} - \frac{ch^2}{72r} \Bigg] \frac{\partial^4 u}{\partial x^4} \Bigg\}
\end{aligned}
\qquad (3.3.8)
$$

For the simple heat conduction equation this error reduces to

$$k^2\left[\frac{1}{2}(1-2\theta)+\frac{1}{12r}\right]\frac{\partial^4 u}{\partial x^4}+\ldots. \qquad (3.3.9)$$

and thus by choosing

$$\theta=\frac{1}{2}+\frac{1}{12r} \qquad (3.3.10)$$

the truncation error is simplified to include only terms higher than fourth order derivatives. As previously mentioned, the use of (3.3.10) gives rise to the high accuracy formula derived by Douglas (1956).

The stability of (3.3.5) is examined by first replacing $u_{i,j}$ by $u_{m,n}$ and then letting $u_{m,n}=e^{im\gamma}\xi^n$, where γ is an arbitrary real number and $\xi=e^{i\lambda}$, λ being a complex parameter. Equation (3.3.5) thus becomes

$$(1-\beta_1\theta)e^{i(m-1)\gamma}\xi^{n+1}+4(1+\beta_2\theta)e^{im\gamma}\xi^{n+1}+(1-\beta_3\theta)e^{i(m+1)\gamma}\xi^{n+1}$$

$$=\{1+\beta_1(1-\theta)\}e^{i(m-1)\gamma}\xi^n+4\{1-\beta_2(1-\theta)\}e^{im\gamma}\xi^n+\{1+\beta_3(1-\theta)\}e^{i(m+1)\gamma}\xi^n$$

Dividing by $e^{im\gamma}\xi^n\neq 0$ and rearranging gives

$$\xi=\frac{\{1+\beta_1(1-\theta)\}e^{-i\gamma}+4\{1-\beta_2(1-\theta)\}+\{1+\beta_3(1-\theta)\}e^{i\gamma}}{(1-\beta_1\theta)e^{-i\gamma}+4(1+\beta_2\theta)+(1-\beta_3\theta)e^{i\gamma}}$$

If we now replace β_1, β_2, β_3 by their full expressions and let h and k tend to zero in such a way that r remains fixed we obtain

$$\xi = \frac{\{1 + 6ar(1-\theta)\}(e^{-i\gamma}+e^{i\gamma}) + 4\{1 - 3ar(1-\theta)\}}{(1 - 6ar\theta)(e^{-i\gamma}+e^{i\gamma}) + 4(1+3ar\theta)} \qquad (3.3.11)$$

Since $2\cos\gamma = e^{-i\gamma}+e^{i\gamma}$,

and $\cos\gamma = 1 - 2\sin^2\frac{\gamma}{2}$

it follows that, in view of the fact that ξ is purely real, the stability condition on ξ is

$$-1 \leqslant \frac{3 - 2(1 + 6ar(1-\theta))\sin^2\frac{\gamma}{2}}{3 - 2(1 - 6ar\theta)\sin^2\frac{\gamma}{2}} \leqslant 1 \qquad (3.3.12)$$

Denoting the denominator in this expression by D, we see that since $r > 0$, $a > 0$ and $\theta \geqslant 0$ then $D > 0$. Thus (3.3.12) becomes

$$-3 + 2(1-6ar\theta)\sin^2\frac{\gamma}{2} \leqslant 3 - 2(1+6ar(1-\theta))\sin^2\frac{\gamma}{2} \leqslant 3 - 2(1-6ar\theta)\sin^2\frac{\gamma}{2} . \qquad (3.3.13)$$

From the right-hand inequality in (3.3.13) we have

$$-12ar\sin^2\frac{\gamma}{2} \leqslant 0 \qquad (3.3.14)$$

which is satisfied for all $r > 0$; thus the left-hand inequality will yield the required stability criteria. From the left-hand inequality we obtain the expression

$$12ar(1-2\theta)\sin^2\frac{\gamma}{2} \leqslant 6 - 4\sin^2\frac{\gamma}{2} . \qquad (3.3.15)$$

Thus, if $1-2\theta > 0$, we can rearrange (3.3.15) to give

$$r \leqslant \frac{3 - 2\mathrm{Sin}^2\frac{\gamma}{2}}{6a(1-2\theta)\mathrm{Sin}^2\frac{\gamma}{2}} \quad . \tag{3.3.16}$$

Since $\mathrm{Sin}^2\frac{\gamma}{2} \in [0,1]$, then by choosing $\mathrm{Sin}^2\frac{\gamma}{2}$ to give the most restricted condition on stability, we obtain

$$r \leqslant \frac{1}{6a(1-2\theta)} \quad . \tag{3.3.17}$$

Alternatively, if $1-2\theta \leqslant 0$, rearrangement of (3.3.15) gives

$$r \geqslant \frac{3 - 2\mathrm{Sin}^2\frac{\gamma}{2}}{6a(1-2\theta)\mathrm{Sin}^2\frac{\gamma}{2}} \tag{3.3.18}$$

and thus $r \geqslant \alpha$, where $\alpha < 0$. This implies that the scheme (3.3.5) is unconditionally stable for $1-2\theta \leqslant 0$.

The scheme (3.3.5) therefore has the following condition governing its stability

(a) if $\theta \geqslant \frac{1}{2}$, it is unconditionally stable.

(b) if $\theta < \frac{1}{2}$, it is stable provided that

$$r \leqslant \{6a(1-2\theta)\}^{-1} \quad . \tag{3.3.19}$$

3.4 Variable Coefficients

As shown in section 3.2 spline techniques can be applied to hyperbolic partial differential equations with variable coefficients. In this section we require solutions to the parabolic equation with variable coefficients

$$\frac{\partial u}{\partial t} = \frac{\partial}{\partial x}\left[a(x,t)\,\frac{\partial u}{\partial x} \right] + b(x,t)\,\frac{\partial u}{\partial x} + c(x,t)u \qquad (3.4.1)$$

where again $a(x,t) > 0$ at all points in the solution domain.

As in previous sections, if we replace the time derivative in (3.4.1) by a finite difference approximation and the space derivatives by a cubic spline we obtain at (ih, jk)

$$\begin{aligned}\frac{u_{i,j+1} - u_{i,j}}{k} &= \theta a_{i,j+1} M_{i,j+1} + (1-\theta) a_{i,j} M_{i,j} \\ &\quad + \theta(a'_{i,j+1} + b_{i,j+1})L_{i,j+1} + (1-\theta)(a'_{i,j} + b_{i,j})L_{i,j} \\ &\quad + \theta c_{i,j+1} u_{i,j+1} + (1-\theta) c_{i,j} u_{i,j} \qquad (3.4.2)\end{aligned}$$

$(i=0,1,\ldots,N \; ; \; j=1,2,\ldots \; ; \; Nh=1 \; ; \; \theta \geq 0)$.

To obtain the required scheme incorporating cubic splines we perform the following operations:

(i) multiply (3.1.7) by $a_{i,j}(1-\theta)$;

(ii) multiply (3.1.9) by $\theta a_{i,j+1}$;

(iii) multiply (3.1.14) by $(a'_{i,j}+b_{i,j})(1-\theta)$;

(iv) multiply (3.1.16) by $\theta(a'_{i,j+1}+b_{i,j+1})$;

(v) add the expressions obtained in (i)-(iv) together; this gives the following expression

$$\begin{aligned}&a_{i,j}(1-\theta)\left(\frac{1}{6}M_{i-1,j} + \frac{2}{3}M_{i,j} + \frac{1}{6}M_{i+1,j}\right) + a_{i,j+1}\theta\left(\frac{1}{6}M_{i-1,j+1} + \frac{2}{3}M_{i,j+1} + \frac{1}{6}M_{i+1,j+1}\right) \\ &+(a'_{i,j}+b_{i,j})(1-\theta)\left(\frac{1}{6}L_{i-1,j} + \frac{2}{3}L_{i,j} + \frac{1}{6}L_{i+1,j}\right) + (a'_{i,j+1}+b_{i,j+1})\theta\left(\frac{1}{6}L_{i-1,j+1} \right. \\ &\qquad \left. + \frac{2}{3}L_{i,j+1} + \frac{1}{6}L_{i+1,j+1}\right) \\ &= a_{i,j}(1-\theta)\left(\frac{u_{i-1,j} - 2u_{i,j} + u_{i+1,j}}{h^2}\right) + a_{i,j+1}\theta\left(\frac{u_{i-1,j+1} - 2u_{i,j+1} + u_{i+1,j+1}}{h^2}\right) \\ &+(a'_{i,j}+b_{i,j})(1-\theta)\left(\frac{u_{i+1,j} - u_{i-1,j}}{2h}\right) + (a'_{i,j+1}+b_{i,j+1})\theta\left(\frac{u_{i+1,j+1} - u_{i-1,j+1}}{2h}\right) \\ &\qquad\qquad (3.4.3)\end{aligned}$$

(vi) use (3.4.2) directly and with i replaced by both (i-1) and (i+1) to eliminate the $M_{i,j}$ and $L_{i,j}$ values in (3.4.3). In the case of constant coefficients the required scheme results immediately. In this case however, use must also be made of Taylor Series expansions before the M's and L's can be eliminated. For example, (3.4.2) with i replaced by (i-1) can be written as

$$\frac{u_{i-1,j+1} - u_{i-1,j}}{k} = \theta\left(a_{i,j+1} - ha'_{i,j+1} + \frac{h^2}{2!}a''_{i,j+1}\cdots\right)M_{i-1,j+1}$$
$$+(1-\theta)\left(a_{i,j} - ha'_{i,j} + \frac{h^2}{2!}a''_{i,j}\cdots\right)M_{i-1,j}$$
$$+\theta\left(a'_{i,j+1} - ha''_{i,j+1}+\ldots+b_{i,j+1} - hb'_{i,j+1} + \frac{h^2}{2!}b''_{i,j+1}\cdots\right)L_{i-1,j+1}$$
$$+(1-\theta)\left(a'_{i,j} - ha''_{i,j}+\ldots+b_{i,j} - hb'_{i,j} + \frac{h^2}{2!}b''_{i,j}\cdots\right)L_{i-1,j}$$
$$+\theta c_{i-1,j+1}\,u_{i-1,j+1} + (1-\theta)c_{i-1,j}\,u_{i-1,j} \qquad (3.4.4)$$

A similar expression can also be obtained for (3.4.2) with i replaced by (i+1). These expressions are then used to carry out the elimination of the $M_{i,j}$ and $L_{i,j}$ values as required. The following scheme thus results

$$(\phi_{i-1,j+1} - \phi\psi_{i,j+1}) \overset{u_{i-1,j+1}}{} + 4(\phi_{i,j+1} + 3\theta\gamma_{i,j+1})u_{i,j+1}$$

$$+ (\phi_{i+1,j+1} - \theta\chi_{i,j+1})u_{i+1,j+1}$$

$$=\{\phi_{i-1,j} + kc_{i-1,j} + (1-\theta)\psi_{i,j}\}u_{i-1,j} + 4\{\phi_{i,j} + kc_{i,j} - 3(1-\theta)\gamma_{i,j}\}\, u_{i,j}$$

$$+\{\phi_{i+1,j} + kc_{i+1,j} + (1-\theta)\chi_{i,j}\}\, u_{i+1,j}$$

$$(i=1,2,\ldots,(N-1) \qquad (3.4.5)$$

where

$$\phi_{i,j} = 1 - k\theta c_{i,j} \quad , \quad \gamma_{i,j} = ra_{i,j} \quad , \quad \psi_{i,j} = 6\gamma_{i,j} - \beta_{i,j} \quad ,$$

$$\chi_{i,j} = 6\gamma_{i,j} + \beta_{i,j} \quad , \quad \beta_{i,j} = 3\,\frac{k}{h}\,(a'_{i,j} + b_{i,j}).$$

As in section 3.2, the stability condition for the scheme (3.4.5) is derived by applying the von Neumann Method locally. It can thus be shown that

(i) if $\theta \geq \frac{1}{2}$, it is unconditionally stable

(ii) if $\theta < \frac{1}{2}$, it is stable provided

$$r \leq \{\, 6a(x,t)(1-2\theta)\}^{-1} \qquad (3.4.6)$$

is satisfied independently at each point of the solution domain.

The truncation error associated with (3.4.5) may again be derived by expanding the terms in the scheme using Taylor

series. As in section 3.2, the expression is complicated by derivatives of the variable coefficients. For conciseness the details are not given here, but it can be shown that the error of (3.4.5) is $O(k^2)$.

CHAPTER 4

Initial Value Partial Differential Equations with Unequally Spaced Knots.

4.1 The Use of Unequal Step Lengths

The numerical solution of partial differential equations using finite difference schemes in which the mesh points are non-uniformly distributed has been considered by various authors. For example, Saul'yev (1964) suggested the use of non-rectangular grids for solving the heat conduction equation in which the initial condition g(x) has the form illustrated in Figure 1.

Saul'yev recommends that, due to the changing nature of the function g(x) in such a situation the step lengths should be chosen to be smaller in the first third of the range $[0,1]$ and larger in the reamining two-thirds.

More complicated problems in which the solution varies rapidly over a small part of the domain but very slowly over the rest are found in boundary layer problems in fluid dynamics. Crowder and Dalton (1971) and Kàlnay de Rivas (1972) have considered the use of non-uniform grids which can be used to place sufficient mesh points in the region of the boundary layer and fewer points in the remaining solution domain.

Finite difference approximations with unequally spaced mesh points have also been shown to be advantageous in moving boundary problems in heat flow (see for example Murray and

Landis (1959), Douglas and Gallie (1955), Lotkin (1960) and Crank and Gupta (1972a).

4.2 Hyperbolic Partial Differential Equations with Constant Coefficients

In this section we obtain solutions u(x,t) to (3.1.1) using spline techniques in which the knot partition (3.1.4) is considered to be unequally spaced and where the distance between successive knots is given in (2.2.2).

From equation (2.2.3) the spline function on the j^{th} time line has the form

$$S_j(x) = M_{i-1,j}\frac{(x_i - x)^3}{6h_i} + M_{i,j}\frac{(x - x_{i-1})^3}{6h_i} + \left(u_{i-1,j} - \frac{h_i^2}{6}M_{i-1,j}\right)\frac{(x_i - x)}{h_i}$$

$$+\left(u_{i,j} - \frac{h_i^2}{6}M_{i,j}\right)\frac{(x - x_{i-1})}{h_i} . \quad (i=1,2,\ldots,N) \qquad (4.2.1)$$

Similarly the expression (2.2.6) for the second derivative of the spline function becomes on the j^{th} time level

$$\frac{h_i}{6}M_{i-1,j} + \frac{h_i + h_{i+1}}{3}M_{i,j} + \frac{h_{i+1}}{6}M_{i+1,j}$$

$$= \frac{h_i u_{i+1,j} - (h_i + h_{i+1})u_{i,j} + h_{i+1}u_{i-1,j}}{h_i h_{i+1}} \qquad (4.2.2)$$

$$(i=1,2,\ldots,(N-1))$$

A relationship similar to (3.1.14) is now required for unequally spaced knots. From (3.1.10) to (3.1.13) the following expressions are obtained

$$h_i L_{i,j} = \frac{h_i^2}{6} M_{i-1,j} + \frac{h_i^2}{3} M_{i,j} + u_{i,j} - u_{i-1,j} \qquad (4.2.3)$$

$$h_{i+1} L_{i,j} = -\frac{h_{i+1}^2}{3} M_{i,j} - \frac{h_{i+1}^2}{6} M_{i+1,j} + u_{i+1,j} - u_{i,j} \qquad (4.2.4)$$

$$h_{i+1} L_{i+1,j} = \frac{h_{i+1}^2}{6} M_{i,j} + \frac{h_{i+1}^2}{3} M_{i+1,j} + u_{i+1,j} - u_{i,j} \qquad (4.2.5)$$

$$h_i L_{i-1,j} = -\frac{h_i^2}{3} M_{i-1,j} - \frac{h_i^2}{6} M_{i,j} + u_{i,j} - u_{i-1,j} \qquad (4.2.6)$$

Adding (4.2.3) and (4.2.4) to half the sum of (4.2.5) and (4.2.6) gives the expression

$$\frac{h_i}{6} L_{i-1,j} + \frac{h_i + h_{i+1}}{3} L_{i,j} + \frac{h_{i+1}}{6} L_{i+1,j}$$

$$= \frac{(h_i^2 - h_{i+1}^2)}{12} M_{i,j} + \frac{u_{i+1,j} - u_{i-1,j}}{2} \qquad (4.2.7)$$

$$(i=1,2,\ldots,(N-1))$$

Approximations similar to (4.2.2) and (4.2.7) also hold on the $(j-1)^{th}$ and $(j+1)^{th}$ time lines. As explained in section 3.1 we now take combinations of the above mentioned relationships and use (3.1.5) to eliminate the $M_{i,j}$ and $L_{i,j}$ terms where possible. The following three time level scheme is thus obtained

$$(\phi_i - \gamma_i\theta)u_{i-1,j+1} + 2(1 + \chi_i\theta)u_{i,j+1} + (\beta_i - \psi_i\theta)u_{i+1,j+1}$$

$$+ \frac{bk^2}{2}(h_{i+1} - h_i)(\theta M_{i,j-1} + (1-2\theta)M_{i,j} + \theta M_{i,j+1})$$

$$=\{2\phi_i + \gamma_i(1-2\theta)\}u_{i-1,j} + 2\{2 - \chi_i(1-2\theta)\}u_{i,j} + \{2\beta_i + \psi_i(1-2\theta)\}u_{i+1,j}$$

$$-(\phi_i - \gamma_i\theta)u_{i-1,j-1} - 2(1 + \chi_i\theta)u_{i,j-1} - (\beta_i - \psi_i\theta)u_{i+1,j-1} \qquad (4.2.8)$$

$$(i=1,2,\ldots,(N-1))$$

where

$$\gamma_i = 6ar_i - 3bh_{i+1}s_i + ch_ih_{i+1}s_i$$

$$\chi_i = 6a\nu_i - ck^2$$

$$\psi_i = 6as_i + 3bh_ir_i + ch_ih_{i+1}r_i$$

$$\phi_i = \frac{h_i}{h_i + h_{i+1}}, \quad \beta_i = \frac{h_{i+1}}{h_i + h_{i+1}}$$

and the mesh ratios r_i, s_i and ν_i are given by

$$r_i = \frac{k^2}{h_i(h_i + h_{i+1})}, \quad s_i = \frac{k^2}{h_{i+1}(h_i + h_{i+1})}, \quad \nu_i = \frac{k^2}{2h_ih_{i+1}}.$$

If the coefficiant b in (3.1.1) is non-zero the solution of the scheme (4.2.8) is complicated by the presence of $M_{i,j-1}$, $M_{i,j}$ and $M_{i,j+1}$. Assuming that the scheme is fully developed in that values for u and M are known on the j^{th} and $(j-1)^{th}$ time lines, then we must determine $M_{i,j+1}$ values before further solutions $u_{i,j+1}$ can be found.

This problem is overcome using the following numerical procedure:

(i) Using the initial condition (3.1.3) the expression (4.2.2) becomes

$$\frac{h_i}{6}M_{i-1,0} + \frac{h_i + h_{i+1}}{3}M_{i,0} + \frac{h_{i+1}}{6}M_{i+1,0}$$

$$= \frac{h_i\, g_1(x_{i+1}) - (h_i + h_{i+1})g_1(x_i) + h_{i+1}g_1(x_{i-1})}{h_i h_{i+1}} \quad . \tag{4.2.9}$$

$$(i=1,2,\ldots,(N-1)$$

Given that $M_{0,j} = M_{N,j} = 0$ $(j=0,1,2,\ldots.)$, the tri-diagonal system is easily solved for $M_{i,0}$ $(i=1,2,\ldots.,(N-1))$.

(ii) By setting $\theta=0$ and using the derivative initial condition in (3.1.3), the scheme (4.2.8) becomes, with $j=0$

$$2\phi_i\, u_{i-1,1} + 4u_{i,1} + 2\beta_i\, u_{i+1,1} + \frac{bk^2}{2}(h_{i+1} - h_i)M_{i,0}$$

$$= (2\phi_i + \gamma_i)g_1(x_{i-1}) + 2(2-\chi_i)g_1(x_i) + (2\beta_i + \psi_i)g_1(x_{i+1})$$

$$+ 2k\phi_i g_2(x_{i-1}) + 4kg_2(x_i) + 2k\beta_i g_2(x_{i+1}). \tag{4.2.10}$$

$$(i=1,2,\ldots.,(N-1))$$

The solutions $u_{i,1}(i=1,2,\ldots,(N-1))$ are thus obtained from tri-diagonal system (4.2.10).

(iii) Putting j=1 in the expression (4.2.2) gives an easily solvable tri-diagonal system of equations producing the values $M_{i,1}$ $(i=1,2,....,(N-1))$.

(iv) Since we have now determined $M_{i,0}$, $M_{i,1}$, $u_{i,0}$ and $u_{i,1}$ we can develop a general scheme for obtaining $M_{i,j+1}$ and hence $u_{i,j+1}$. This is done using a simple iterative process, beginning with an initial approximation $M_{i,j+1}^{(0)}$ to $M_{i,j+1}$, given by the extrapolated relationship

$$M_{i,j+1}^{(0)} = 2M_{i,j} - M_{i,j-1} \quad (i=0,1,....,N). \qquad (4.2.11)$$

We substitute (4.2.11) into the scheme (4.2.8) thus obtaining initial approximations $u_{i,j+1}^{(0)}$, to $u_{i,j+1}$.

(v) Assuming now that the iterative process is fully developed and that we wish to obtain improved approximations $M_{i,j+1}^{(n+1)}$, to $M_{i,j+1}$, then from (4.2.2) we have the expression

$$\frac{h_i}{6} M_{i-1,j+1}^{(n+1)} + \frac{h_i + h_{i+1}}{3} M_{i,j+1}^{(n+1)} + \frac{h_{i+1}}{6} M_{i+1,j+1}^{(n+1)}$$

$$= \frac{h_i u_{i+1,j+1}^{(n)} - (h_i + h_{i+1}) u_{i,j+1}^{(n)} + h_{i+1} u_{i-1,j+1}^{(n)}}{h_i h_{i+1}} \cdot (4.2.12)$$

Given that $M_{0,j+1}^{(n+1)} = M_{N,j+1}^{(n+1)} = 0$, the system (4.2.12) is easily solved for the required improved approximations $M_{i,j+1}^{(n+1)}$ $(i=1,2,....,(N-1))$.

(vi) The $M_{i,j+1}^{(n+1)}$ values obtained in (v) are now used in the scheme (4.2.8), which in iterative notation is

$$(\phi_i - \gamma_i\theta)u_{i-1,j+1}^{(n+1)} + 2(1+\chi_i\theta)u_{i,j+1}^{(n+1)} + (\beta_i - \psi_i\theta)u_{i+1,j+1}^{(n+1)}$$

$$+ \frac{bk^2}{2}(h_{i+1} - h_i)(\theta M_{i,j-1} + (1-2\theta)M_{i,j} + \theta M_{i,j+1}^{(n+1)})$$

$$= \{2\phi_i + \gamma_i(1-2\theta)\}u_{i-1,j} + 2\{2 - \chi_i(1-2\theta)\}u_{i,j} + \{2\beta_i + \psi_i(1-2\theta)\}u_{i+1,j}$$

$$-(\phi_i - \gamma_i\theta)u_{i-1,j-1} - 2(1+\chi_i\theta)u_{i,j-1} - (\beta_i - \psi_i\theta)u_{i+1,j-1}$$

$$(i=1,2,\ldots,(N-1)) \qquad (4.2.13)$$

By solving (4.2.13) we obtain improved approximations $u_{i,j+1}^{(n+1)}$, to $u_{i,j+1}$.

(vii) A test is now performed on these $u_{i,j+1}^{(n+1)}$ values by examining numerical values of the inequality

$$\left| u_{i,j+1}^{(n+1)} - u_{i,j+1}^{(n)} \right| \leq \varepsilon \qquad (i=1,2,\ldots,(N-1)) \quad (4.2.14)$$

for some fixed tolerance ε. If (4.2.14) is satisfied for all i then the $u_{i,j+1}^{(n+1)}$ are taken as the required solutions. However, if (4.2.14) is not satisfied, then the $u_{i,j+1}^{(n+1)}$ must be re-employed in (4.2.12) and the process repeated until the required accuracy is achieved.

The obtaining of solutions to (3.1.1) using this iterative process is obviously more computationally expensive than the previously described equally spaced knot schemes. However,

the M values obtained in this process are of further benefit in the following instances:

(a) As explained in Wisher (1977), a major advantage of splines schemes over finite difference approximations is that by making use of the spline function (4.1.1), we can easily obtain solutions to (3.1.1) at points intermediate to the knot points.

(b) In a later section of this thesis an algorithm is derived for obtaining 'optimal' knot positions for the spline solution of partial differential equations. This algorithm requires the evaluation of the $M_{i,j}$ values on each time line.

The truncation error for the scheme (4.2.8) may again be derived using Taylor Series expansions. For example, expanding $u_{i+1,j}$ and $u_{i-1,j}$ about (x_i, t_j) we have

$$u_{i+1,j} = u_{i,j} + h_{i+1}\left(\frac{\partial u}{\partial x}\right)_{i,j} + \frac{h_{i+1}^2}{2!}\left(\frac{\partial^2 u}{\partial x^2}\right)_{i,j} + \ldots . \qquad (4.2.15)$$

and

$$u_{i-1,j} = u_{i,j} - h_i\left(\frac{\partial u}{\partial x}\right)_{i,j} + \frac{h_i^2}{2!}\left(\frac{\partial^2 u}{\partial x^2}\right)_{i,j} - \ldots . \qquad (4.2.16)$$

The following expression for the truncation error is thus obtained

$$k^2\left[c^2k^2f(\theta)u + \left\{2bck^2f(\theta) + \frac{1}{3}c^2k^2\theta(h_i-h_{i+1})\right\}\frac{\partial u}{\partial x}\right.$$

$$+\left\{k^2(2ac+b^2)f(\theta) + \frac{1}{6}b(h_i-h_{i+1})(1+ck^2\theta) - \frac{1}{3}c^2k^2\theta\left(\frac{h_i^3+h_{i+1}^3}{h_i+h_{i+1}}\right)\right\}\frac{\partial^2 u}{\partial x^2}$$

$$+\left\{2abk^2f(\theta) + \frac{1}{6}k^2\theta(h_i-h_{i+1})(2ac+3b^2) - \frac{1}{18}c\left(\frac{h_i^4-h_{i+1}^4}{h_i+h_{i+1}}\right)\right.$$

$$\left.-\frac{1}{6}bck^2\theta\left(\frac{h_i^3+h_{i+1}^3}{h_i+h_{i+1}}\right)\right\}\frac{\partial^3 u}{\partial x^3}$$

$$+\left\{a^2k^2f(\theta)+\frac{1}{2}abk^2\theta(h_i - h_{i+1}) + \frac{1}{12}a\left(\frac{h_i^3 + h_{i+1}^3}{h_i + h_{i+1}}\right)(1-2ck^2\theta)\right.$$

$$\left.+\frac{1}{24}b\left(\frac{h_i^4 - h_{i+1}^4}{h_i + h_{i+1}}\right) - \frac{1}{72}c\left(\frac{h_i^5 + h_{i+1}^5}{h_i + h_{i+1}}\right)\right\}\frac{\partial^4 u}{\partial x^4}\Bigg] \qquad (4.2.17)$$

where $f(\theta)$ is given by (3.1.19)

Due to the unequally spaced knot points employed in the scheme (4.2.8) it is not possible to examine the stability of this scheme using the usual von Neumann method. This is because the method requires that the step lengths h and k tend to zero in such a way that the mesh ratio r remains fixed. In (4.2.8) each mesh ratio involves both h_i and h_{i+1},

which we would have to let tend to zero at the same rate. However, the scheme (4.2.8) reduces to (3.1.17) when $h_i = h_{i+1} = h$ and we would thus expect the stability conditions for the two schemes to be very similar.

This problem has been considered by Saul'yev (1964) in the use of non-uniform finite difference approximations. Using his notation the reasoning of the above paragraph suggests that the scheme (4.2.8) has the following stability condition

(a) if $\theta \geq \frac{1}{4}$, it is unconditionally stable

(b) if $\theta < \frac{1}{4}$, it is stable provided that

$$\frac{k^2}{\min\{h_i h_{i+1}\}} \leq \frac{1}{3a(1-4\theta)} \qquad (4.2.18)$$

Numerical evidence confirming this stability condition is given in the later chapters on case studies where values of θ, k, h_i and h_{i+1} are used which either satisfy or violate the condition.

4.3 Parabolic Partial Differential Equations with Constant Coefficients

Here we consider spline solutions to the parabolic equation (3.3.1). As in the previous section the knot partition (3.1.4) is chosen to be unequally spaced where h_i, the distance between successive knots, is given by (2.2.2).

Using the technique explained in section 3.3, we take combinations of the relationships (4.2.2) and (4.2.7) and use (3.3.4) to eliminate the $M_{i,j}$ and $L_{i,j}$ terms where possible. The two time level scheme thus obtained is as follows

$$(\phi_i - \gamma_i\theta)u_{i-1,j+1} + 2(1 + \chi_i\theta)u_{i,j+1} + (\beta_i - \psi_i\theta)u_{i+1,j+1}$$

$$+ \frac{bk}{2}(h_{i+1} - h_i)(\theta M_{i,j+1} + (1-\theta)M_{i,j})$$

$$= \{\phi_i + \gamma_i(1-\theta)\}u_{i-1,j} + 2\{1-\chi_i(1-\theta)\}u_{i,j} + \{\beta_i + \psi_i(1-\theta)\}u_{i+1,j}$$

$$(i=1,2,\ldots,(N-1)) \qquad (4.3.1)$$

where γ_i, ψ_i, ϕ_i and β_i are as defined in section 4.2 and

$$\chi_i = 6a\nu_i - ck,$$

$$r_i = \frac{k}{h_i(h_i + h_{i+1})}, \quad \blacksquare_i = \frac{k}{h_{i+1}(h_i + h_{i+1})}, \quad \nu_i \frac{k}{2h_i h_{i+1}}.$$

As described in section 4.2, when the coefficient b in (3.3.1) is non-zero the scheme (4.3.1) requires the calculation of $M_{i,j+1}$ and $M_{i,j}$ before solutions can be produced. A numerical procedure similar to that of the previous section is employed, although in this case the process is considerably simplified since (4.3.1) is only a two time level scheme. The numerical procedure is briefly as follows:

(i) Using the expression (4.2.2) determine $M_{i,0}(i=1,2,\ldots,(N-1))$.

(ii) Set $\theta = 0$ in (4.3.1) and hence evaluate the solutions $u_{i,1}(i=1,2,\ldots,(N-1))$.

(iii) Using (4.2.2) determine $M_{i,1}(i=1,2,\ldots,(N-1))$.

(iv) Evaluate $u_{i,2}(i=1,2,\ldots,(N-1))$ from the scheme (4.3.1).

The procedure is now fully developed and further solutions are obtained using (4.2.2) and (4.3.1) alternately.

In a similar manner to previous sections, we again derive the truncation error associated with the scheme (4.3.1) using Taylor series expansions. It can thus be shown that (4.3.1) becomes

$$\left[-\gamma_i+2\chi_i-\psi_i\right] u + \left[k(3-\gamma_i\theta+2\chi_i\theta-\psi_i\theta)\right]\frac{\partial u}{\partial t}$$

$$+\left[\frac{k^2}{2}(3-\gamma_i\theta+2\chi_i\theta-\psi_i\theta)\right]\frac{\partial u^2}{\partial t^2} + \left[\frac{k^3}{6}(3-\gamma_i\theta+2\chi_i\theta-\psi_i\theta)\right]\frac{\partial^3 u}{\partial t^3}$$

$$+\left[\frac{k^4}{24}(3-\gamma_i\theta+2\chi_i\theta-\psi_i\theta)\right]\frac{\partial^4 u}{\partial t^4} + \left[h_i\gamma_i - h_{i+1}\psi_i\right]\frac{\partial u}{\partial x}$$

$$+\left[-k(h_i - h_{i+1})+ k(h_i\gamma_i\theta - h_{i+1}\psi_i\theta)\right]\frac{\partial^2 u}{\partial x\partial t}$$

$$+\left[\frac{-k^2}{2}(h_i - h_{i+1})+ \frac{k^2}{2}(h_i\gamma_i\theta - h_{i+1}\psi_i\theta)\right]\frac{\partial^3 u}{\partial x\partial t^2}$$

$$+\left[\frac{-k^3}{6}(h_i-h_{i+1})+ \frac{k^3}{6}(h_i\gamma_i\theta-h_{i+1}\psi_i\theta)\right]\frac{\partial^4 u}{\partial x\partial t^3} + \left[\frac{-h_i^2}{2}\gamma_i-\frac{h_{i+1}^2}{2}\psi_i\right]\frac{\partial^2 u}{\partial x^2}$$

$$+\left[\frac{k}{2}(h_i^2(\phi_i-\gamma_i\theta)+h_{i+1}^2(\beta_i-\psi_i\theta))\right]\frac{\partial^3 u}{\partial x^2\partial t}$$

$$+\left[\frac{k^2}{4}(h_i^2(\phi_i-\gamma_i\theta)+h_{i+1}^2(\beta_i-\psi_i\theta))\right]\frac{\partial^4 u}{\partial x^2\partial t^2} + \left[\frac{h_i^3}{6}\gamma_i - \frac{h_{i+1}^3}{6}\psi_i\right]\frac{\partial^3 u}{\partial x^3}$$

$$+\left[\frac{-k}{6}(h_i^3(\phi_i-\gamma_i\theta)-h_{i+1}^3(\beta_i-\psi_i\theta))\right]\frac{\partial^4 u}{\partial x^3\partial t} + \left[\frac{-h_i^4}{24}\gamma_i - \frac{h_{i+1}^4}{24}\psi_i\right]\frac{\partial^4 u}{\partial x^4} \qquad (4.3.2)$$

This expression again contains time and mixed derivative terms. As in section 3.3, these can be replaced using (3.3.1), although the resulting expression is extremely complicated due to the variable step lengths.

In the simple case of the heat conduction equation ((3.3.1) with a=1, b=c=0) the truncation error to fourth order derivative terms has the form

$$k\left[\frac{k}{2} + \frac{1}{12}\left(\frac{h_i^3 + h_{i+1}^3}{h_i + h_{i+1}}\right) - k\theta\right]\frac{\partial^4 u}{\partial x^4} + \ldots. \qquad (4.3.3)$$

In addition, the scheme (4.3.1) has the following conditions governing its stability

(a) if $\theta \geq \frac{1}{2}$, it is unconditionally stable

(b) if $\theta < \frac{1}{2}$, it is stable provided that

$$\frac{k}{\min\{h_i h_{i+1}\}} \leq \frac{1}{6a(1-2\theta)} . \qquad (4.3.4)$$

CHAPTER 5

Methods for Obtaining Knot Partitions

5.1 Preamble

In this chapter three techniques are presented for obtaining 'optimal' knot partitions. These techniques will be called the 'local', 'global' and 'transformation' methods for reasons which will become apparent. The knot partitions obtained are chosen to best suit (in some sense) the initial condition of the partial differential equation, but which are then fixed throughout time.

As explained in the work of de Boor (1978), we cannot hope to place each knot optimally. This is because in approximating a function f(x) by a spline function S(x) we must have sufficient information about f(x) to evaluate $||f-S||_\infty$ before each knot can be optimally located. In the solution of differential equations f(x) is only known implicitly and hence in this thesis we endeavour to obtain an optimum knot distribution which we believe to be a general improvement on existing equally spaced knot methods. More exactly one could consider the knots as sub-optimal. Here-after the word optimal will have this meaning.

5.2 A Local Method

The technique described in this section for obtaining optimal knot positions is an adaptation of the well-known work of Curtis and Powell (1967). In that work, the authors developed an algorithm for use in approximating simple functions using cubic splines. They stated than an estimate ε_i of the error $\varepsilon(x)=f(x)-S(x)$ at each knot x_i is given by

$$\varepsilon_i = ||f - S||_\infty \simeq \frac{1}{384}(x_i - x_{i-1})^3 d_i \qquad (5.2.1)$$

where d_i, the discontinuity in the third derivative of the spline function, is defined as

$$d_i = S'''(x_i+) - S'''(x_i-). \qquad (5.2.2)$$

A full derivation of (5.2.1) is given in Schultz (1973). We now require an expression for this discontinuity in terms of function values f(x).

Rewriting (3.1.7) we have

$$S''(x_{i-1}) + 4S''(x_i) + S''(x_{i+1}) = \frac{6}{h^2}\left[f(x_{i-1}) - 2f(x_i) + f(x_{i+1})\right] \qquad (5.2.3)$$

which in operator notation can be written as

$$(E^{-1} + 4 + E)h^2 S''(x_i) = 6(E^{-1} - 2 + E)f(x_i) \qquad (5.2.4)$$

and after rearrangement

$$h^2 S''(x_i) = \frac{6(E^{-1} - 2 + E)}{E^{-1} + 4 + E} f(x_i) . \qquad (5.2.5)$$

Using a simple forward difference approximation, $S'''(x_i+)$ can be expressed as

$$S'''(x_i+) = \frac{S''(x_{i+1}) - S''(x_i)}{h} \qquad (5.2.6)$$

and thus by substituting for the second derivatives using (5.2.5), we have the expression

$$h^3 S'''(x_i+) = \frac{6(E^{-1}-2+E)}{E^{-1}+4+E} f(x_{i+1}) - \frac{6(E^{-1}-2+E)}{E^{-1}+4+E} f(x_i) . \qquad (5.2.7)$$

Employing the shift operator again, (5.2.7) becomes

$$h^3 S'''(x_i+) = \frac{6(1-2E+E^2)}{E^{-1}+4+E} f(x_i) - \frac{6(E^{-1}-2+E)}{E^{-1}+4+E} f(x_i) . \qquad (5.2.8)$$

and thus after suitable rearrangement the following expression for $S'''(x_i+)$ is derived

$$h^3 S'''(x_i+) = \frac{6(3-3E+E^2-E^{-1})}{E^{-1}+4+E} f(x_i). \qquad (5.2.9)$$

Similarly, using the approximation

$$S'''(x_i-) = \frac{S''(x_i) - S''(x_{i-1})}{h} \qquad (5.2.10)$$

an expression for $S'''(x_i-)$ becomes

$$h^3 S'''(x_i-) = \frac{6(3E^{-1} - 3 + E - E^{-2})}{E^{-1}+4+E} f(x_i) . \qquad (5.2.11)$$

Subtracting the relationships (5.2.11) from (5.2.9)

results in the expression

$$S'''(x_i+) - S'''(x_i-) = \frac{6(6 - 4E + E^2 - 4E^{-1} + E^{-2})}{E^{-1} + 4 + E} f(x_i) \quad (5.2.12)$$

and thus

$$S'''(x_i+) - S'''(x_i-) \approx \frac{6hf^{iv}(x_i)}{E^{-1} + 4 + E}. \quad (5.2.13)$$

By expanding the denominator terms in (5.2.13) we obtain

approximately

$$S'''(x_i+) - S'''(x_i-) = h\left[1 + \frac{h^2D^2}{6} + \frac{h^4D^4}{72} + \ldots\right]^{-1} f^{iv}(x_i). \quad (5.2.14)$$

and hence, by ignoring $O(h^4)$ terms, (5.2.14) results in the

required expression for d_i

$$d_i = S'''(x_i+) - S'''(x_i-) = hf^{iv}(x_i) + O(h^3). \quad (5.2.15)$$

Employing Taylor's theorem to remove the higher order

terms in (5.2.15), the error estimate (5.2.1) thus becomes

$$\varepsilon_i = \frac{1}{384} h^4 f^{iv}(\xi) \quad (5.2.16)$$

where ξ is some value lying between x_{i-1} and x_i.

In the Curtis and Powell algorithm a cubic spline is

fitted to the function f(x) using a small number of

equally spaced knots and if ε_i exceeds some pre-assigned

error bound, extra knots are inserted half-way between

existing knots. The process is repeated until the error estimates $|\varepsilon_i|$ are all less than the error bound.

To obtain unequal knot positions for use in the spline solution of partial differential equations we rewrite the error estimate (5.2.16) in the form

$$|\varepsilon_i| = |S_i - u_i| = \frac{1}{384} h_i^4 |u^{iv}(\xi)| \qquad (5.2.17)$$

where S_i and u_i are, respectively, the spline and exact solutions at the knot x_i. Rearrangement of (5.2.17) yields the expression

$$h_i = \left[\frac{384\ \varepsilon_i}{|u^{iv}(\xi)|}\right]^{1/4} . \qquad (5.2.18)$$

Substitution of (5.2.18) into (2.2.2) gives the approximation

$$x_i = x_{i-1} + \left[\frac{384\ \varepsilon_i}{|u^{iv}(\xi)|}\right]^{1/4} \quad (i=1,2,\ldots,N) \qquad (5.2.19)$$

which may be used as a basis for generating suitable knot partitions, in which the function $u^{iv}(\xi)$ is evaluated as the fourth derivative of the initial condition at the knot x_{i-1}. As will be later shown, equation (5.2.19) is implemented with $\varepsilon = \varepsilon_1 = \varepsilon_2 = \ldots. = \varepsilon_N$, the aim being to choose a suitable ε value which gives a desired number of knots over $[0,1]$. This is only to enable us to compare the various

methods and in practice a bound would initially be fixed on ε_i. The number and position of knots would then be determined by this bound.

5.3 A Global Method

Here the technique described for obtaining knot partitions for use in the spline solution of partial differential equations is largely based on the work of de Boor (1973 and 1974). Using results obtained by Rice (1969), Phillips (1970), McClure (1970), Dobson (1972), de Boor and Swartz (1973) and Burchard (1974), de Boor considered the approximation of a given function f on $[a,b]$ by S_Δ^k, a spline of order k (degree k-1) with a knot partition Δ, where

$$\Delta: \quad a = t_1 < t_2 < \ldots < t_N < t_{N+1} = b. \tag{5.3.1}$$

For convenience only, (5.3.1) is here used rather than (2.1.1); note that the notations are made compatible at the end of this section.

To obtain suitable knot distributions, de Boor suggests that the following condition should be satisfied

$$||f - S_\Delta||_i \lesssim C|\Delta t_i|^k \, ||f^{(k)}||_i + O(|\Delta|^k) \tag{5.3.2}$$

where

$$||h||_i \approx \sup_{t\varepsilon[t_i, t_{i+1}]} |h(t)| \quad , \tag{5.3.3}$$

$$|\Delta| = \max_i \Delta t_i = \max_i (t_{i+1} - t_i) \tag{5.3.4}$$

and C is a constant > 0. The norm $||f^{(k)}||_i$ can be illustrated pictorially as in Figure 2(a), and for sufficiently small $|\Delta|$ the expression (5.3.2) has the form shown in Figure 2(b).

Generalising (5.3.2) to the whole partition $\left[t_1, t_{N+1}\right]$ we obtain the condition

$$||f - S_\Delta||_\infty \leq \max_i ||f - S_\Delta||_i \approx C \max_i |\Delta t_i|^k ||f^{(k)}||_i \qquad (5.3.5)$$

which again is illustrated in Figure 3. This suggests that the knots $t_2, t_3, \ldots, t_N$ should be chosen such that

$$\max_i ||f - S_\Delta||_i \qquad (5.3.6)$$

is minimised. Since C is constant we thus require to minimise

$$\max_i \left[|\Delta t_i|^k \sup_{\left[t_i, t_{i+1}\right]} |f^{(k)}| \right] \qquad (5.3.7)$$

$$= \max_i \left[|t_{i+1} - t_i|^k \sup_{\left[t_i, t_{i+1}\right]} |f^{(k)}| \right] . \qquad (5.3.8)$$

Consider now a particular interval $\left[\alpha, \beta\right]$ and define the function $s(\alpha,\beta)$ to be

$$s(\alpha,\beta) = (\beta-\alpha)^k \sup_{\left[\alpha,\beta\right]} |f^{(k)}| . \qquad (5.3.9)$$

Fixing α and letting $\beta=\beta_1$ (say) we have from (5.3.9)

$$s(\alpha,\beta_1) = (\beta_1 - \alpha)^k \sup_{[\alpha,\beta_1]} |f^{(k)}| \ . \tag{5.3.10}$$

If we now increase β to $\beta_2 = \beta_1 + \delta\beta_i$ then

$$\sup_{[\alpha,\beta_2]} |f^{(k)}| \geq \sup_{[\alpha,\beta_1]} |f^{(k)}| \tag{5.3.11}$$

since in the new interval $[\alpha,\beta_2]$ $|f^{(k)}|$ may achieve a new maximum or may not. In addition, since

$$(\beta_2 - \alpha)^k > (\beta_1 - \alpha)^k \tag{5.3.12}$$

then

$$s(\alpha,\beta_2) > s(\alpha,\beta_1). \tag{5.3.13}$$

Similarly, if β is decreased to $\beta_2 = \beta_1 - \delta\beta_1$ we have

$$\sup_{[\alpha,\beta_2]} |f^{(k)}| \leq \sup_{[\alpha,\beta_1]} |f^{(k)}| \tag{5.3.14}$$

and since

$$(\beta_2 - \alpha)^k < (\beta_1 - \alpha)^k \tag{5.3.15}$$

then

$$s(\alpha,\beta_2) < s(\alpha,\beta_1) \ . \tag{5.3.16}$$

We can thus conclude that the function $s(\alpha,\beta)$ is monotone increasing in β with α fixed.

Consider now the case when β is fixed and $\alpha = \alpha_1$ (say).

The expression (5.3.9) then becomes

$$s(\alpha_1,\beta) = (\beta - \alpha_1)^k \sup_{[\alpha_1,\beta]} |f^{(k)}| \,. \tag{5.3.17}$$

If α is increased to $\alpha_2 = \alpha_1 + \delta\alpha_1$ then

$$\sup_{[\alpha_2,\beta]} |f^{(k)}| \leq \sup_{[\alpha_1,\beta]} |f^{(k)}| \tag{5.3.18}$$

and since

$$(\beta-\alpha_2)^k < (\beta-\alpha_1)^k \tag{5.3.19}$$

we have

$$s(\alpha_2,\beta) < s(\alpha_1,\beta). \tag{5.3.20}$$

Similarly, if α is decreased to $\alpha_2 = \alpha_1 - \delta\alpha_1$ then it can be shown that

$$s(\alpha_2,\beta) > s(\alpha_1,\beta) \tag{5.3.21}$$

and thus the function $s(\alpha,\beta)$ is monotone decreasing in α with β fixed.

Let us now consider a single break point t_2, with adjacent knots t_1 and t_3 fixed, as shown diagrammatically in Figure 4(a). If, as illustrated,

$$s(t_1,t_2) > s(t_2,t_3) \tag{5.3.22}$$

then by moving t_2 to $t_2' = t_2 - \delta t_2$, we have

$$s(t_1,t_2') < s(t_1,t_2) \tag{5.3.23}$$

as shown in Figure 4(b). In addition

$$s(t_2',t_3) > s(t_2,t_3) \tag{5.3.24}$$

and we thus find that

$$|s(t_1,t_2') - s(t_2',t_3)| < |s(t_1,t_2) - s(t_2,t_3)|. \tag{5.3.25}$$

Therefore to minimise the deviation $|s(t_1,t_2) - s(t_2,t_3)|$ t_2' should be chosen such that

$$s(t_1,t_2') = s(t_2',t_3). \tag{5.3.26}$$

Similarly, (5.3.26) holds if the condition (5.3.22) has the form

$$s(t_1,t_2) < s(t_2,t_3). \tag{5.3.27}$$

Generalising the above to the whole knot partition Δ it can thus be shown that $t_2,t_3,\ldots,t_N$ should be chosen such that

$$s(t_i,t_{i+1}) = \text{constant} \qquad (i=1,2,\ldots,N) \tag{5.3.28}$$

in which case (5.3.8) is minimised . The expression (5.3.28) can be rewritten as

$$|t_{i+1} - t_i|\left(||f^{(k)}||_\infty\right)^{1/k} = \text{constant} \tag{5.3.29}$$

and thus the knots $t_2, t_3, \ldots, t_N$ should be chosen such that

$$\int_{t_i}^{t_{i+1}} |f^{(k)}(x)|^{1/k} dx = \frac{1}{N} \int_0^1 |f^{(k)}(x)|^{1/k} dx . \qquad (5.3.30)$$

$$(i=1,2,\ldots,N)$$

To employ this technique in deriving knot partitions for the spline solution of partial differential equations we again apply the strategy of section 5.2 and take the function f(x) to be the given initial condition (denoted by g(x) in chapter 3). Since in this thesis we use cubic splines with knots $x_0, x_1, \ldots, x_N$ as defined by (3.1.4), the integral expression (5.3.30) becomes

$$\int_{x_i}^{x_{i+1}} |g^{iv}(x)|^{1/4} dx = \frac{1}{N} \int_0^1 |g^{iv}(x)|^{1/4} dx . \qquad (5.3.31)$$

$$(i=0,1,\ldots,(N-1))$$

5.4 A Transformation Method

As shown by Kàlnay de Rivas (1972) and Blottner (1975) the determination of suitable mesh points for the finite difference solution of boundary layer problems is available using co-ordinate transformations. Their idea is to make a change of independent variable, mapping the domain into a new co-ordinate system where the variations of the solution are less rapid. Assuming that the transformation is defined by

$$x = X(\xi) \tag{5.4.1}$$

where x is the old independent variable and ξ the new one, then to resolve the boundary layers, a transformation is required which stretches the independent variable in areas of rapid change and compresses it elsewhere (see Figure 5). This technique has been applied to several practical problems by Jones and Thompson (1980) who also suggest several possible types of transformation. For example, to resolve a boundary layer near x=0, the transformation

$$x(\xi) = \xi^2 \tag{5.4.2}$$

is suggested and alternatively for boundary layers at both x=0, and x=1, the transformation

$$X(\xi) = \sin^2(\pi\xi/2) \tag{5.4.3}$$

is appropriate.

In all the above references, the authors choose the mesh points ξ_i to be equally spaced and generate the non-uniform grid points x_i from the transformation (5.4.1). They then obtain the required solutions by using simple equally spaced finite difference approximations on the transformed differential equation. In the present work, once the unequally spaced knot partition has been obtained using (5.4.1), the solutions are obtained using the schemes of chapter 4. This avoids any analytical differentiation of the transformation function $X(\xi)$.

As in the two previous sections the choice of a suitable transformation (5.4.1) here depends on the shape of the initial condition of the partial differential equation. Suppose, for example, that the initial condition $g(x)$ is a continuous function having one peak (for example, as in figure 1) at some point $x=\alpha$. The required transformation should be chosen so as to 'bunch' the knots around $x=\alpha$ which can be achieved by choosing $x=\xi^{\frac{1}{2}}$ to the left of the peak and $x=\xi^2$ to the right of the peak as illustrated in figure 6.

Considering the area to the right of $x=\alpha$, we require

$$x = A(\xi-\alpha)^2 + \alpha \qquad (5.4.4)$$

to be satisfied for some constant A. Since we also require $x=1$ when $\xi=1$, then

$$A = \frac{1}{1-\alpha} \qquad (5.4.5)$$

and thus to the right of the peak the knots are chosen according to the relationship

$$x = \frac{1}{1-\alpha}(\xi-\alpha)^2 + \alpha \ . \qquad (5.4.6)$$

Similarly, it can be shown that to the left of the peak the knots should be chosen from the expression

$$x = (\alpha\xi)^{\frac{1}{2}} \qquad (5.4.7)$$

Additionally, a knot is positioned at the peak $x=\alpha$.

Assuming, for example, that the initial condition has a peak at $x=0.8$, then the relationships (5.4.6) and (5.4.7) give the following knots for $\xi = 0(0.1)1$:

ξ	0	0.1	0.2	0.3	0.4	0.5	0.6	0.7	0.8	0.9	1
x	0	.28	.40	.49	.57	.63	.69	.75	.80	.85	1

Alternatively, assuming that the peak is at $x=0.5$ then the following knots are generated:

ξ	0	0.1	0.2	0.3	0.4	0.5	0.6	0.7	0.8	0.9	1
x	0	.2236	.3162	.3873	.4472	.5	.5250	.58	.68	.82	1

As a further illustration of this technique suppose that the initial condition of the partial differential equation has a peak at $x=\alpha$ and a trough at $x=\beta$. For such a condition, using functions of the type (5.4.4) and (5.4.7), (5.4.1) may be represented as

$$x = (\alpha\xi)^{\frac{1}{2}} \qquad x < \alpha \tag{5.4.8}$$

$$x = \frac{2}{\beta-\alpha}(\xi-\alpha)^2 + \alpha \qquad \alpha < x < \frac{\alpha+\beta}{2} \tag{5.4.9}$$

$$x = \left(\frac{\beta-\alpha}{2}\right)^{\frac{1}{2}}\left[\xi - \left(\frac{\alpha+\beta}{2}\right)\right]^{\frac{1}{2}} + \frac{\alpha+\beta}{2} \qquad \frac{\alpha+\beta}{2} < x < \beta \tag{5.4.10}$$

$$x = \frac{1}{1-\beta}(\xi-\beta)^2 + \beta \qquad x > \beta \tag{5.4.11}$$

with knots additionally positioned at both $x=\alpha$ and $x=\beta$.

However, suppose for example that the initial condition has the form

$$u(x,0) = \sin\pi x \qquad 0 \leq x \leq 1. \tag{5.4.12}$$

Here one would expect the 'best' knots to be symmetrical about the peak $x=0.5$. The actual knots generated by the transformation (5.4.6) and (5.4.7) as given earlier, illustrate a drawback in this method. The major difficulty lies in generalising about the choice of the transformation function (5.4.1), while trying to take on board initial condition variations which cannot be explicitly bought into play.

Further discussion on the implementation of all three techniques described in this chapter is given in the following chapter on case studies.

CHAPTER 6

Case Studies 1

6.1 Case Study Philosophy

In this first chapter of case studies we assess the effectiveness of the knot placement techniques derived in the previous chapter. For various partial differential equations, knot partitions are obtained from the methods of sections 5.2 to 5.4; these are then employed to obtain solutions using the schemes of chapter 4. The efficiency of using non-uniform knot placings is assessed by making comparisons with solutions produced for uniform knot partitions, having a corresponding number of knots.

In obtaining results for the case studies of this chapter the knots are chosen subject to the initial condition g(x) and are then fixed throughout time. This has the disadvantage that if the solution to the partial differential equation changes significantly in shape from that of the initial condition as time progresses, the knots will no longer be in optimal positions.

6.2 Case Study 1.1

As an illustration of the application of spline techniques in the numerical solution of hyperbolic partial differential equations we first consider the simple wave equation (3.1.1) with a=1, b=c=0

$$\frac{\partial^2 u}{\partial t^2} = \frac{\partial^2 u}{\partial x^2} \qquad (0 \leq x \leq 1,\ t > 0) \tag{6.2.1}$$

with the boundary conditions

$$u(0,t) = u(1,t) = 0 \tag{6.2.2}$$

and the initial conditions

$$u(x,0) = \sin\pi x \tag{6.2.3}$$

$$\frac{\partial u}{\partial t}(x,0) = 0 \ . \tag{6.2.4}$$

To draw comparisons between the accuracy of the results produced using non-uniform knot partitions and constant knot spacings we require an equal number of knots in each case. For the constant knot spacing case we use h=0.1, which gives 9 internal knots in the range $[0,1]$.

Employing the initial condition (6.2.3) the recursive process (5.2.19) of the local method becomes

$$x_i = x_{i-1} + \left[\frac{384\ \varepsilon}{\pi^4 \sin\pi x_{i-1}} \right]^{1/4} \qquad (i=1,2,\ldots,10) \tag{6.2.5}$$

where ε is chosen to give 9 internal knots. An obvious problem in implementing (6.2.5) arises since the denominator is zero when x=0. This is easily overcome by fixing a knot at the peak x=0.5 and determining the knots from that point. Using the symmetry of (6.2.3) the internal knot positions produced are as shown in Table 1.

To determine suitable knots using the global method of section 5.3 the initial condition (6.2.3) is again employed, the integral expression (5.3.31) thus becoming

$$\pi \int_{x_i}^{x_{i+1}} (\sin\pi x)^{1/4} dx = \frac{\pi}{10} \int_{0}^{1} (\sin\pi x)^{1/4} dx \,. \qquad (6.2.6)$$

$$(i=0,1,\ldots,9)$$

The right hand side of (6.2.6) is initially evaluated using an IBM numerical integration routine employing the trapezoidal rule. The knots are then chosen so that the value of the integral between each pair of successive knots is arbitrarily close to one-tenth of the value of the integral between 0 and 1. This has been achieved using an interval halving technique which generates the knot positions which satisfy (6.2.6) to any desired accuracy, in this case taken to be 0.5×10^{-5}. The knots produced in this manner are again given in Table 1.

Further discussion on the application of both the local and global methods to this particular case study is given in Raggett and Wisher (1979a and 1979b).

The initial condition (6.2.3) obviously only has one peak in $x \varepsilon [0,1]$, this being at $x=0.5$. The expressions (5.4.6) and (5.4.7) thus become, respectively

$$x_i = 2 (\xi_i - 0.5)^2 + 0.5 \qquad x > 0.5 \qquad (6.2.7)$$

and

$$x_i = (0.5\xi_i)^{1/2} \qquad x < 0.5 \qquad (6.2.8)$$

$$(i=0,1,\ldots,10)$$

The knot positions thus produced by the transformation method are also given in Table 1.

Equation (6.2.1) is now solved using the scheme (4.2.8) and the accuracy of the results produced using the three knot partitions shown in Table 1 are compared with results obtained using constant knot spacings. The accuracy is examined by evaluating the maximum absolute value of the error between the numerical solutions and the analytic solution, evaluated at each knot point, out to a chosen point in time. The analytic solution to the wave equation (6.2.1) with the prescribed boundary and initial conditions (6.2.2) and (6.2.3) is derived in Appendix 1 and is found to be

$$u(x,t) = \text{Sin}\pi x \cos\pi t. \qquad (6.2.9)$$

Numerical solutions to (6.2.1) have been evaluated for a range of values of the parameter θ. Table 2(a) gives such results using a time step length of k=0.05, the errors being examined for 10 time steps out to t=0.5. Similarly, Table 3(a) shows maximum errors using k=0.01, in this case evaluated to t=0.1.

In certain more difficult problems the analytic solution may not be available and the accuracy of results obtained may be examined by evaluating the numerical value of the truncation error at each knot. This has been done for this particular

case study and the maximum absolute values of the trauncation error to fourth order derivative terms using k=0.05 are given for the various knot partitions in Table 4. Results here are again for a range of θ values examined for 10 time steps. As can be seen from Table 4 these results suggest that the use of the local and global knot partitions may prove advantageous to using constant knot spacing. The truncation errors for the transformation knots are also seen to be significantly larger than those of the other knot partitions. This is because the order of truncation error depends on k, h_i, h_{i+1} and from Table 1 it can be seen that the distance between successive knots is relatively large near x=0 and x=1. It should also be emphasised that due to the changing nature of the derivative terms in the truncation error this method of examining accuracy is unreliable and is not employed in future case studies.

As suggested in section 3.1, the truncation error (4.2.15) can be considerably simplified by choosing θ so that (3.1.20) is satisfied. In this case, θ is thus chosen to be 1/12. Extending this idea, it was earlier shown that for simple problems involving only uniform knot partitions the parameter θ can be chosen to eliminate the leading term of the truncation error. This technique was examined in detail by Crandell (1955) when using finite difference schemes for solving the heat conduction equation. Further, Wisher (1977) suggested that for schemes in which the knot partition is non-uniform, the

leading term of the truncation error can be eliminated by suitably choosing θ at each knot point. When solving the wave equation the truncation error (4.2.15) reduces to

$$k^2\left[k^2\left(\frac{1}{12}-\theta\right)+\frac{1}{12}\left(\frac{h_i^3+h_{i+1}^3}{h_i+h_{i+1}}\right)\right]\frac{\partial^4 u}{\partial x^4}+\ldots. \qquad (6.2.10)$$

and thus to eliminate the fourth order term the parameter θ should be chosen such that

$$\theta_i = \frac{1}{12}\left[1+\frac{h_i^3+h_{i+1}^3}{k^2(h_i+h_{i+1})}\right]. \qquad (6.2.11)$$

Results using $\theta = 1/12$ and θ according to (6.2.11) are also given in Tables 2(b) and 3(b).

In analysing the results given in Table 2(a) it is difficult to draw any firm conclusions for this particular case study. As can be seen, for $\theta \lesssim \frac{1}{3}$ the knot partitions produced using both the local and global methods result in smaller errors than when equally spaced knots are used. For $\theta > \frac{1}{3}$ the reverse is true and the errors using constant knot spacings are smaller than those for either the local or global methods. Considering the results produced using the knots of the transformation method, only when $\theta=1$ is any improvement seen, and this is very marginal.

The knots resulting from the transformation method also give numerical support to the stability condition (4.2.18). For example, when $\theta=0$, the scheme (4.2.8) is stable provided

$$k^2 \leq \frac{\min\{h_i h_{i+1}\}}{3} \quad . \tag{6.2.12}$$

For the transformation knots given in Table 1, $\min\{h_i h_{i+1}\} = 0.001056$ and thus for stability we require

$$k^2 \leq 0.000352. \tag{6.2.13}$$

Using $k=0.05$ this condition is violated and thus, as can be seen from Table 2(a), the results are unstable. If $k=0.01$, as in Table 3(a), then (6.2.13) is satisfied and stability is achieved.

As might be expected, the most accurate results for all choices of knots are produced when θ is chosen to remove the leading term of the truncation error. In fact, if θ is chosen subject to (6.2.11), the results produced using a uniform knot partition are superior to any of those using variable knot spacings. However, the results of Table 3(a), giving maximum errors only as far as $t=0.1$ using $k=0.01$, show that the local and global knot partitions give more accurate solutions than when using equally spaced knots. These results are consistent with the introductory remarks of this chapter.

6.3 Case Study 1.2

Here we again consider the simple one-dimensional wave equation (6.2.1) with boundary conditions (6.2.2) but choose the initial conditions to be

$$u(x,0) = x^4(1 - x) \tag{6.3.1}$$

and

$$\frac{\partial u}{\partial t}(x,0) = 0. \tag{6.3.2}$$

As shown in Figure 7, (6.3.1) is non-symmetrical in $x\varepsilon\,[0,1]$ and is in fact a particular case of the Beta probability distribution

$$f(x) = x^{\alpha-1}(1 - x^{\beta-1}) \qquad \alpha,\beta > 0 \quad . \tag{6.3.3}$$

The initial condition (6.3.1) is again employed to determine non-uniform knot partitions using both the local and global techniques of chapter 5. The recursive relationship (5.2.19) of the local method and the integral expression (5.3.31) from the global method respectively become

$$x_i = x_{i-1} + \left[\frac{384\varepsilon}{|24 - 120x_{i-1}|}\right]^{1/4} \qquad (i=1,2,\ldots,10) \tag{6.3.4}$$

and

$$\int_{x_i}^{x_{i+1}} |24 - 120x|^{1/4}\, dx = \frac{1}{10}\int_{0}^{1} |24 - 120x|^{1/4}\, dx \quad . \tag{6.3.5}$$

$$(i=0,1,\ldots,9)$$

The knots produced by evaluating each of the expressions (6.3.4) and (6.3.5) are given in Table 5. These knot partitions and uniformly spaced knots with h=0.1 are now used in (4.2.8) producing solutions for this case study. Comparisons in accuracy are again made by evaluating the maximum absolute value of the error between the numerical solutions and the following Fourier series analytic solution (derived in Appendix 2)

$$u(x,t) = \sum_{n=1}^{\infty} 2\left[\frac{24}{(n\pi)^5} - \left(\frac{-8}{(n\pi)^3} + \frac{96}{(n\pi)^5}\right)\cos n\pi\right] \mathrm{Sin} n\pi x \cos n\pi t. \qquad (6.3.6)$$

Results given in Table 6(a) show these maximum errors for k=0.05 using a range of θ values. The errors have again been examined for 10 time steps out to t=0.5. The results show that when θ=0 and θ=1/4 the errors produced using the local and global knots are smaller than those using equally spaced knots, the results of the global method being superior. However, for the remaining θ values used constant knot spacing proves more accurate. The results of Table 6(a) are therefore again inconclusive. Overall, as can be seen in Table 6(b), the errors of smallest magnitude occur when θ is chosen to remove the leading term of the truncation error when the knots of the local method are used.

These rather inconclusive results can best be explained by graphing the analytic solution (6.3.6) for various time levels. As can be seen in Figure 7 the peak of the solution moves in the x direction as time progresses and by t=0.5 the shape of the wave is completely different from its original initial condition (6.3.1). The local and global knot partitions are thus no longer optimally placed. We would, however, expect the local and global knots to give improved accuracy close to the initial line t=0 since for small t the shape of the solution is very close to that of the initial condition. As can be seen in Table 7 this is in fact found to be the case. Further numerical evidence of this is given in Table 8 where the maximum errors are listed using k=0.01 for 10 time steps. These results show that for all the θ values used the solutions produced using the local and global knot partitions always have smaller errors than when uniformly spaced knots are employed. However, the above reasoning is contradicted by the results shown in Table 9 where maximum errors are again given using k=0.01. In this case the errors are examined for 50 time steps out to t=0.5 and as can be seen, the local and global knots still prove more accurate. While this result is somewhat surprising, it is also gratifying that the proposed new methods seem to be an improvement on constant knot spacing when the time steps are chosen relatively small.

6.4 Case Study 1.3

As a final illustration of the use of spline techniques for solving hyperbolic partial differential equations we assume that the coefficients a and b in (3.1.1) have the values unity and zero respectively, and thus the equation under consideration is

$$\frac{\partial^2 u}{\partial t^2} = \frac{\partial^2 u}{\partial x^2} + cu \quad . \ (0 \leq x \leq 1, \ t > 0) \tag{6.4.1}$$

Equation (6.4.1) is assumed to be subject to the boundary conditions (6.2.2) and the initial conditions (6.2.3) and (6.2.4). The analytic solution to (6.4.1) is as derived in Appendix 3 and is given by

$$u(x,t) = \text{Sin}\pi x \cos(\pi^2 - c)^{1/2} t. \tag{6.4.2}$$

To examine the effect of the lower order term cu, various values of the coefficient c are used, although in each case c is chosen to be negative to avoid any occurrence of negative square roots in (6.4.2).

As in previous case studies, numerical solutions are obtained using constant knot spacing with h=0.1 and also using the knot partitions resulting from the local and global methods

of chapter 5. Since the initial condition used here is the same as that employed in case study 1.1, the knots resulting from the local and global methods are again as given in Table 1. As previously, accuracy is examined by evaluating the maximum absolute error between the numerical solutions and the analytic solution (6.4.2) at the knots out to a certain point in time. Results given in Tables 10 and 11 show maximum errors for a range of values of c using k=0.05 and k=0.01 respectively. In each case results are examined out to t=0.5 and the parameter θ is chosen as $\frac{1}{3}$. The errors given in Table 10 show that only when c=-1 do the variable knot spacings prove superior to constant knot spacing. In Table 11, increased accuracy is observed when the local and global knot partitions are used for both c=-1 and c=-10.

As can be seen in both Tables 10 and 11, for large negative values of c, the errors resulting from the use of all knot partitions are large in magnitude and no improvement is gained by employing non-uniform knot spacings. It should however be noted that since the coefficient c in (6.4.1) is effectively multiplied by k^2 then, particularly for large negative values of c, as k is decreased in size the accuracy of the results obtained increases.

The equation (6.4.1) is also useful for assessing the effect of lower order terms on the stability of the scheme (4.2.8). Various authors (see for example Fox (1962), Richtmyer and Morton (1967) and Griffiths (1982)) have suggested that it is reasonable to assume that the presence of the lower order terms, $b\frac{\partial u}{\partial x}$ and cu, have no great effect on the stability condition of a particular finite difference scheme. In section 4.2 it is shown that the stability of the scheme (4.2.8) is unaffected by the presence of a cu term in (3.1.1) and that the scheme (4.2.8) is unconditionally stable when $\theta \geq \frac{1}{4}$. This is confirmed by the results of Tables 10 and 11. Further, when $\theta < \frac{1}{4}$, the scheme (4.2.8) is stable provided that the condition (4.2.18) is satisfied. For this case study, when equally spaced knots are employed for example, the condition (4.2.18) reduces to $\theta \geq -\frac{1}{12}$ when k=0.05. The results shown in Table 12 are produced when the parameter θ is chosen to be zero and, as can be seen, stability is still achieved.

6.5 Case Study 1.4

In this case study we illustrate the application of the spline scheme derived in section 4.3 for obtaining numerical solutions to parabolic partial differential equations. We consider the simple one-dimensional heat conduction equation ((3.3.1) with a=1, b=c=0)

$$\frac{\partial u}{\partial t} = \frac{\partial^2 u}{\partial x^2} \qquad (0 \leq x \leq 1, \quad t > 0) \qquad (6.5.1)$$

together with the initial condition

$$u(x,0) = \sin\pi x \qquad (6.5.2)$$

and the boundary conditions

$$u(0,t) = u(1,t) = 0 \ . \qquad (6.5.3)$$

As in previous case studies, solutions are obtained using 9 internal knots and thus in the equally spaced knot case, h=0.1 is used. Since the initial conditions (6.5.2) and (6.2.3) are the same, the knots of the local and global methods are again given by (6.2.5) and (6.2.6) respectively. These knot positions are given in Table 1. Numerical solutions to (6.5.1) subject to (6.5.2) and (6.5.3) have been obtained employing the knots of Table 1, solutions being derived using the spline scheme (4.3.1). As shown in Appendix 4, the analytic solution for this case study is given by

$$u(x,t) = e^{-\pi^2 t} \sin\pi x \ . \qquad (6.5.4)$$

The results given in Table 13(a) are the maximum absolute values of the errors between the numerical solutions and the analytic solution (6.5.4) using a time step length of k=0.05, results being examined for 10 time steps. As can be seen the errors produced using all three knot partitions are very similar in magnitude. The only case when the use of variable

knot spacings gives improved accuracy over constantly spaced knots is when the parameter θ is chosen to be 1/2. It should be noted, however, that this value of θ is the most suitable choice when no additional information is available since it gives equal weighting to both time levels. The results of Table 14(a), where maximum errors for 50 time steps (using k=0.01) are given, confirm this. Results produced using θ=1/4 are included to provide numerical evidence to the stability condition (4.3.4). For example, using the local knots (4.3.4) is satisfied provided $\theta \geq 0.486$ when k=0.05 is used and provided $\theta \geq 0.430$ in the case of k=0.01.

As suggested in section 6.2, in certain instances the leading term of the truncation error may be eliminated by suitable choice of the parameter θ. For this particular case study the truncation error is given by (4.3.3) and thus by choosing θ such that

$$\theta_i = \frac{1}{2} + \frac{1}{12k}\left(\frac{h_i^3 + h_{i+1}^3}{h_i + h_{i+1}}\right) \qquad (6.5.5)$$

the fourth order derivative term is reduced to zero. Results obtained using (6.5.5) are given in Tables 13(b) and 14(b). In both cases the errors resulting from the use of the local

and global knot partitions are smaller than those when equally spaced knots are employed. In addition, as might be expected, choosing θ from (6.5.5) results in the most accurate solutions obtained.

6.6 Case Study 1.5

As a final illustration of the suitability of the local and global methods we again consider the heat conduction equation (6.5.1). In this case study we assume (6.5.1) has the initial condition

$$u(x,0) = e^{-ax} \tag{6.6.1}$$

and the boundary conditions

$$u(0,t) = 1 \tag{6.6.2}$$

and $$u(1,t) = e^{-a} \tag{6.6.3}$$

where a is a constant > 0. Since we again choose to have 9 internal knot points in $x\varepsilon[0,1]$ the knots of the local method are given by the recursive process

$$x_i = x_{i-1} + \left[\frac{384\varepsilon}{a^4 e^{-ax_i}}\right]^{1/4} \quad (i=1,2,\ldots,10) \tag{6.6.4}$$

Similarly, applying the global method of section 5.3 the knot partition results from the following expression

$$\int_{x_i}^{x_{i+1}} \left(a^4 e^{-ax}\right)^{1/4} dx = \frac{1}{10} \int_{o}^{1} \left(a^4 e^{-ax}\right)^{1/4} dx. \qquad (6.6.5)$$

$$(i=0,1,....,9)$$

In carrying out numerical computations we have chosen the constant a to take the values 1 and 10. The shapes of the initial condition (6.6.1) using these values of a are shown in Figure 8. The knot partitions resulting from the expressions (6.6.4) and (6.6.5) using a=1 and a=10 are given in Tables 15 and 16 respectively.

As in the previous case studies we assess the usefulness of the local and global methods by comparing the results produced using these knots with results obtained using equally spaced knots. For this particular case study the analytic solution, which is derived in Appendix 5, is given by

$$u(x,t) = \left[1 + (e^{-a} - 1)x\right] + \sum_{n=o}^{\infty} \frac{2}{n\pi} (e^{-a}\cos n\pi - 1)\left(\frac{a^2}{(n\pi)^2 + a^2}\right)\sin n\pi x e^{-n^2\pi^2 t} \qquad (6.6.6)$$

This analytic solution is evaluated at each knot point and the accuracy is again examined by calculating the maximum absolute error between the numerical solution and the analytic solution (6.6.6) for a chosen number of time levels.

For the case when the constant a is chosen to be unity Tables 17(a) and 18(a) show the maximum errors using k=0.05 and k=0.01 respectively. Similarly, when a=10 the maximum errors obtained are given in Tables 19(a) (for k=0.05) and 20(a) (for k=0.01). In all computations the errors have been examined out to t=0.5.

Analysing the results for a=1 first, we see that, as in the previous case study, only when $\theta = \frac{1}{2}$ do the non-uniform knot partitions result in smaller errors than when uniformly spaced knots are used. This is the case for both k=0.05 and k=0.01. Again the choice of $\theta = \frac{1}{2}$, which gives equal weighting to each of the time levels, is a logical choice without prior knowledge which may result in increased accuracy. It should however be noted that the errors resulting from each of the knot partitions are very similar in magnitude for individual θ values.

As in case study 1.4, θ may be chosen to remove the leading term of the truncation error (4.3.3). Again this is done by choosing the parameter θ from the relationship (6.5.5). As is shown in Tables 17(b) and 18(b), this choice of θ results in the most accurate solutions obtained for each of the knot

partitions for both k=0.05 and k=0.01. However, using this value of θ the local and global knots only result in smaller maximum errors when the time step length k=0.05. When k=0.01 constant knot spacing is more accurate.

Considering now the case when a=10, the maximum errors resulting from uniformly spaced knots are always smaller in magnitude than those when variable knot spacings are employed if k=0.01. When a time step length of k=0.05 is used, $\theta = \frac{1}{2}$ is again the only case where the local and global methods give any improvement. This includes choosing the parameter θ such that the leading term of the truncation error is removed.

It is worthwhile to here consider in more detail the results obtained when the constant a in (6.6.1) is equal to ten. For this value of a the analytic solution (6.6.6) has the form shown in Figure 9 for various time levels. As can be seen, the shape of the analytic solution becomes less 'severe' as time progresses and by t=0.5 the solution is approximately linear. The knots produced using the local and global methods will therefore not be optimally placed for large t. As in case study 1.2, it might be expected that the local and global knot partitions give improved accuracy close to the initial line t=0. We have however found that close to t=0 the numerical

solutions oscillate either side of the analytic solution for successive time lines and that the maximum errors quoted in Tables 19 and 20 always occur on the second time line; improvement is therefore not observed in this case.

CHAPTER 7

Varying the Knots on Each Time Line

7.1 Preamble

In the case studies of Chapter 6 numerical solutions are obtained using knot partitions which are derived subject to the initial condition g(x) of the partial differential equation. These knots are then fixed throughout time. As was seen in case studies 1.2 and 1.5, when the shape of the solution to the partial differential equation changes significantly as time progresses then the knots will no longer be optimally placed. It would therefore be desirable to have an algorithm in which optimal knot partitions are derived on each time line. Obviously, if the position of the mesh points in any finite difference scheme change on each time line, then that scheme becomes much more complex (see for example, Murray and Landis (1959), where such a scheme was used in the solution of moving boundary problems in heat flow). Fortunately, in using spline functions, an interpolating polynomial is available which can be used to obtain solutions at points intermediate to the existing knot points.

The technique used in the following section to determine a new partition of optimal knots on each new time line, is based on the previously described global method and is an extension of the work of Dobson (1972) who used spline techniques in approximation problems. As was shown in section 5.3, the optimal knot partition of the global method results from the integral expression (5.3.30). This expression requires knowledge of the fourth derivative of the function f(x) with respect to x. In the case studies of Chapter 6, f(x) was taken to be the given initial condition. If the global method is used as a basis for generating new knots on each new time line then f(x) will be unknown as time progresses. This problem can be overcome by making use of the spline function S(x) as given by (4.2.1). It would therefore seem reasonable to approximate $f^{iv}(x)$ in (5.3.30) by $S^{iv}(x)$. However, since in this work we use cubic splines, then only the first and second derivatives are continuous and $S^{iv}(x) = 0$ in each knot interval. This problem is overcome using the following algorithm.

7.2 Procedure for Determining Optimal Knot Partition

Assume that a partition of knots π_j (as defined in (3.1.4)) and the corresponding numerical solutions $u_{i,j}$ at these knots are known on the j^{th} time line. On the initial line, the knots π_o can either be taken as equally spaced or obtained using one of the methods of Chapter 5.

(i) Determine the mid-points of the knots of π_j,

$$x_{i-\frac{1}{2}} = \frac{x_{i-1} + x_i}{2} \qquad (i=1,2,\ldots,N) \qquad (7.2.1)$$

(ii) Evaluate the third derivative of the spline function at the mid-points from the relationship

$$S_j'''(x_{i-\frac{1}{2}}) = \frac{1}{h_i}(M_{i,j} - M_{i-1,j}) \qquad (7.2.2)$$

$$(i=1,2,\ldots,N)$$

the $M_{i,j}(i=0,1,\ldots,N)$ first being determined from (4.2.2) with $M_{o,j} = M_{N,j} = 0$.

(iii) Obtain an approximation to $S_j^{iv}(x)$ at the knots x_i,

$$S_j^{iv}(x_i) = \frac{S_j'''(x_{i+\frac{1}{2}}) - S_j'''(x_{i-\frac{1}{2}})}{x_{i+\frac{1}{2}} - x_{i-\frac{1}{2}}} \qquad (i=1,2,\ldots,(N-1)) \qquad (7.2.3)$$

where the $S_j^{iv}(x_i)$ will be piecewise constants with discontinuities at the mid-points $x_{i-\frac{1}{2}}$.
While we realise that this is a crude approximation ($S_j^{iv}(x)$ is not well-defined at the knots), this procedure has been used with success by Dobson (1972) and de Boor (1978).

(iv) Compute the values of

$$\left|S_j^{iv}(x_i)\right|^{1/4} \qquad (i=1,2,\ldots,(N-1)). \qquad (7.2.4)$$

These will have the form illustrated in Figure 10, the functions $\left|S_j^{iv}(x_1)\right|^{1/4}$ and $\left|S_j^{iv}(x_{N-1})\right|^{1/4}$ being extended to include all the range [0,1].

(v) Using the expression (5.3.30) the new knots $x_i'(i=0,1,\ldots,N)$ on the j^{th} time line should thus be chosen such that

$$\int_{x_i}^{x_{i+1}'} \left|S_j^{iv}(x)\right|^{1/4} dx = \frac{1}{N} \int_0^1 \left|S_j^{iv}(x)\right|^{1/4} dx. \qquad (7.2.5)$$

$$(i=0,1,\ldots,(N-1))$$

The right-hand-side of the integral expression (7.2.5) is evaluated by summing the areas of the rectangles shown in Figure 10.

The relationship (7.2.5) thus becomes

$$\int_{x_i}^{x_{i+1}'} \left|S_j^{iv}(x)\right|^{1/4} dx = A_S \qquad (7.2.6)$$

where the constant A_S is given by

$$A_S = \frac{1}{N}\left\{ \left|S_j^{iv}(x_1)\right|^{1/4} . x_{\frac{1}{2}} + \sum_{i=1}^{N-1} \left|S_j^{iv}(x_i)\right|^{1/4} (x_{i+\frac{1}{2}} - x_{i-\frac{1}{2}}) + \left|S_j^{iv}(x_{N-1})\right|^{1/4} (1 - x_{N-\frac{1}{2}}) \right\}. \qquad (7.2.7)$$

The knots are thus determined using the following procedure. Assume that a knot x_i' has been determined, as illustrated in Figure 11. The knot x_{i+1}' is found as follows:

(a) Evaluate

$$A_n = \left|S_j^{iv}(x_M)\right|^{1/4} (x_{M+\frac{1}{2}} - x_i')$$

and let $A_L = 0$.

(b) If $A_n > A_S$, then

$$x_{i+1}' = x_i' + \frac{A_S - A_L}{\left|S_j^{iv}(x_M)\right|^{1/4}}$$

(c) If $A_n = A_S$, then

$$x_{i+1}' = x_{M+\frac{1}{2}}.$$

(d) If $A_n < A_S$, then let

$$x_i' = x_{M+\frac{1}{2}},$$

$$A_L = A_n$$

and $M = M+1$.

Evaluate

$$A_n = A_n + \left|S_j^{iv}(x_M)\right|^{1/4} (x_{M+\frac{1}{2}} - x_{M-\frac{1}{2}})$$

and return to (b).

As previously mentioned, this technique has been used by Dobson (1972), in approximating a function f by splines of various order. In that work, the author performed several iterations of the algorithm and examined the errors produced using the knots of each iteration. It was found that only one or two iterations were usually required, after which no improvement in accuracy was gained. As shown in the following section, we here perform only one iteration of the knot placement algorithm per time line, since with several iterations the process becomes computationally expensive. However, in the following chapter on case studies, it is noticed that certain conditions on the size of the time step length, and hence on the relative position of the knot partitions, should be observed.

7.3 Implementation of the Splines Schemes

With knots varying on each time line, numerical solutions to a given partial differential equation are again to be derived using the splines schemes (4.2.8) for hyperbolic equations and (4.3.1) for parabolic equations. In the case of hyperbolic partial differential equations the implementation of (4.2.8) is accomplished as follows:

Assume that the scheme is fully developed in that solutions $u_{i,j}(j \geq 1)$ are known on the time lines t=o to t=jk. Using the algorithm described in section 7.2, a new partition of knots π_j is obtained. Solutions $u_{i,j-1}$ and $u_{i,j-2}$ at these spatial knots are found using the spline function (4.2.1), these being used in (4.2.8) to determine new solutions $u_{i,j}$. The scheme (4.2.8) is employed again to find solutions $u_{i,j+1}$, the process then being repeated. As previously stated, on the initial line the knots π_o are chosen to be equally spaced or derived using one of the methods of Chapter 5. Employing the derivative initial condition of (3.1.3), solutions $u_{i,1}$ are found from (4.2.8). A new partition of knots π_1 is then obtained from the algorithm of section 7.2. Solutions $u_{i,o}$ at these knots are found from the initial condition (3.1.3), these being used in (4.2.8) to determine new solutions $u_{i,1}$. The scheme (4.2.8) is employed again to determine $u_{i,2}$, the process then being fully developed.

In the case of parabolic partial differential equations the procedure is as above but is simplified since the scheme (4.3.1) is only two time level. Having found a new partition of knots π_j, the spline function (4.2.1) is required only once, this being to obtain solutions $u_{i,j-1}$ at these knots on the previous time line.

CHAPTER 8

Case Studies 2

8.1 Case Study Philosophy

Here we again consider each of the case studies of Chapter 6 and derive solutions by choosing optimal knot partitions on each time line using the technique described in the previous chapter. The application of the technique to both hyperbolic and parabolic partial differential equations is therefore considered. Results obtained by varying the knots on each time line are compared with both those resulting from constantly spaced knots and the knots of the local and global methods. In the tables referred to in the following case studies, the results obtained in Chapter 6 are therefore listed again to enable comparisons to be made.

It should be noted that in sections 6.3 and 6.6 it was suggested that, due to the changing nature of the solution of the respective partial differential equations', improvement might be expected from a scheme in which optimal knots are chosen on each new time line.

8.2 Case Study 2.1

The simple one-dimensional wave equation (6.2.1) subject to (6.2.2), (6.2.3) and (6.2.4) is reconsidered here. Using the algorithm described in section 7.2, optimal knot partitions are derived on each time line and solutions obtained employing the procedure of section 7.3. To enable comparisons to be made with the results of case study 1.1, 9 internal knots are chosen on each time line and solutions are obtained for a range of values of the parameter θ. Accuracy is again examined by evaluating the maximum absolute difference between the numerical solutions and the analytic solution (6.2.9) at the knots, out to a chosen point in time.

The errors given in Table 21 are those obtained using a time step length of k=0.05, results being examined out to t=0.5. As can be seen, for $\theta \leq \frac{1}{3}$ results produced by varying the knots on each time line are an improvement on results obtained using equally spaced knots. However, the errors of smallest magnitude are observed when the knots of the earlier described global method are employed. When $\theta > \frac{1}{3}$, using equally spaced knots gives greatest accuracy.

The results of Table 21 suggest that for this particular case study no improvement in accuracy is to be gained by varying the knots on each time line. This might be expected since, as can be seen from (6.2.9), the solution has the form of a symmetrical wave. Figure 12 shows the partitions of knots derived using the algorithm of section 7.2 for certain time lines when the parameter θ is chosen to be $\frac{1}{3}$. As can be seen, little variation in the knot partitions is observed as time progresses and thus, due to the additional computation required, no increase in accuracy is obtained by varying the knots on each time line.

8.3 Case Study 2.2

Here we again consider case study 1.2 and derive solutions to the hyperbolic partial differential equation (6.2.1) with boundary conditions (6.2.2) and initial conditions (6.3.1) and (6.3.2).

Using the technique described in Chapter 7 solutions are obtained, the algorithm being employed to produce 9 internal knots on each time line. The results given in Table 22 are the maximum absolute errors between the numerical solutions and the analytic solution (6.3.6), where results were examined out to t=0.5 using a time step length of k=0.05.

As mentioned earlier, and illustrated in Figure 7, the analytic solution (6.3.6) is such that the peak of the wave moves in the x direction as time progresses. We would therefore hope that by varying the knots on each time line some improvement in accuracy would be observed. The results given in Table 22 show that this is not the case for this particular choice of k. As can be seen, for all choices of the parameter θ the errors produced by varying the knots on each time line are always larger in magnitude than those resulting from either uniformly spaced knots or from the variable knot spacings of the local and global methods.

To further test the algorithm, solutions were derived using a time step length of k=0.01; again 9 internal knot points were used. The results shown in Table 23 are the maximum absolute errors between the numerical solutions and the analytic solution (6.3.6) using k=0.01 in which errors were examined at the knot points for 50 time steps out to t=0.5. In this case the errors produced by varying the knots on each time line are considerably smaller than those obtained earlier in case study 1.2. For all choices of the parameter θ shown, the results obtained by varying the knots on each

time line are always more accurate than those produced by using either constant knot spacing or the knots of the local and global methods. By using a small time step length we thus see that significant improvement is gained by choosing different knot partitions on each time line.

Some explanation of the above can be obtained by examining the positions of the knots resulting from the application of the knot placement algorithm for each choice of step length k. Figures 13 and 14 show the partitions of knots produced by the algorithm on certain time lines when k=0.05 and k=0.01, respectively. Comparing these partitions with the shape of the analytic solution shown in Figure 7, we see that when k=0.01 the knots marginally better match the changing nature of the analytic solution than those derived when k=0.05, particularly on the early time lines. The situation is further clarified when more than 9 internal knot points are produced on each time line. Figures 15 and 16 show the partitions of knots produced when 19 internal knots are allowed and the time step length is chosen to be k=0.05 and k=0.01, respectively. As can be seen, considerable improvement in the positioning of the knots is obtained when the smaller step length k=0.01 is used. When k=0.05, the

knots resulting from the application of the knot placement algorithm given in section 7.2 remain 'bunched' close to $x=1$ and do not match the analytic solution (6.3.6). Additionally, Figure 17 shows the knots produced by the algorithm on $t=0.5$ when the analytic solution (6.3.6) is used instead of the numerical solutions. This has been done for comparison purposes and it is interesting to note that the knots produced in this way are very similar to those in Figure 16 when $k=0.01$ was used.

We thus here conclude that improvement in accuracy is to be gained by varying the knots on each time line if a small time step length is employed.

8.4 Case Study 2.3

In this section we reconsider case study 1.3 and derive solutions to equation (6.4.1) by producing different knot partitions on each time line. To enable comparisons to be made with earlier obtained results we again choose 9 internal knots on each time line and obtain solutions for various negative values of the coefficient c.

The results given in Tables 24 and 25 are the maximum absolute errors between the numerical solutions and the analytic

solution (6.2.4) out to t=0.5 using time step lengths of k=0.05 and k=0.01, respectively. All results shown have again been obtained when the parameter θ is taken to be $\frac{1}{3}$. Examining the errors given we see that for both choices of k, no improvement in accuracy is observed by using different knot partitions on each time line. In certain instances (namely, c=-1 when k=0.05 and c=-1, c=-10 when k=0.01) the errors produced by varying the knots on each time line are smaller than those resulting from equally spaced knots. However, in each of these cases, the results derived using either the local or global knot partitions are a further improvement. If the coefficient c is chosen to be -100 or -200, the errors for k=0.05 are almost identical for each of the methods presented. When the time step length k is taken to be 0.01, Table 25 shows that, for these large values of c, constant knot spacing gives greatest accuracy.

When considering the results obtained by choosing different knot partitions on each time line it should be noted that the analytic solution (6.4.2) is symmetrical in [0,1] for all values of the coefficient c. As was seen in case study 2.1, little benefit is therefore gained by varying the knots at each stage in time.

8.5 Case Study 2.4

In this case study we now apply the technique described in Chapter 7 to parabolic partial differential equations. We again consider the one-dimensional heat conduction equation (6.5.1) subject to the initial condition (6.5.2) and the boundary conditions (6.5.3). The algorithm given in section 7.2 is again used to produce 9 internal knot points on each time line and these are employed in the scheme (4.3.1) using the technique described in section 7.3. Figure 18 shows the partitions of knots produced by the algorithm on certain time lines when the parameter θ is chosen to be $\frac{1}{2}$ and when a time step length of k=0.05 is used.

The results shown in Tables 26 and 27 are the maximum errors between the numerical solutions and the analytic solution (6.5.4) using k=0.05 and k=0.01, respectively. Results have been examined at the knot points, out to t=0.5 in each case. As can be seen, for both choices of k, the errors obtained by varying the knots on each time line are smaller than those resulting from both uniformly spaced knots and the knots of the local method when $\theta = \frac{1}{2}$. However, in each case further improvement is obtained by using the knots of the global method. For $\theta > \frac{1}{2}$, using a constant knot spacing

of h=0.1 proves most accurate for both k=0.05 and k=0.01.

For this particular parabolic partial differential equation the analytic solution (6.5.4) has a symmetrical form for all time with the solution dying out as time progresses. As shown in Figure 18 the knot partitions produced in this case study are very similar on each time line and are approximately constantly spaced. Little is therefore to be gained by varying the knots on each time line.

8.6 Case Study 2.5

Here we reconsider the parabolic partial differential equation (6.5.1) together with the initial condition (6.6.1) and the boundary conditions (6.6.2) and (6.6.3). To enable comparisons to be made with the results obtained in case study 1.5 we again let the constant a in (6.6.1) take the values 1 and 10. In each case, solutions have been derived by using the algorithm in section 7.2 to produce new knot partitions on each time line. The accuracy of the solutions obtained is examined by comparing them with the known analytic solution (6.6.6) at each knot point. The results given in Tables 28 and 29 are the maximum absolute errors between the numerical solutions and the analytic solution when the constant a is equal to 1 and time step lengths of k=0.05 and k=0.01, respectively, are used.

Similarly, the results shown in Tables 30 and 31 are the maximum errors produced using k=0.05 and k=0.01, respectively, when a is chosen to be 10. Errors in all tables have been examined out to t=0.5. In addition, Figures 19 to 22 show the partitions of knots generated by the knot placement algorithm for both a=1 and a=10 using time step lengths of k=0.05 and k=0.01. In each case, 9 internal knots are chosen on each time line and the partitions produced are those when the parameter θ is taken to be $\frac{1}{2}$.

Examining the results for a=1 first, we see from Table 28 that when $\theta = \frac{1}{2}$ and $\theta = \frac{3}{4}$ the results obtained by varying the knots on each time line are an improvement over those produced using either equally spaced knots or the knots of the local and global methods. In the case when θ is chosen to be unity, constant knot spacings prove most accurate. When k=0.01, Table 29 shows that for $\theta = \frac{1}{2}$ the errors resulting from varying the knots on each time line are smaller than those for each of the other knot partitions used. When $\theta = \frac{3}{4}$ and $\theta = 1$, using equally spaced knots again results in the smallest errors. The results of Tables 28 and 29 are encouraging since the choice of $\theta = \frac{1}{2}$ is the most suitable in that it gives equal weighting to each of the time lines in the scheme (4.3.1).

We now turn our attention to the results produced when the constant a in (6.6.1) is equal to 10. As can be seen from Table 30, when the time step length k=0.05 is employed smaller errors result by choosing different knot partitions on each time line than by using either equally spaced knots or the knots of the local and global methods when θ is set to $\frac{1}{2}$. The results for $\theta = \frac{3}{4}$ and $\theta = 1$ again show that constantly spaced knots are most accurate. In the case when k=0.01, the results of Table 31 show that the smallest errors for all choices of the parameter θ are produced by choosing the knots to be equally spaced.

The results for a=10 are surprising if one considers the distributions of knots produced by the knot placement algorithm for both k=0.05 and k=0.01. Figures 21 and 22 indicate that more reasonable paritions of knots are produced when the smaller time step k=0.01 is employed (see figure 9 for analytic solution) since the knots for k=0.05 remain 'bunched' close to x=o for all time. These partitions of knots are consistent with those produced in case study 2.2 where a small time step length again gave better partitions.

However, the results of Table 31 show that no improvement in accuracy is gained by varying the knots on each time line when k=0.01 is used. The reason for this, as indicated in case study 1.5, is because close to t=o the numerical solutions oscillate either side of the analytic solution and the maximum error always occurs on the second time line for any choice of knots used. The benefit from the more reaslistic knot partitions is therefore not realised.

CHAPTER 9

Conclusions and Extensions

9.1 Conclusions

Before drawing general conclusions about the proposed methods we here first briefly review the results obtained in the earlier case studies. This may repeat some of the comments made in chapters 6 and 8 but will enable easier comparisons.

In case studies 1.1 and 2.1 we considered the one-dimensional wave equation having a symmetric initial condition. The results obtained showed that for the smaller values of the parameter θ used, the knots of the global method gave greatest accuracy. For larger θ values, using equally spaced knots resulted in the relatively smaller errors. In certain cases, varying the knots on each time line produced greater accuracy than equally spaced knots, although in these cases the errors were still larger than those resulting from the knots of the global method. For this case study, without any additional information, the value $\theta = 1/3$, is the most logical a priori choice since it gives equal weighting to each of the time lines in the scheme (4.2.8) used. For this particular θ value the global knot partition results in

greatest accuracy. Employing the knots of the global method is therefore advantageous in this case. As mentioned earlier, due to the symmetrical initial condition, no overall improvement in accuracy is gained here by varying the knots on each of the time lines.

The one-dimensional wave equation was again considered in case studies 1.2 and 2.2. In this case the initial condition was chosen to be non-symmetrical and resulted in a wave form in which the peak of the wave moves in the x direction as time progresses. From the results obtained it was found that the knots of the local and global methods gave increased accuracy in certain cases, particularly for small time step lengths k. Since the wave form moves as time progresses it was noted that the local and global knot partitions, being based on the initial condition, would no longer be optimally placed away from the initial line. The results obtained by choosing different optimal knot partitions on each time line showed that, for a larger time step length of k=0.05, no improvement in accuracy over the use of local or global knots was observed; moreover in only one instance were the errors smaller than those of constant knot spacing. However, when a smaller time step length of k=0.01 was employed, the

technique of varying the knots on each time line produced a significant increase in accuracy. For all θ values used, the errors resulting from these knot partitions were always considerably smaller in magnitude than those of either equally spaced knots or the knots of the local and global methods.

A final example on the application of the techniques to hyperbolic partial differential equations was discussed in case studies 1.3 and 2.3. Here the constants a and b in (3.1.1) were chosen to be unity and zero respectively, whilst the coefficient c was allowed to take various negative values. The results obtained indicate that for smaller negative values of c, some improvement in accuracy over equally spaced knots is to be gained by using either the local or global knot partitions. In some instances, the errors produced by varying the knots on each time line are also smaller in magnitude than constant knot spacing, although a further reduction in the magnitude of the errors is always produced by employing the local or global knots. This is to be expected since the initial condition used in this case study is again symmetrical. For larger values of the coefficient c, the magnitude of the errors increases with little to choose between the results of the various knot partitions.

In case studies 1.4 and 2.4 we considered the one-dimensional heat conduction equation, again choosing the initial condition to be symmetrical in shape. The results derived showed that when the parameter $\theta = 1/2$, the errors produced by varying the knots on each time line are smaller in magnitude than the errors resulting from uniformly spaced knots. However, as previously, the results of either the local or global knot partitions give a further improvement in accuracy. For the remaining θ values used, constantly spaced knots proves most accurate. It should however be noted that the choice of $\theta=1/2$ gives the natural 'Crank-Nicolson like' equal weighting to each of the time lines in the scheme (4.3.1) and for this value of θ the global knots result in the most accurate solutions. Due to the symmetrical shape of the solutions little is again gained by choosing different knots on each of the time lines.

The final partial differential equation considered was that of case studies 1.5 and 2.5, in which the heat conduction equation was assumed to have an exponential initial condition with the parameter being chosen to be a=1 and a=10. For a=1, the results produced by varying the knots on each time line

are superior to those found using equally spaced knots, or the knots of the local or global methods when θ is chosen to give equal weighting to each of the time lines. A similar improvement is gained by using $\theta=3/4$ when the time step length is $k=0.05$, although for the remaining values of θ and k equally spaced knots results in the errors of smallest magnitude. These encouraging results are not observed when the parameter a equals 10. In this case, only when $\theta=1/2$ and $k=0.05$ are the results produced by varying the knots on each time line an improvement over the other methods. The remaining results show that constant knot spacing is superior. The practice of using a small time step length to gain improvement in accuracy when varying the knots on each time line (as observed in case study 2.2) is not observed here. As previously explained in section 8.6, this is because oscillations in the numerical solutions occur close to the initial line and maximum errors always occur on the second time line for each value of k used.

We now consider an overall view of the proposed methods by initially examining computing time required in the evaluation of the results. When the knots are fixed throughout time, numerical solutions are obtained from the schemes (4.2.8) or (4.3.1) depending on the problem concerned. Irrespective

of the knot partition used each of the schemes resulted in a tri-diagonal system of equations which was solved using an efficient numerical algorithm (see for example, Mitchell and Griffiths (1980)) giving the required solutions. Obtaining these solutions using either constant knot spacing, or the knots of the local and global methods therefore requires the same computer time. Using the IBM 370/135 machine installed at Sheffield City Polytechnic this computing time for hyperbolic equations was found to be 15.2 seconds. In addition, the derivation of the knot partitions using the local and global methods is a relatively simple procedure requiring 2 seconds and 3.3 seconds of computer time, respectively. When the technique of chapter 7 is employed to obtain solutions by deriving different knot partitions on each time line, then the amount of computation required obviously increases. We have found that, to obtain numerical solutions to hyperbolic equations using this procedure requires 34.4 seconds of computer time. For parabolic partial differential equations slightly less computing time is required for each of the methods since the scheme (4.3.1) employed is only two time level. The times required are however comparable, with the technique in which knots are chosen on each time line taking approximately twice as

long as the methods in which the knots are fixed throughout time.

In general, the results of the case studies suggest that when the solution of the partial differential equation is of symmetrical form for all time, then nothing is gained by varying the knots on each time line. However, in these cases the results show that improvement in accuracy over equally spaced knots is generally achieved by using either the local or global knot partitions and choosing the parameter θ to give equal weighting to each of the time lines. In addition, when the solution of the partial differential equation exhibits the form of a wave whose peak moves in the x direction as time progresses, then considerable benefit appears to be gained by varying the knots on each time line provided the step length k is chosen to be small. The algorithm for positioning the knots on each time line is automatic and does not require knowledge about the shape of the solution a priori. This technique may therefore be useful in obtaining solutions to other numerical problems. Two possible extensions are given in the following section.

9.2 Possible Extensions

(i) Parabolic partial differential equations of the form

$$\frac{\partial u}{\partial t} = D \frac{\partial^2 u}{\partial x^2} + v \frac{\partial u}{\partial x} \quad , \tag{9.2.1}$$

where D>0 and v are constants, are called "diffusion-convection" equations because of the physical processes they describe. Typically, u might be the concentration of a material which is convected with velocity v and diffusing according to the diffusion coefficient D. Particular interest has been focussed on problems in which the cell Peclet number P is given by

$$P = \frac{vh}{2D} \tag{9.2.2}$$

is large. In such situations spurious oscillations are introduced into finite difference solutions (see for example, Price, Cavendish and Varga (1968)) when the analytic solution is known to be non-oscillatory. Various methods have been proposed to overcome this problem, the most well-known being the technique of "upwinding" which has been used by Spalding (1972) in finite difference approximations and by Christie, Griffiths, Mitchell and Zienkiewicz (1976) in the use of finite elements. In the analysis of difference schemes Siemieniuch and Gladwell (1978) observed that solutions of (9.2.1) may be kept non-oscillatory by restricting the step

size h with respect to the coefficient v. However, for large values of v this is computationally expensive and a scheme which can restrict the step length h locally (in the region of the oscillations) may therefore be beneficial.

(ii) For moving boundary problems in heat flow the physical situation usually arises where an interface, or internal boundary, exists which moves as time progresses. The interface often takes the form shown in Figure 23 where region A contains a material in its solid form, region B the material in its liquid form and the boundary PQ varies due to melting or freezing of the material. If the position of the interface at time t is given by $x=S(t)$ then, in one space dimension, a typical set of governing equations may be of the form (see for example, Meyer (1976))

$$\frac{\partial}{\partial x}\left[k_1(x,t)\,\frac{\partial u_1}{\partial x}\right] - c_1(x,t)\,\frac{\partial u_1}{\partial t} = F_1(x,t),\quad o<x<S(t)$$

$$\frac{\partial}{\partial x}\left[k_2(x,t)\,\frac{\partial u_2}{\partial x}\right] - c_2(x,t)\,\frac{\partial u_2}{\partial t} = F_2(x,t),\quad S(t)<x<1 \qquad (9.2.3)$$

Specific conditions are assumed at the interface $x=S(t)$, on the boundaries $x=o$ and $x=1$ and on the initial line $t=o$. A summary of the numerical methods devised for the solution of

such "Stefan problems" is given in Ockendon and Hodgkins (1975). In general, the solution is such that significant changes in the solution may occur close to the interface. A scheme in which knot points are optimally chosen on each time line may therefore provide a suitable method of solution.

TABLE 1

Internal knot positions used in Case Study 1.1

Local	Global	Transformation
0.117965	0.133776	0.223607
0.220349	0.234013	0.316228
0.316010	0.325845	0.387298
0.408487	0.413714	0.447214
0.500000	0.500000	0.500000
0.591513	0.586286	0.520000
0.683990	0.674155	0.580000
0.779651	0.765987	0.680000
0.882035	0.866224	0.820000

TABLE 2

Errors for Case Study 1.1 using k=0.05 for 10 time steps

	θ	Constant knot spacing h = 0.1	Variable knot spacing		
			Local	Global	Transformation
(a)	0	8.16×10^{-3}	7.46×10^{-3}	7.09×10^{-3}	Unstable
	1/4	3.25×10^{-3}	2.54×10^{-3}	2.10×10^{-3}	3.89×10^{-3}
	1/3	1.63×10^{-3}	9.08×10^{-4}	4.87×10^{-4}	2.25×10^{-3}
	1/2	1.64×10^{-3}	2.34×10^{-3}	2.73×10^{-3}	2.00×10^{-3}
	1	1.12×10^{-2}	1.19×10^{-2}	1.24×10^{-2}	1.10×10^{-2}
(b)	1/12	6.48×10^{-3}	5.81×10^{-3}	5.43×10^{-3}	Unstable
	(6.2.11)	1.11×10^{-5}	4.05×10^{-5}	1.26×10^{-4}	1.21×10^{-3}

TABLE 3

Errors for Case Study 1.1 using k=0.01 for 10 time steps

	θ	Constant knot spacing h = 0.1	Variable knot spacing		
			Local	Global	Transformation
(a)	0	4.71×10^{-4}	4.13×10^{-4}	3.76×10^{-4}	7.88×10^{-4}
	1/4	4.43×10^{-4}	3.63×10^{-4}	3.41×10^{-4}	7.78×10^{-4}
	1/3	3.95×10^{-4}	3.70×10^{-4}	3.32×10^{-4}	7.17×10^{-4}
	1/2	3.72×10^{-4}	3.42×10^{-4}	3.08×10^{-4}	7.37×10^{-4}
	1	3.80×10^{-4}	3.22×10^{-4}	2.96×10^{-4}	7.28×10^{-4}
(b)	(6.2.11)	4.39×10^{-5}	6.19×10^{-5}	2.04×10^{-5}	2.03×10^{-4}

TABLE 4

Truncation Errors for Case Study 1.1 using k=0.05 for 10 time steps

θ	Constant knot spacing	Variable knot spacing		
	h = 0.1	Local	Global	Transformation
0	2.50×10^{-4}	1.87×10^{-4}	9.23×10^{-5}	Unstable
1/4	9.98×10^{-5}	7.34×10^{-5}	3.35×10^{-5}	2.36×10^{-2}
1/3	4.99×10^{-5}	3.55×10^{-5}	1.39×10^{-5}	5.03×10^{-2}
1/2	4.99×10^{-5}	5.27×10^{-5}	2.89×10^{-5}	1.04×10^{-1}
1	3.49×10^{-4}	2.68×10^{-4}	1.43×10^{-4}	2.65×10^{-1}

TABLE 5

Internal knot positions used in Case Study 1.2

Local	Global
0.104019	0.116725
0.228994	0.282605
0.397569	0.399465
0.501907	0.500314
0.595750	0.593166
0.683453	0.680781
0.766875	0.764549
0.847043	0.845305
0.924603	0.923605

TABLE 6

Errors for Case Study 1.2 using k=0.05 for 10 time steps

	θ	Constant knot spacing h = 0.1	Variable knot spacing Local	Variable knot spacing Global
(a)	0	1.10×10^{-2}	1.03×10^{-2}	9.35×10^{-3}
	1/4	3.89×10^{-3}	2.32×10^{-3}	2.01×10^{-3}
	1/3	2.28×10^{-3}	2.88×10^{-3}	2.84×10^{-3}
	1/2	4.38×10^{-3}	6.93×10^{-3}	6.76×10^{-3}
	1	1.21×10^{-2}	1.38×10^{-2}	1.36×10^{-2}
(b)	(6.2.11)	2.61×10^{-3}	1.82×10^{-3}	1.92×10^{-3}

TABLE 7

Errors on second time line for Case Study 1.2

$k = 0.05, \quad \theta = 1/3$

Constant knot spacing	Variable knot spacing	
h = 0.1	Local	Global
1.01×10^{-3}	2.18×10^{-4}	2.65×10^{-4}

TABLE 8

Errors for Case Study 1.2 using k=0.01 for 10 time steps

θ	Constant knot spacing $h = 0.1$	Variable knot spacing	
		Local	Global
0	3.22×10^{-3}	1.81×10^{-3}	1.86×10^{-3}
1/4	3.13×10^{-3}	1.71×10^{-3}	1.77×10^{-3}
1/3	3.10×10^{-3}	1.68×10^{-3}	1.74×10^{-3}
1/2	3.04×10^{-3}	1.62×10^{-3}	1.67×10^{-3}
1	2.86×10^{-3}	1.44×10^{-3}	1.50×10^{-3}

TABLE 9

Errors for Case Study 1.2 using k=0.01 for 50 time steps

θ	Constant knot spacing	Variable knot spacing	
	h = 0.1	Local	Global
0	1.00×10^{-2}	8.74×10^{-3}	8.76×10^{-3}
1/4	9.76×10^{-3}	8.24×10^{-3}	8.34×10^{-3}
1/3	9.65×10^{-3}	8.08×10^{-3}	8.20×10^{-3}
1/2	9.43×10^{-3}	7.72×10^{-3}	7.86×10^{-3}
1	8.83×10^{-3}	6.80×10^{-3}	7.03×10^{-3}

TABLE 10

Errors for Case Study 1.3 using $\theta = \frac{1}{3}$ and k=0.05 for 10 time steps

c	Constant knot spacing	Variable knot spacing	
	h = 0.1	Local	Global
-1	5.58×10^{-4}	1.76×10^{-4}	5.19×10^{-4}
-10	7.54×10^{-3}	7.93×10^{-3}	8.15×10^{-3}
-100	1.52×10^{-1}	1.52×10^{-1}	1.53×10^{-1}
-200	2.93×10^{-1}	2.93×10^{-1}	2.93×10^{-1}

TABLE 11

Errors for Case Study 1.3 using $\theta = \frac{1}{3}$ and k=0.01 for 50 time steps

c	Constant knot spacing	Variable knot spacing	
	h = 0.1	Local	Global
-1	6.29×10^{-3}	6.21×10^{-3}	5.55×10^{-3}
-10	4.11×10^{-3}	3.23×10^{-3}	3.16×10^{-3}
-100	4.58×10^{-3}	4.81×10^{-3}	4.94×10^{-3}
-200	1.41×10^{-2}	1.44×10^{-2}	1.45×10^{-2}

TABLE 12

Errors for Case Study 1.3 using $\theta=0$ and $k=0.05$ for 10 time steps

c	Constant knot spacing	Variable knot spacing	
	h = 0.1	Local	Global
-1	8.09×10^{-3}	7.43×10^{-3}	7.07×10^{-3}
-10	7.54×10^{-3}	7.17×10^{-3}	7.00×10^{-3}
-100	5.75×10^{-2}	5.72×10^{-2}	5.71×10^{-2}
-200	1.47×10^{-1}	1.47×10^{-1}	1.46×10^{-1}

TABLE 13

Errors for Case Study 1.4 using k=0.05 for 10 time steps

	θ	Constant knot spacing h = 0.1	Variable knot spacing Local	Global
(a)	1/4	Unstable	Unstable	Unstable
	1/2	1.08×10^{-2}	1.05×10^{-2}	1.03×10^{-2}
	3/4	3.39×10^{-2}	3.42×10^{-2}	3.44×10^{-2}
	1	7.32×10^{-2}	7.35×10^{-2}	7.37×10^{-2}
(b)	(6.4.5)	7.65×10^{-3}	7.63×10^{-3}	7.61×10^{-3}

TABLE 14

Errors for Case Study 1.4 using k=0.01 for 50 time steps

	θ	Constant knot spacing h = 0.1	Variable knot spacing Local	Global
(a)	1/4	Unstable	Unstable	Unstable
	1/2	3.33×10^{-3}	2.97×10^{-3}	2.77×10^{-3}
	3/4	5.72×10^{-3}	6.07×10^{-3}	6.27×10^{-3}
	1	1.46×10^{-2}	1.49×10^{-2}	1.51×10^{-2}
(b)	(6.4.5)	2.87×10^{-4}	2.71×10^{-4}	2.48×10^{-4}

TABLE 15

Internal knot positions used in Case Study 1.5 when a=1.

Local	Global
0.089594	0.089472
0.181218	0.180988
0.274965	0.274652
0.370935	0.370557
0.469235	0.468818
0.569981	0.569558
0.673296	0.672893
0.779315	0.778977
0.888182	0.887945

TABLE 16

Internal knot positions used in Case Study 1.5 when a=10

Local	Global
0.041330	0.038513
0.087159	0.081132
0.138550	0.128841
0.196988	0.183019
0.264618	0.245703
0.344707	0.320070
0.442549	0.411493
0.567504	0.530205
0.738279	0.699769

TABLE 17

Errors for Case Study 1.5 when a=1 and k=0.05

	θ	Constant knot spacing h = 0.1	Variable knot spacing Local	Global
(a)	1/4	Unstable	Unstable	Unstable
	1/2	3.00×10^{-3}	2.89×10^{-3}	2.89×10^{-3}
	3/4	2.73×10^{-3}	2.74×10^{-3}	2.74×10^{-3}
	1	5.77×10^{-3}	5.83×10^{-3}	5.83×10^{-3}
(b)	(6.4.5)	2.72×10^{-3}	2.67×10^{-3}	2.67×10^{-3}

TABLE 18

Errors for Case Study 1.5 when a=1 and k=0.01

	θ	Constant knot spacing h = 0.1	Variable knot spacing Local	Global
(a)	1/4	Unstable	Unstable	Unstable
	1/2	7.04×10^{-4}	6.99×10^{-4}	6.99×10^{-4}
	3/4	4.63×10^{-4}	4.73×10^{-4}	4.72×10^{-4}
	1	1.17×10^{-3}	1.18×10^{-3}	1.18×10^{-3}
(b)	(6.4.5)	3.92×10^{-4}	4.36×10^{-4}	4.37×10^{-4}

TABLE 19

Errors for Case Study 1.5 when a = 10 and k = 0.05

	θ	Constant knot spacing h = 0.1	Variable knot spacing Loacl	Global
(a)	1/4	Unstable	Unstable	Unstable
	1/2	1.55×10^{-1}	1.48×10^{-1}	1.48×10^{-1}
	3/4	3.54×10^{-2}	3.72×10^{-2}	3.84×10^{-2}
	1	8.01×10^{-2}	8.32×10^{-2}	8.29×10^{-2}
(b)	(6.4.5)	1.43×10^{-1}	1.45×10^{-1}	1.45×10^{-1}

Table 20

Errors for Case Study 1.5 when a = 10 and k = 0.01

	θ	Constant knot spacing h = 0.1	Variable knot spacing Local	Global
(a)	1/4	Unstable	Unstable	Unstable
	1/2	4.49×10^{-2}	4.86×10^{-2}	4.77×10^{-2}
	3/4	1.09×10^{-2}	1.76×10^{-2}	1.73×10^{-3}
	1	3.29×10^{-2}	3.95×10^{-2}	3.93×10^{-2}
(b)	(6.4.5)	2.68×10^{-2}	4.47×10^{-2}	4.43×10^{-2}

TABLE 21

Errors for Case Study 2.1 using k=0.05 for 10 time steps

θ	Constant knot spacing h=0-1	Variable knot spacing Local	Variable knot spacing Global	Varying the knots on each time line
0	8.16×10^{-3}	7.46×10^{-3}	7.09×10^{-3}	7.34×10^{-3}
1/4	3.25×10^{-3}	2.54×10^{-3}	2.10×10^{-3}	2.39×10^{-3}
1/3	1.63×10^{-3}	9.08×10^{-4}	4.87×10^{-4}	7.61×10^{-4}
1/2	1.64×10^{-3}	2.34×10^{-3}	2.73×10^{-3}	2.48×10^{-3}
1	1.12×10^{-2}	1.19×10^{-2}	1.24×10^{-2}	1.21×10^{-2}

TABLE 22

Errors for Case Study 2.2 using k=0.05 for 10 time steps

θ	Constant knot spacing h=0.1	Variable knot spacing		Varying the knots on each time line
		Local	Global	
0	1.10×10^{-2}	1.03×10^{-2}	9.35×10^{-3}	2.17×10^{-2}
1/4	3.89×10^{-3}	2.32×10^{-3}	2.01×10^{-3}	3.48×10^{-3}
1/3	2.28×10^{-3}	2.88×10^{-3}	2.84×10^{-3}	4.17×10^{-3}
1/2	4.38×10^{-3}	6.93×10^{-3}	6.76×10^{-3}	9.85×10^{-3}
1	1.21×10^{-2}	1.38×10^{-2}	1.36×10^{-2}	1.55×10^{-2}

TABLE 23

Errors for Case Study 2.2 using k=0.01 for 50 time steps

θ	Constant knot spacing h=0.1	Variable knot spacing		Varying the knots on each time line
		Local	Global	
0	1.00×10^{-2}	8.74×10^{-3}	8.76×10^{-3}	4.48×10^{-3}
1/4	9.76×10^{-3}	8.24×10^{-3}	8.34×10^{-3}	5.07×10^{-3}
1/3	9.65×10^{-3}	8.08×10^{-3}	8.20×10^{-3}	5.21×10^{-3}
1/2	9.43×10^{-3}	7.72×10^{-3}	7.86×10^{-3}	4.60×10^{-3}
1	8.83×10^{-3}	6.80×10^{-3}	7.03×10^{-3}	5.02×10^{-3}

TABLE 24

Errors for Case Study 2.3 using $\theta = \frac{1}{3}$ and k=0.05 for 10 time steps

c	Constant knot spacing h=0.1	Variable knot spacing Local	Variable knot spacing Global	Varying the knots on each time line
-1	5.58×10^{-4}	1.76×10^{-4}	5.19×10^{-4}	3.22×10^{-4}
-10	7.54×10^{-3}	7.93×10^{-3}	8.15×10^{-3}	8.04×10^{-3}
-100	1.52×10^{-1}	1.52×10^{-1}	1.53×10^{-1}	1.52×10^{-1}
-200	2.93×10^{-1}	2.93×10^{-1}	2.93×10^{-1}	2.93×10^{-1}

TABLE 25

Errors for Case Study 2.3 using $\theta = \frac{1}{3}$ and k=0.01 for 50 time steps

c	Constant knot spacing h=0.1	Variable knot spacing Local	Global	Varying the knots on each time line
-1	6.29×10^{-3}	6.21×10^{-3}	5.55×10^{-3}	5.90×10^{-3}
-10	4.11×10^{-3}	3.23×10^{-3}	3.16×10^{-3}	3.27×10^{-3}
-100	4.58×10^{-3}	4.81×10^{-3}	4.94×10^{-3}	4.92×10^{-3}
-200	1.41×10^{-2}	1.44×10^{-2}	1.45×10^{-2}	1.43×10^{-2}

TABLE 26

Errors for Case Study 2.4 using k=0.05 for 10 time steps

θ	Constant knot spacing h=0.1	Variable knot spacing Local	Variable knot spacing Global	Varying the knots on each time line
1/2	1.08×10^{-2}	1.05×10^{-2}	1.03×10^{-2}	1.04×10^{-2}
3/4	3.39×10^{-2}	3.42×10^{-2}	3.44×10^{-2}	3.43×10^{-2}
1	7.32×10^{-2}	7.35×10^{-2}	7.37×10^{-2}	7.35×10^{-2}

TABLE 27

Errors for Case Study 2.4 using k=0.01 for 50 time steps

θ	Constant knot spacing h=0.1	Variable knot spacing		Varying the knots on each time line
		Local	Global	
1/2	3.33×10^{-3}	2.97×10^{-3}	2.77×10^{-3}	2.90×10^{-3}
3/4	5.72×10^{-3}	6.07×10^{-3}	6.27×10^{-3}	6.14×10^{-3}
1	1.46×10^{-2}	1.49×10^{-2}	1.51×10^{-2}	1.50×10^{-2}

TABLE 28

Errors for Case Study 2.5 when a=1 and k=0.05

θ	Constant knot spacing h=0.1	Variable knot spacing		Varying the knots on each-time line
		Local	Global	
1/4	Unstable	Unstable	Unstable	Unstable
1/2	3.00×10^{-3}	2.89×10^{-3}	2.89×10^{-3}	2.86×10^{-3}
3/4	2.73×10^{-3}	2.74×10^{-3}	2.74×10^{-3}	2.71×10^{-3}
1	5.77×10^{-3}	5.83×10^{-3}	5.83×10^{-3}	5.84×10^{-3}

TABLE 29

Errors for Case Study 2.5 when a=1 and k=0.01

θ	Constant knot spacing h=0.1	Variable knot spacing		Varying the knots on each time line
		Local	Global	
1/4	Unstable	Unstable	Unstable	Unstable
1/2	7.04×10^{-4}	6.99×10^{-4}	6.99×10^{-4}	6.81×10^{-4}
3/4	4.63×10^{-4}	4.73×10^{-4}	4.72×10^{-4}	5.01×10^{-4}
1	1.17×10^{-3}	1.18×10^{-3}	1.18×10^{-3}	1.20×10^{-3}

TABLE 30

Errors for Case Study 2.5 when a=10 and k=0.05

θ	Constant knot spacing h=0.1	Variable knot spacing		Varying the knots on each time line
		Local	Global	
1/4	Unstable	Unstable	Unstable	Unstable
1/2	1.55×10^{-1}	1.48×10^{-1}	1.48×10^{-1}	1.45×10^{-1}
3/4	3.54×10^{-2}	3.72×10^{-2}	3.84×10^{-2}	3.67×10^{-2}
1	8.01×10^{-2}	8.32×10^{-2}	8.29×10^{-2}	8.19×10^{-2}

TABLE 31

Errors for Case Study 2.5 when a=10 and k=0.01

θ	Constant knot spacing h=0.1	Variable knot spacing		Varying the knots on each time line
		Local	Global	
1/4	unstable	Unstable	Unstable	Unstable
1/2	4.49×10^{-2}	4.86×10^{-2}	4.77×10^{-2}	5.01×10^{-2}
3/4	1.09×10^{-2}	1.76×10^{-2}	1.73×10^{-2}	1.45×10^{-2}
1	3.29×10^{-2}	3.95×10^{-2}	3.93×10^{-2}	4.02×10^{-2}

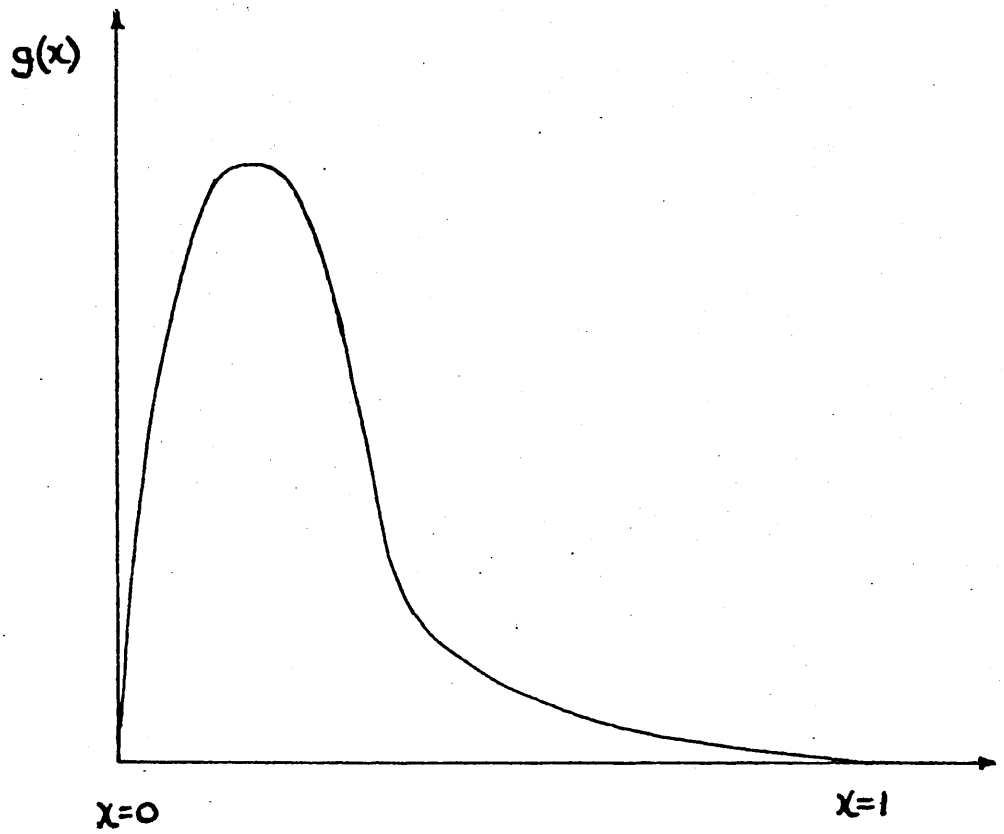

Figure 1

Shape of initial condition u(x,o)=g(x)

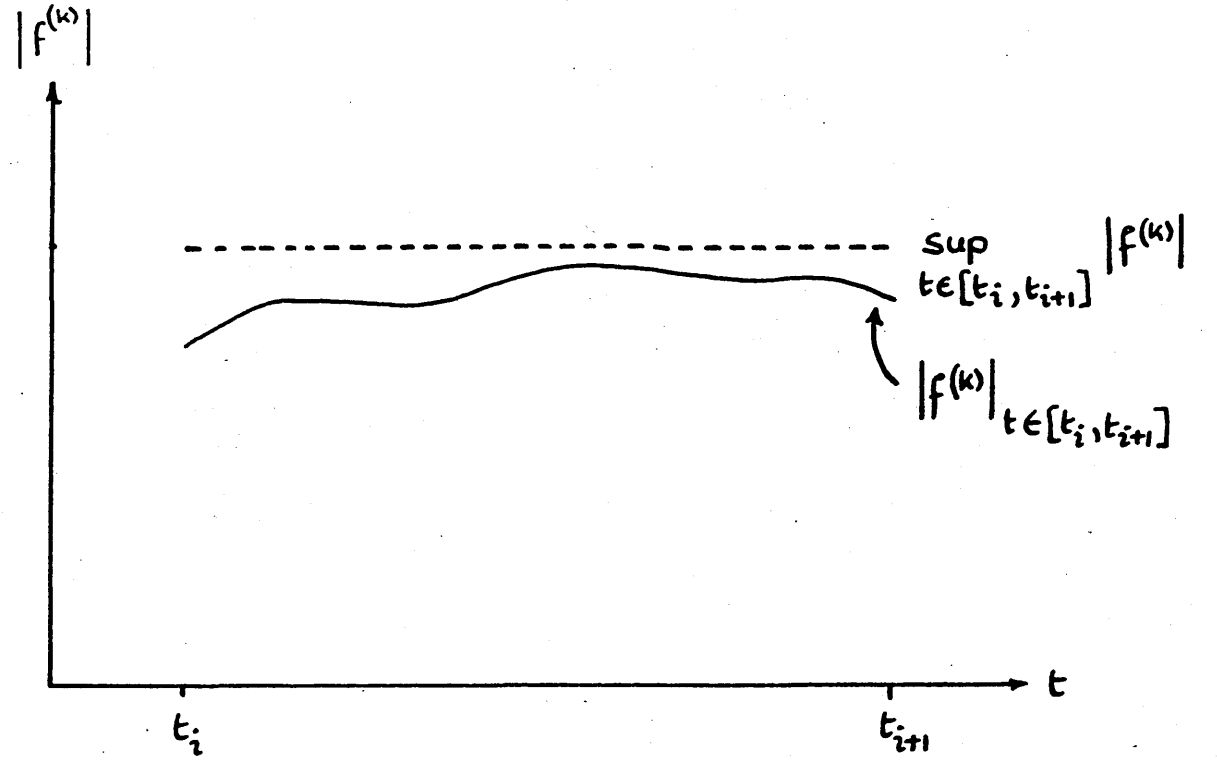

Figure 2(a)

Illustration of $||f^{(k)}||_i$

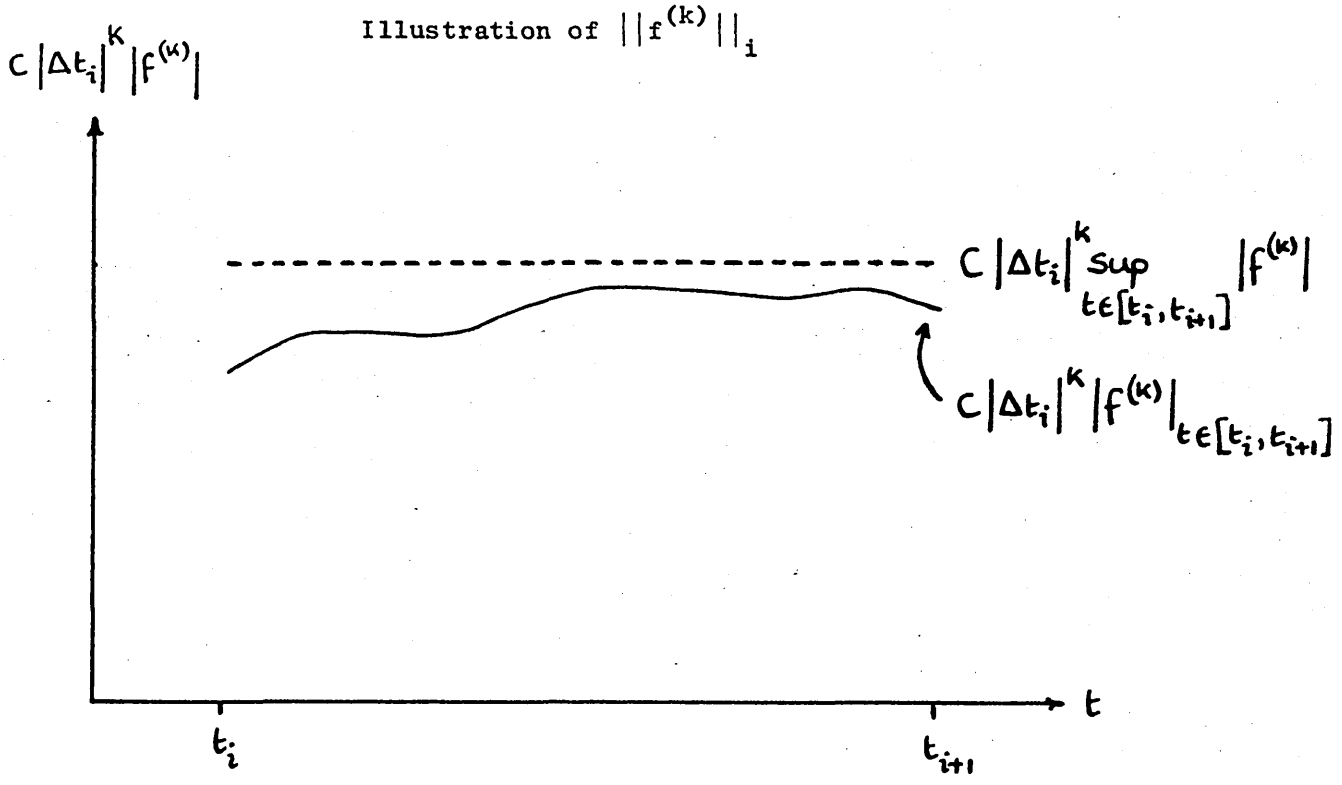

Figure 2(b)

Illustration of (5.3.2)

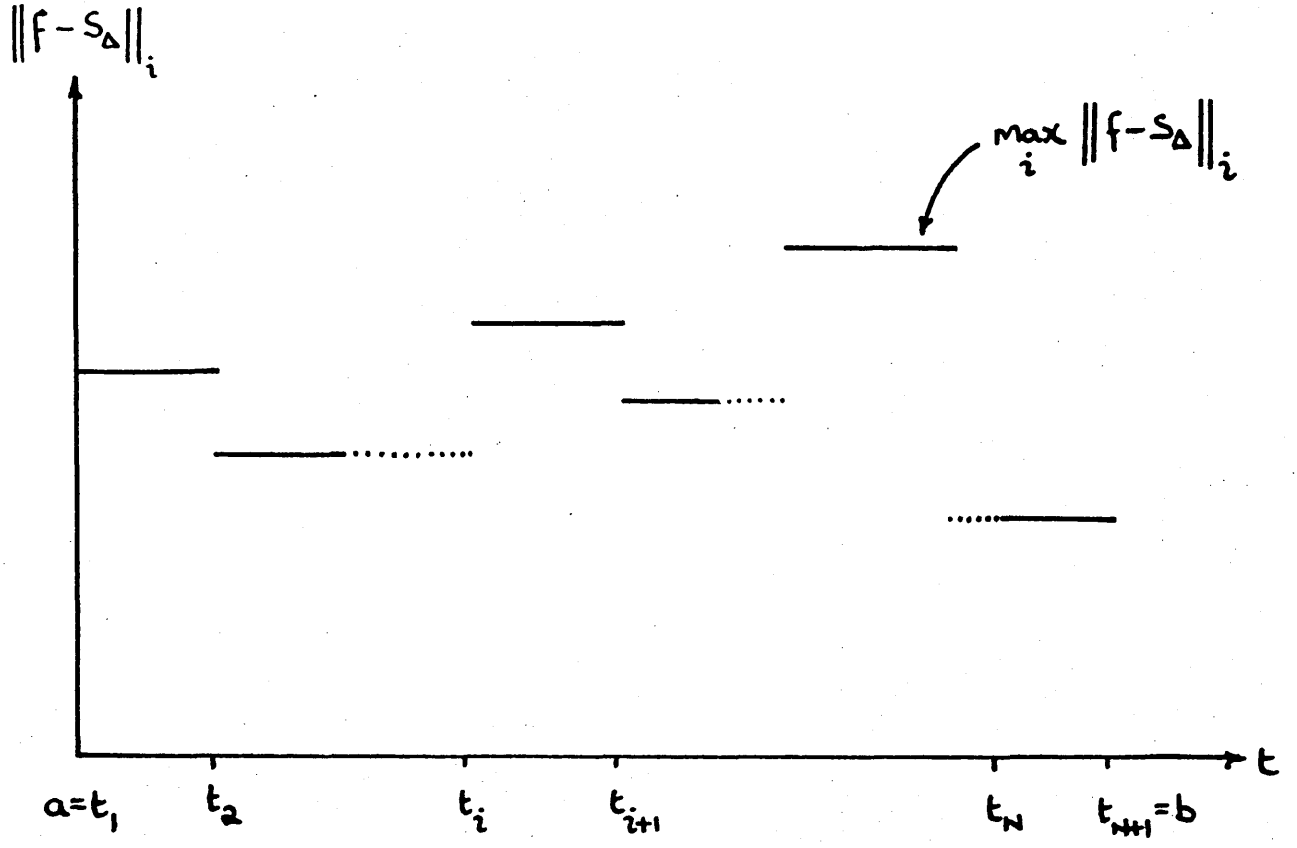

Figure 3

Illustration of $||f-s_\Delta||_\infty$

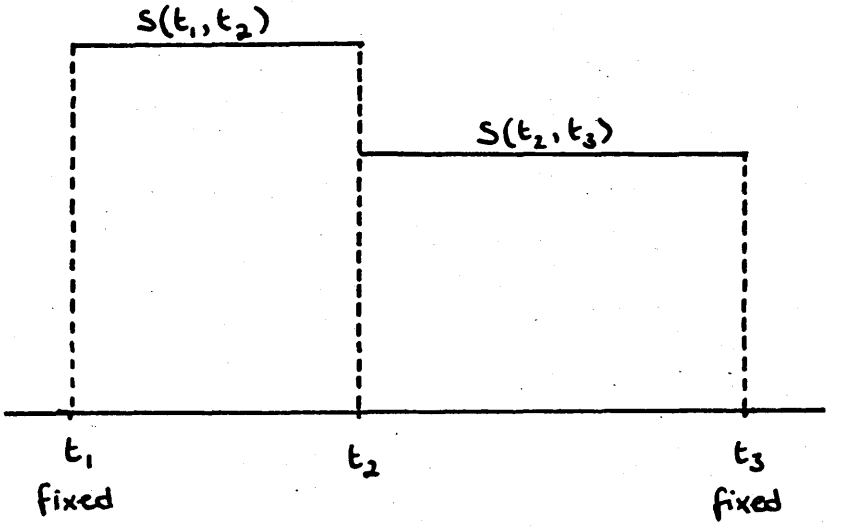

Figure 4(a)

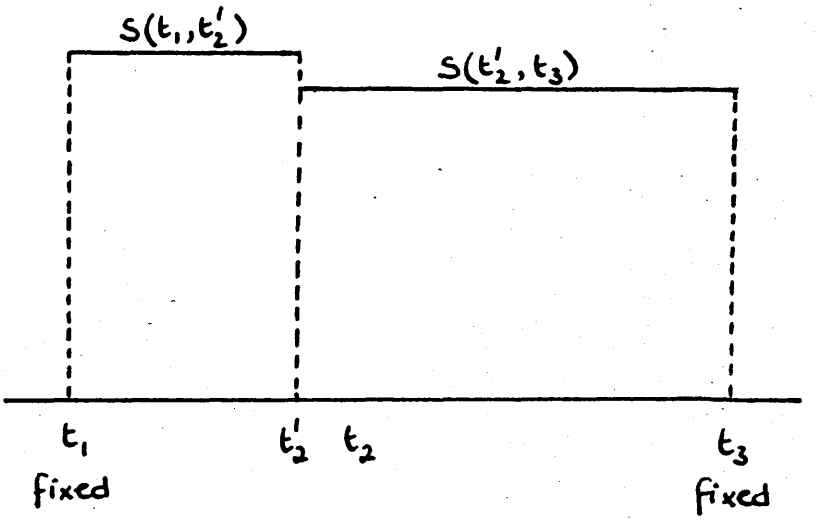

Figure 4(b)

Locating the knot point t_2 - Global Method

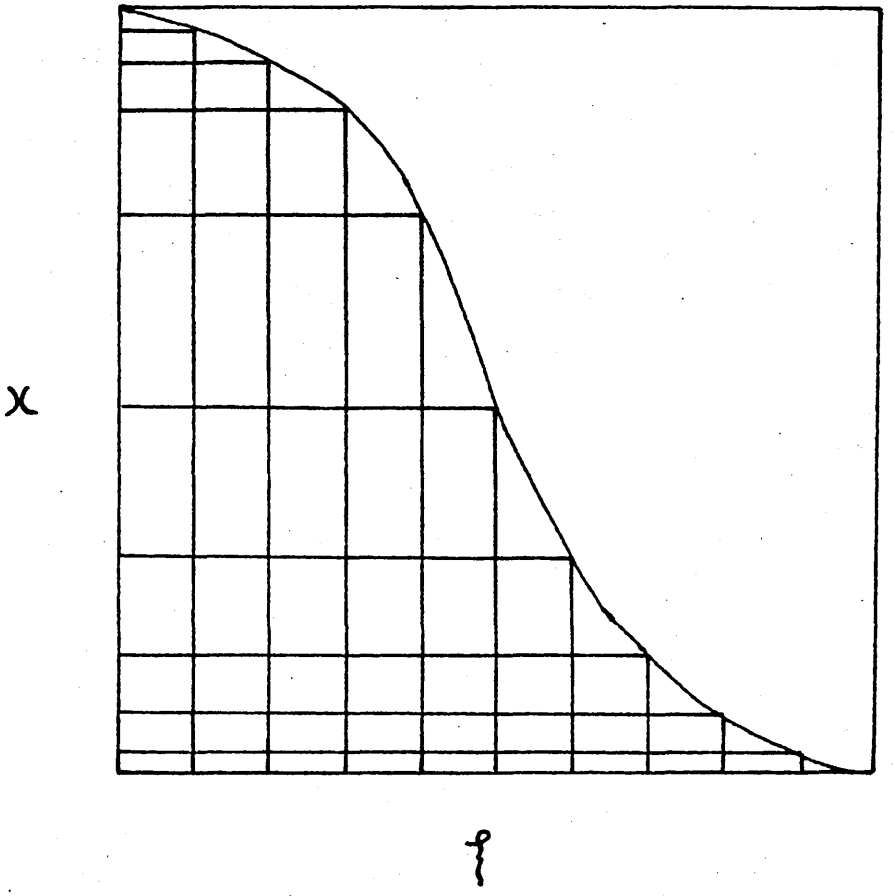

Figure 5

A transformation from a uniform mesh ξ to a non-uniform mesh x.

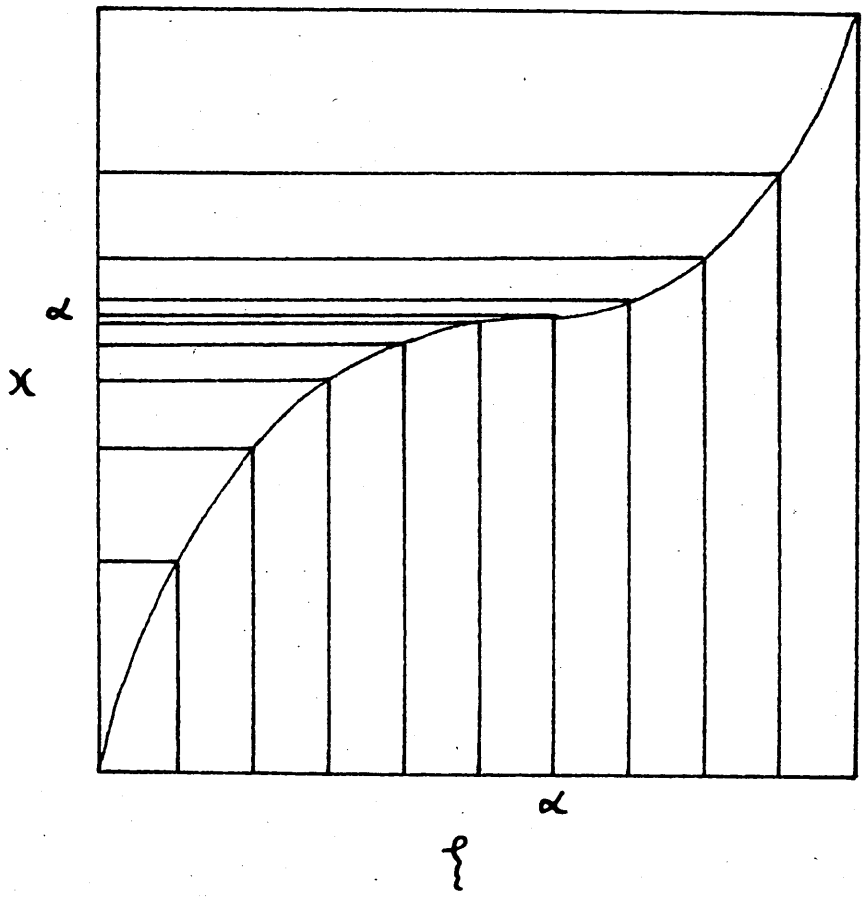

Figure 6

Transformation for a peak at x=α.

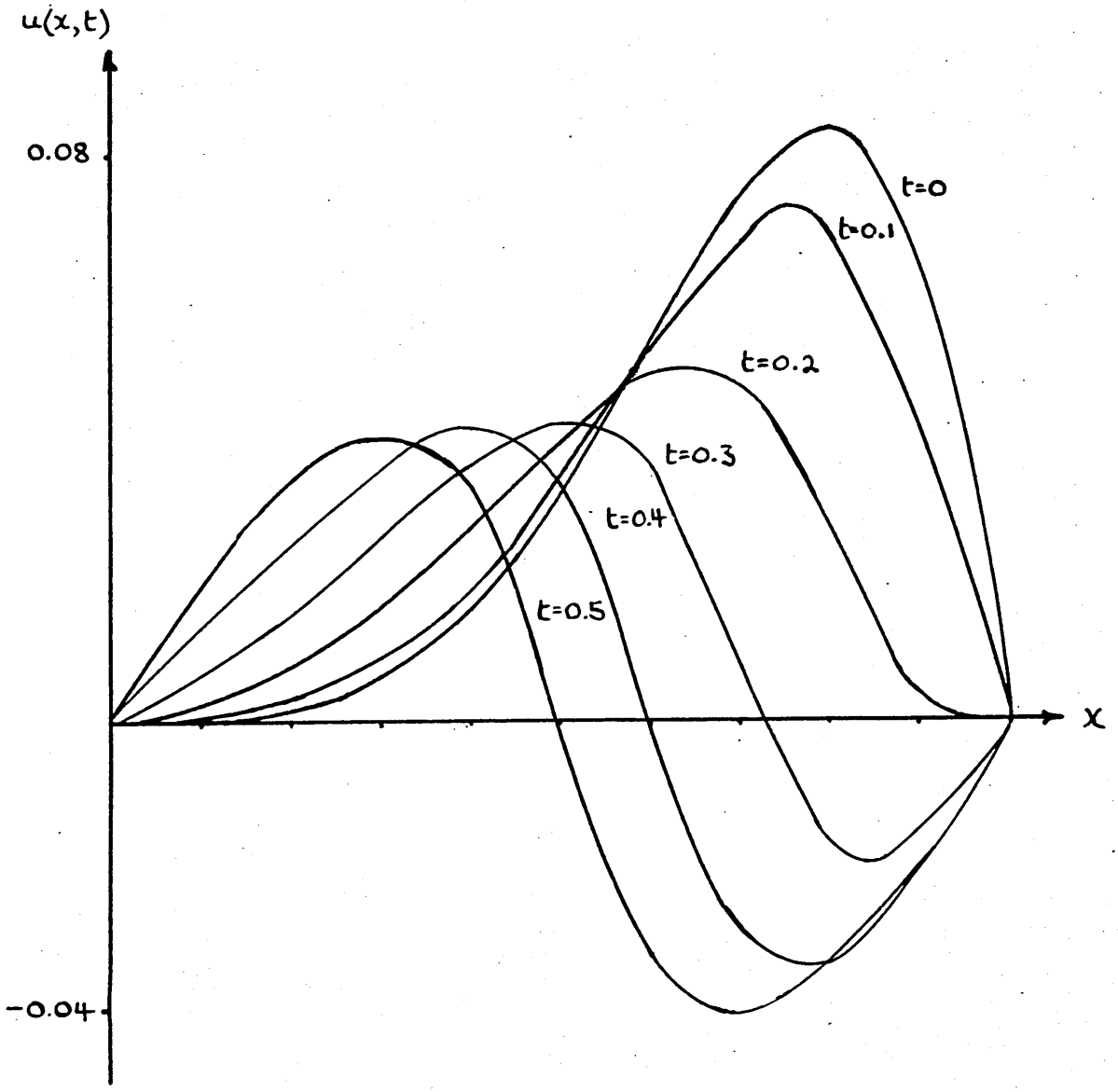

Figure 7

Shape of Analytic Solution (6.3.6) as time progresses

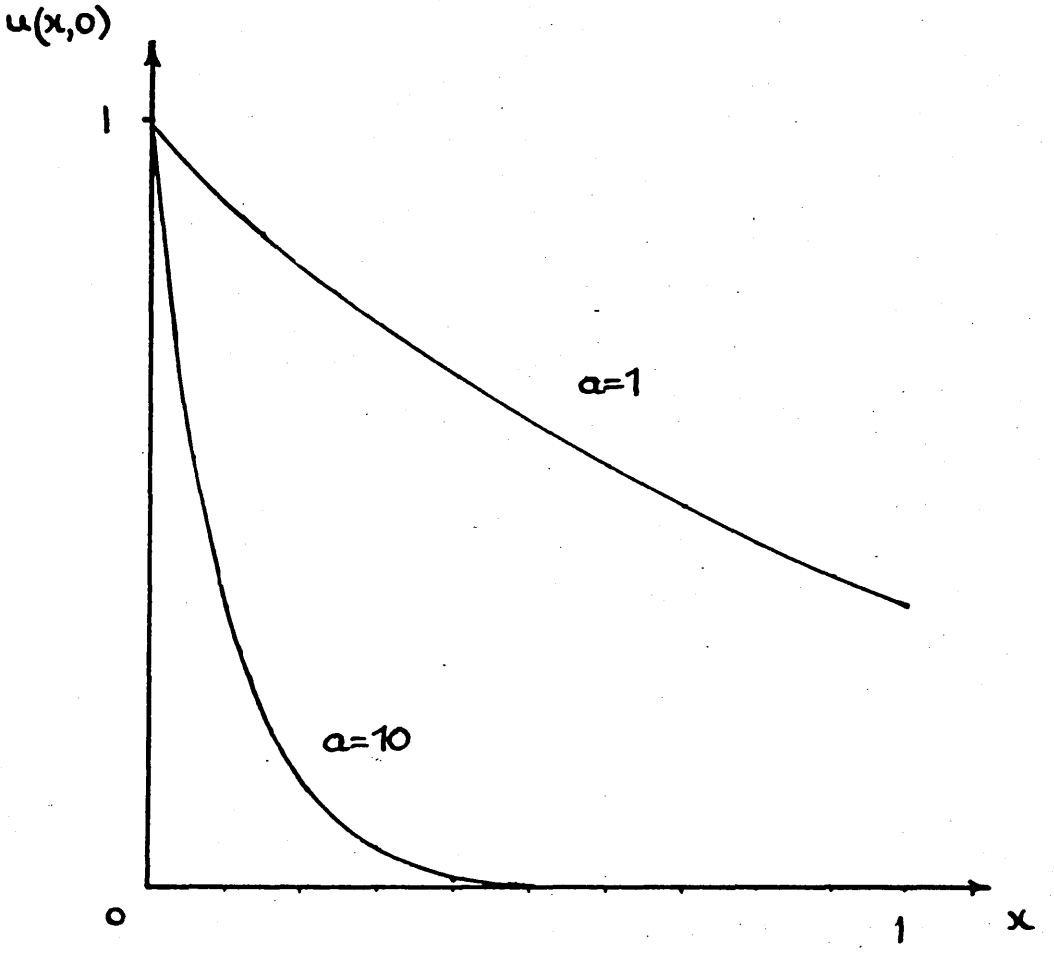

Figure 8

Shape of initial conditions used in Case Study 4

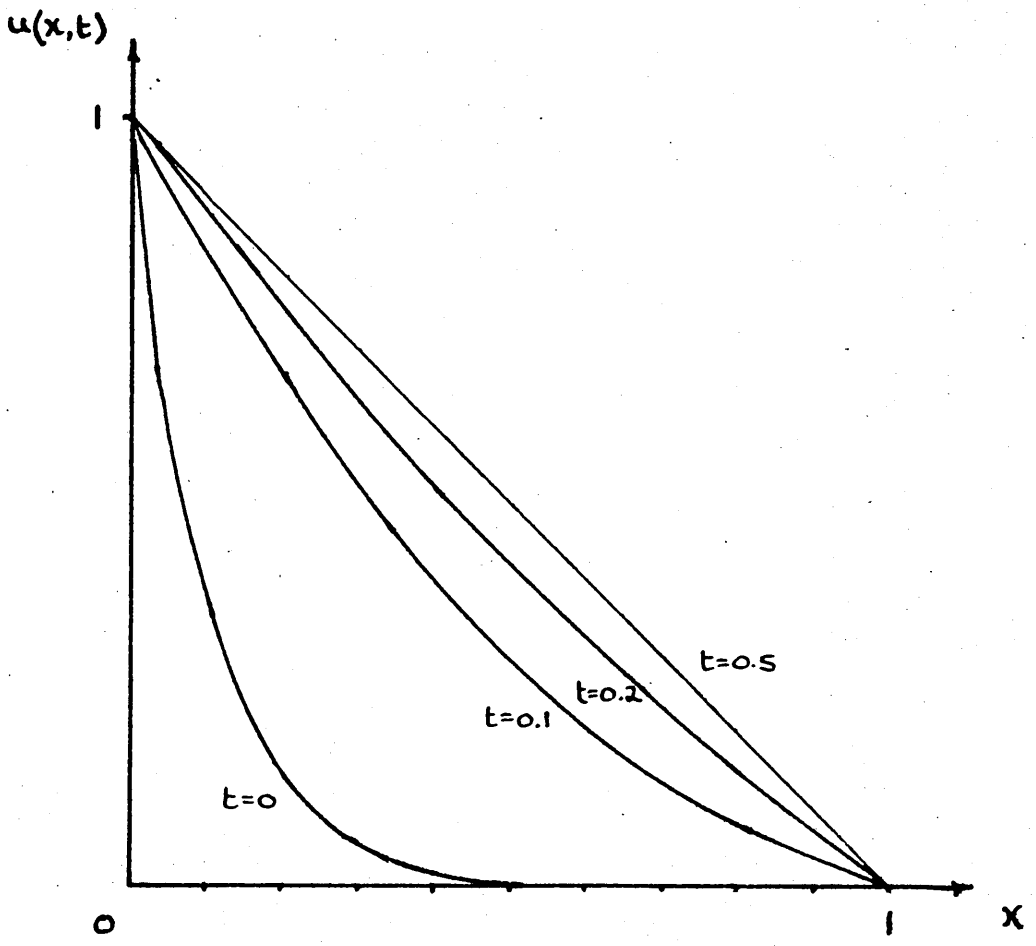

Figure 9

Shape of Analytic Solution (6.5.6), for various time lines, using a=10.

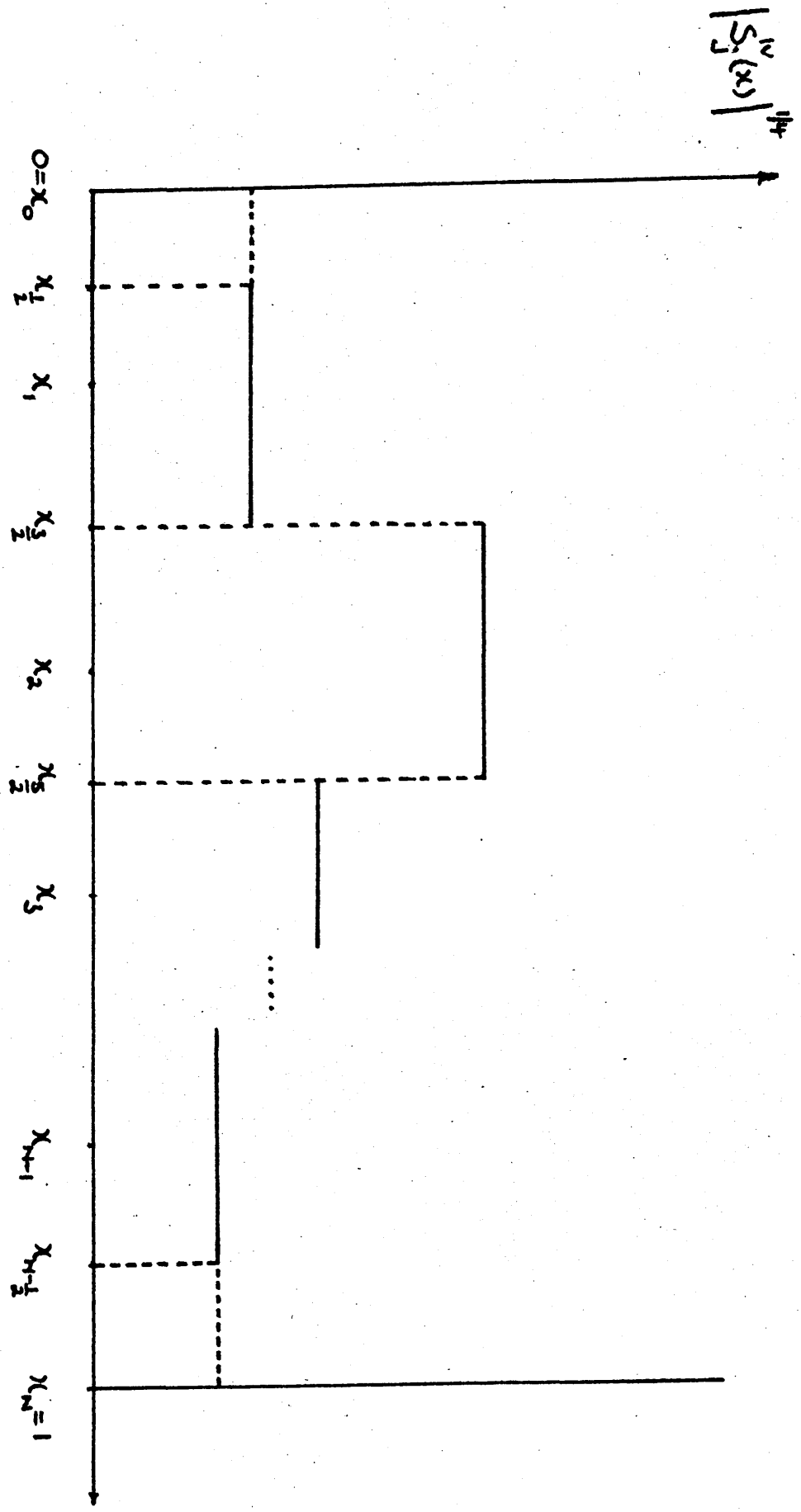

Figure 10

Illustration of (7.2.4)

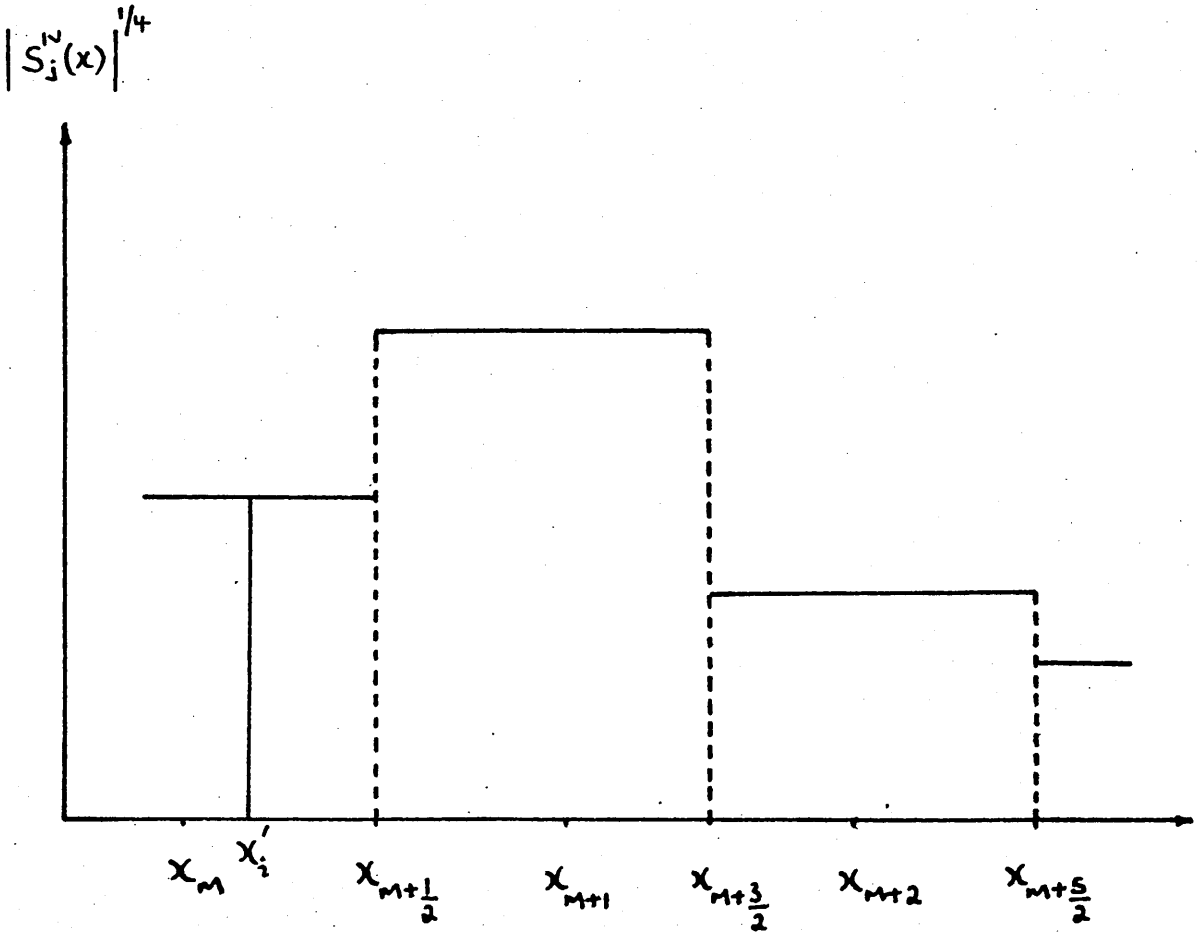

Figure 11

Illustration of procedure for determining new knots

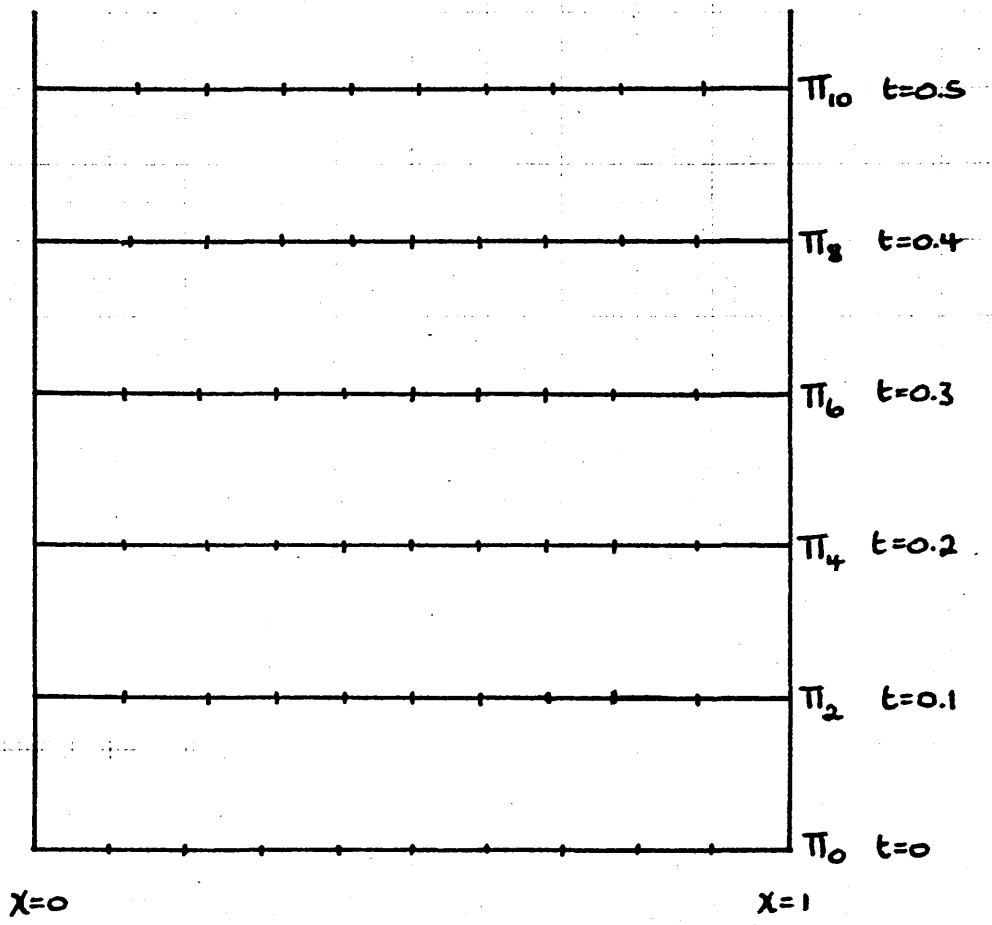

Figure 12

Knot Partitions for Case Study 2.1 with $\theta = \frac{1}{3}$, k=0.05

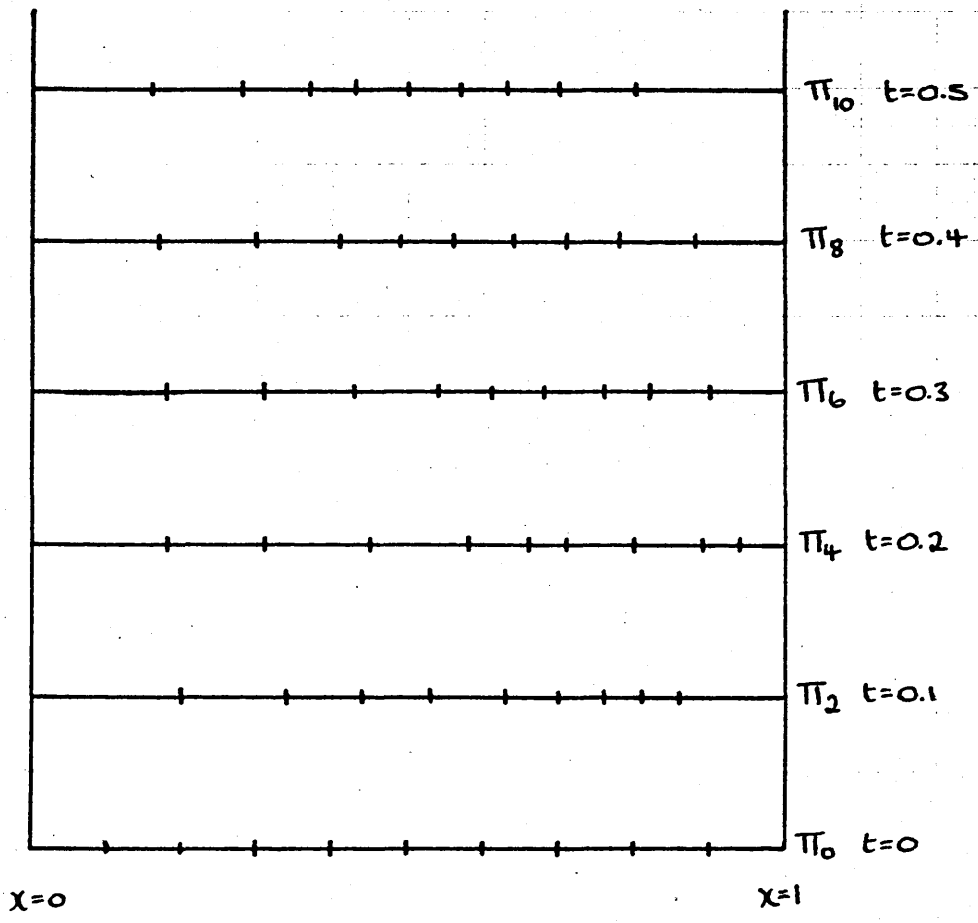

Figure 13

Knot Partitions for Case Study 2.2 with $\theta = \frac{1}{3}$ and k=0.05

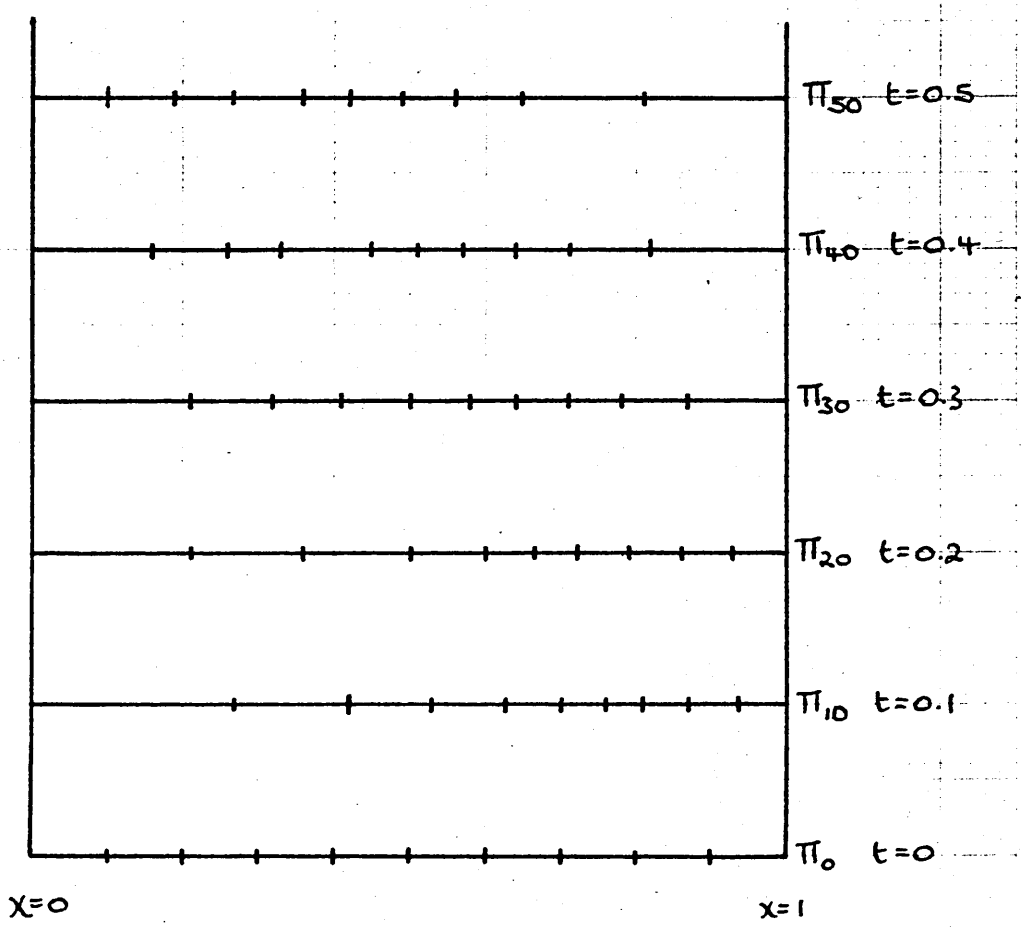

Figure 14

Knot Partitions for Case Study 2.2 with $\theta = \frac{1}{3}$ and k=0.01

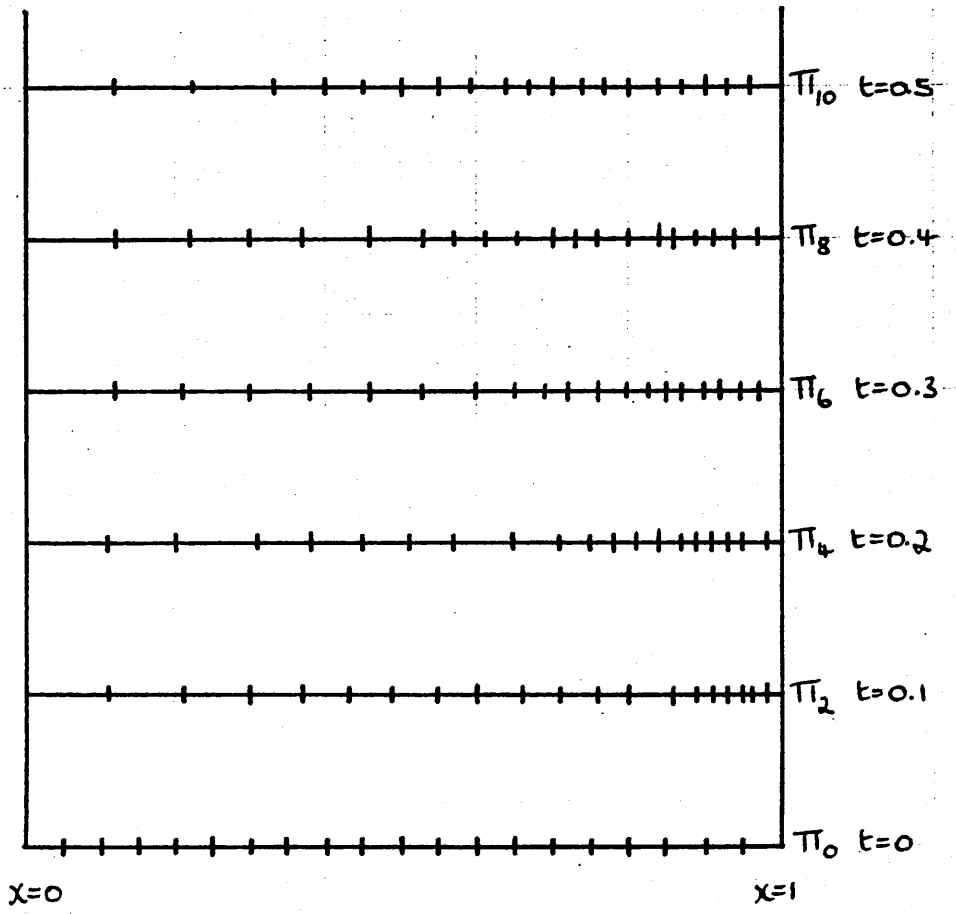

Figure 15

Knot Partitions for Case Study 2.2 with $\theta = \frac{1}{3}$ and k=0.05

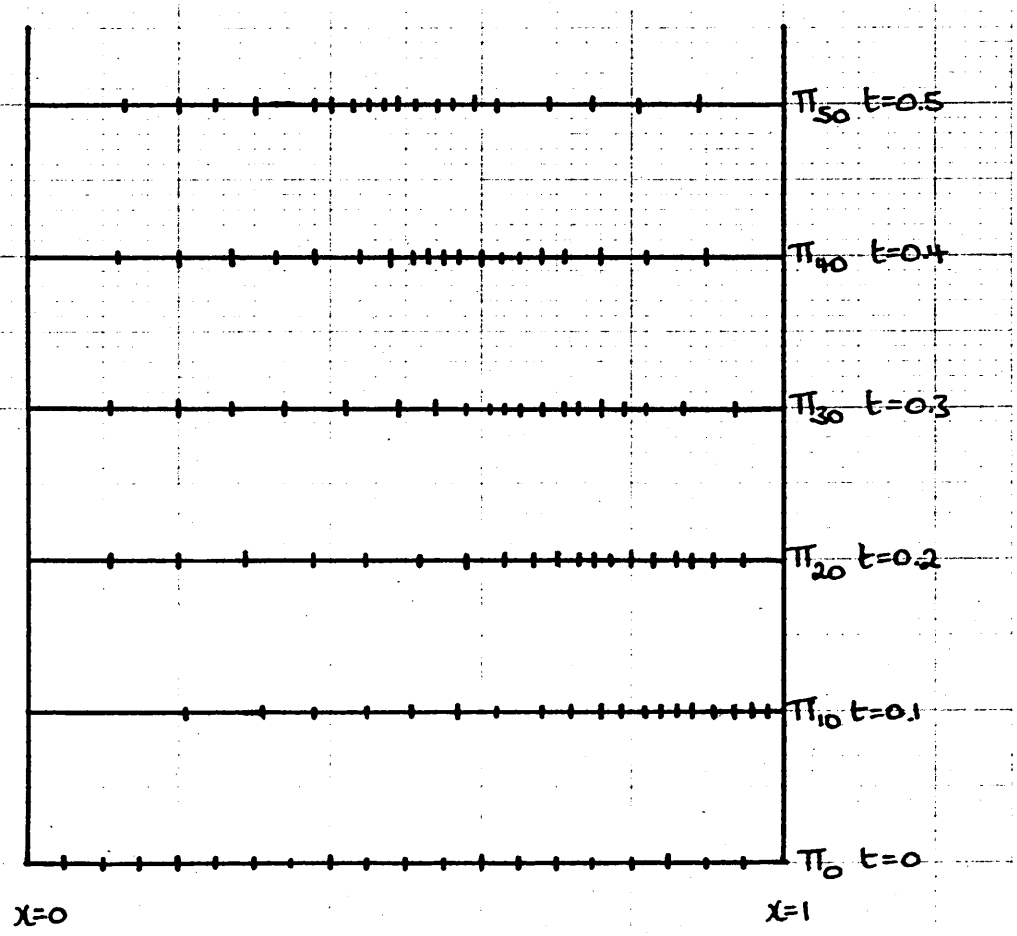

Figure 16

Knot Partitions for Case Study 2.2 with $\theta = \frac{1}{3}$ and k=0.01

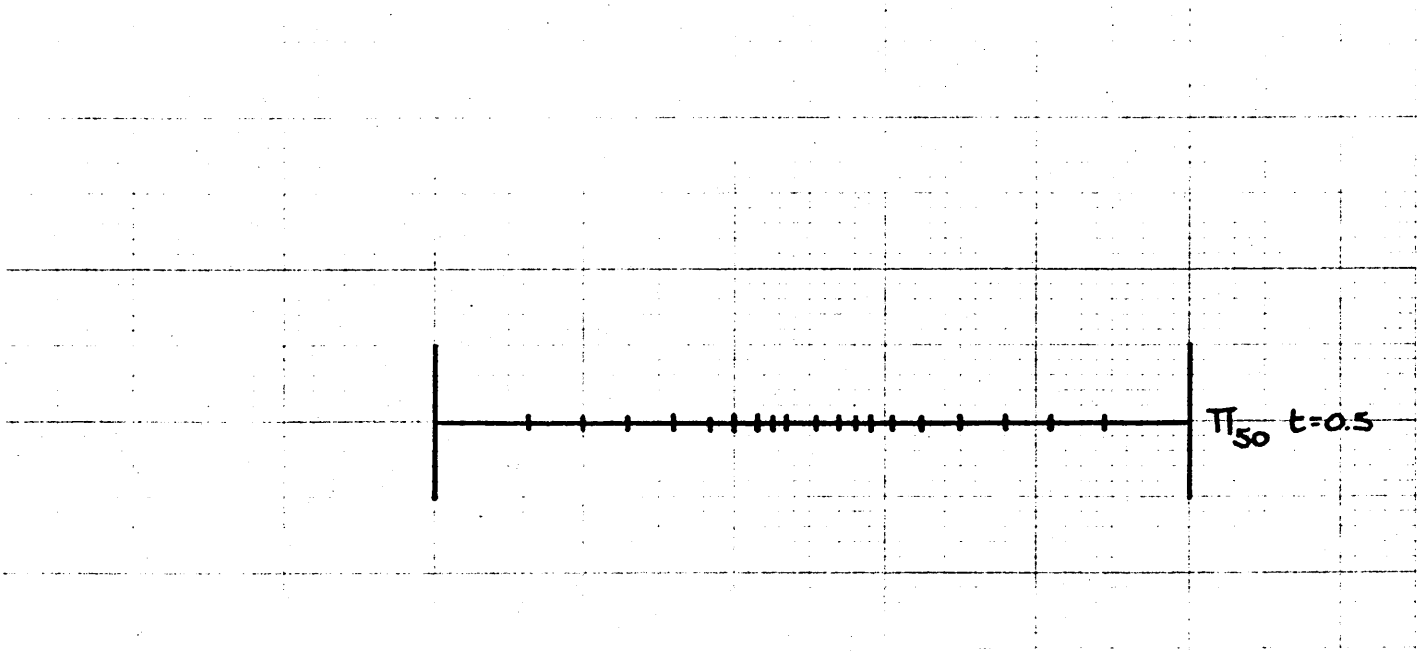

Figure 17

Knot Partitions for Case STudy 2.2 using the Analytic Solution (6.3.6) with k=0.01

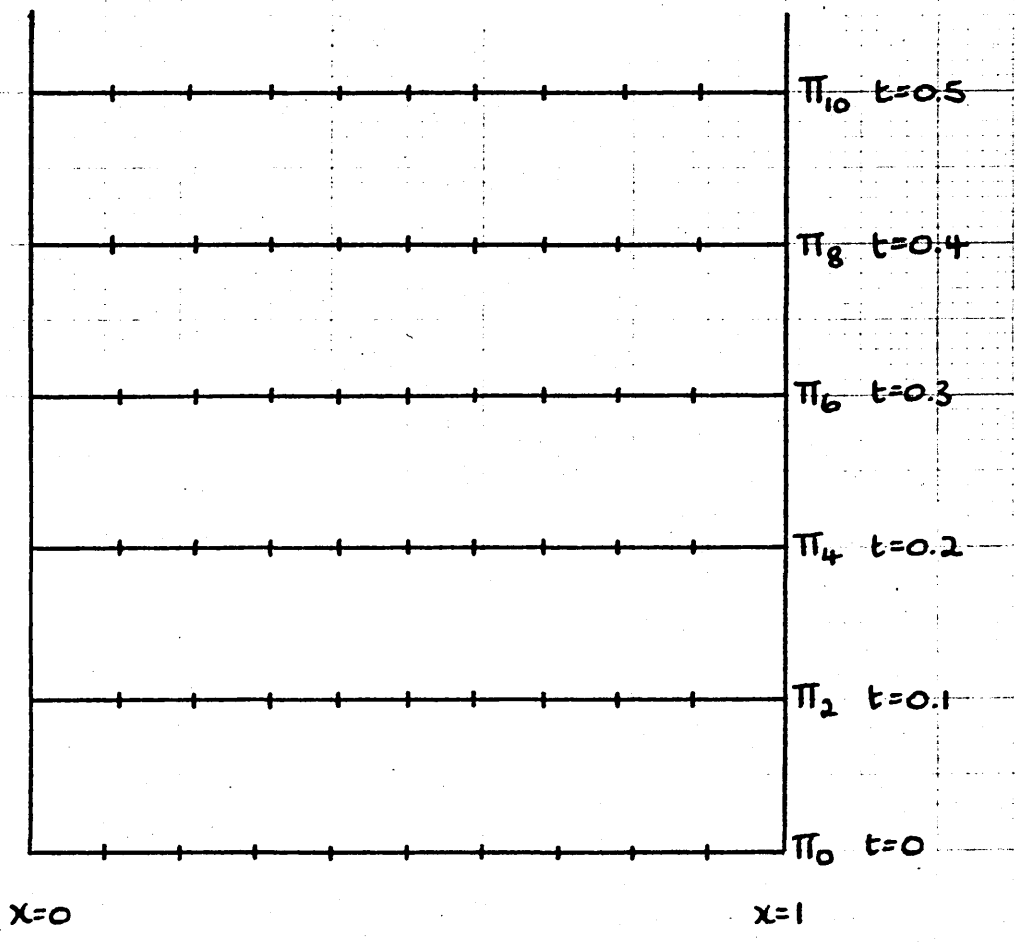

Figure 18

Knot Partitions for Case Study 2.4 with $\theta = \frac{1}{2}$ and k=0.05

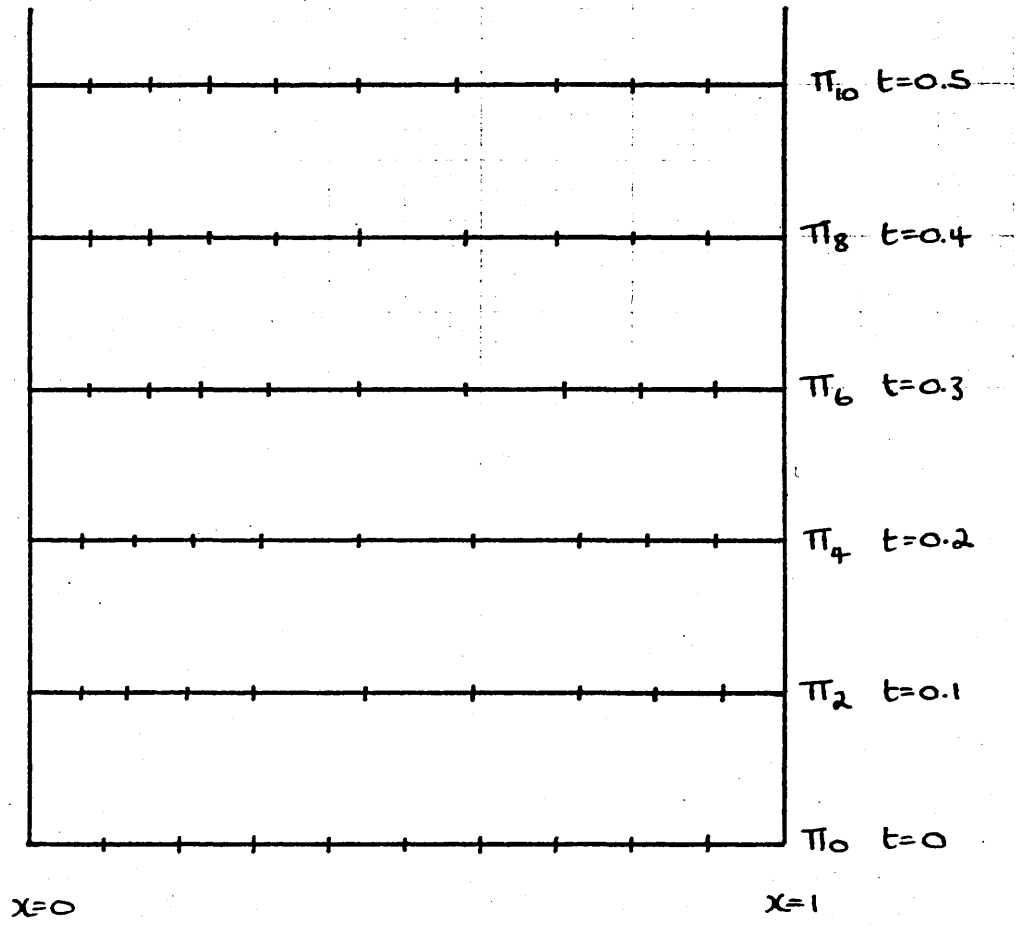

Figure 19

Knot Partitions for Case Study 2.5 with a=1, k=0.05, $\theta = \frac{1}{2}$.

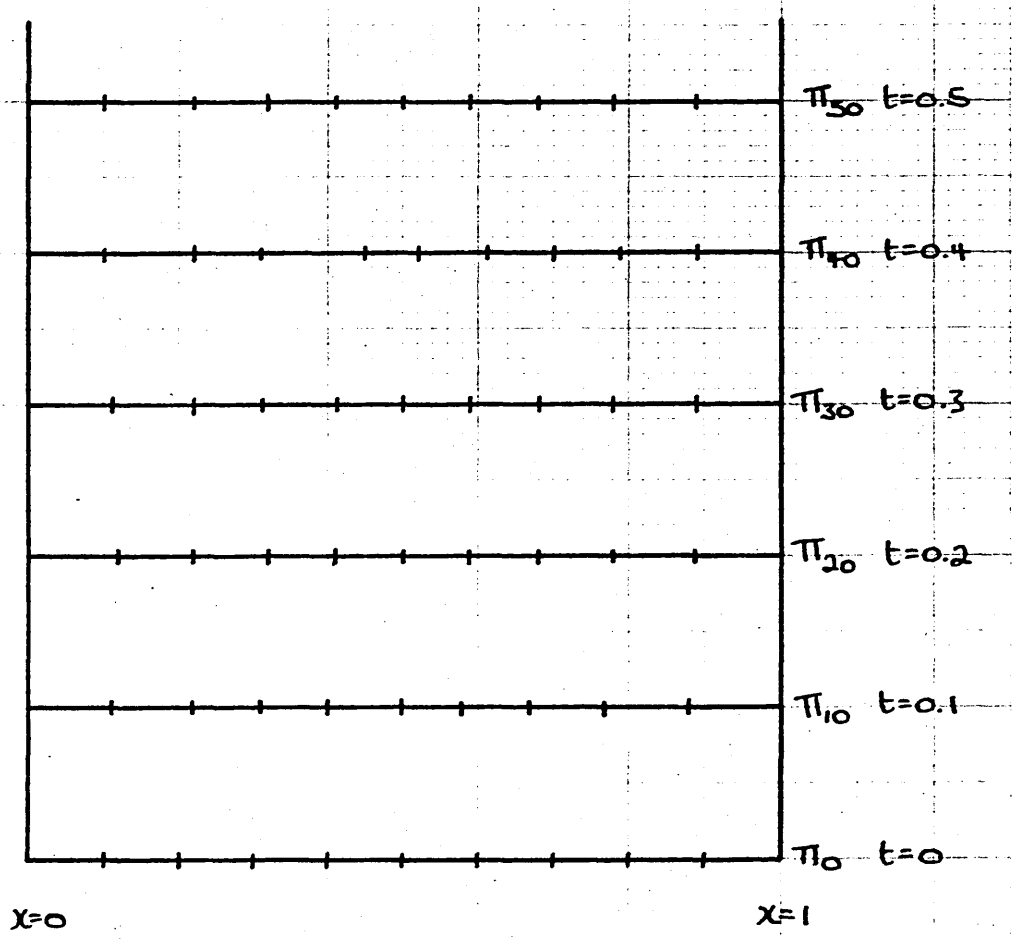

Figure 20

Knot Partitions for Case Study 2.5 with a=1, k=0.01, $\theta = \frac{1}{2}$.

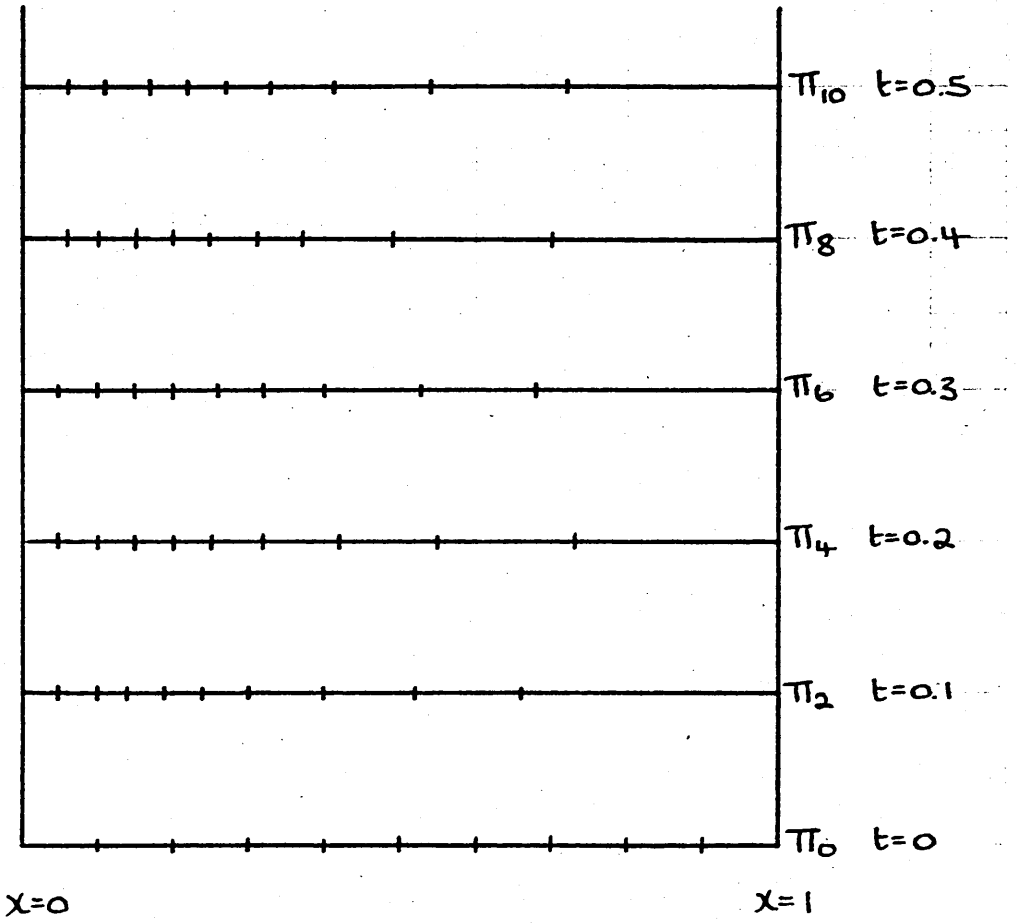

Figure 21

Knot Partitions for Case Study 2.5 with a=10, k=0.05, $\theta = \frac{1}{2}$.

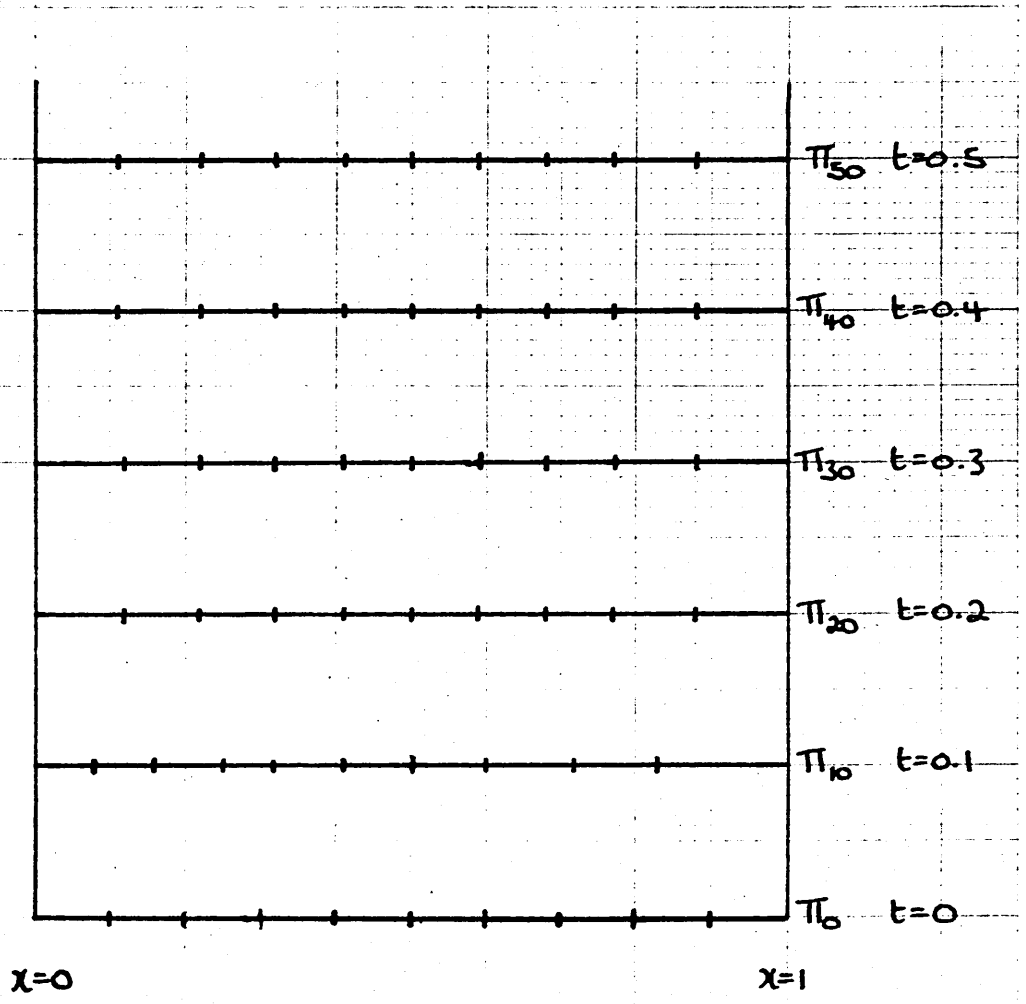

Figure 22

Knot Partitions for Case STudy 2.5 with a=10, k=0.01, $\theta = \frac{1}{2}$.

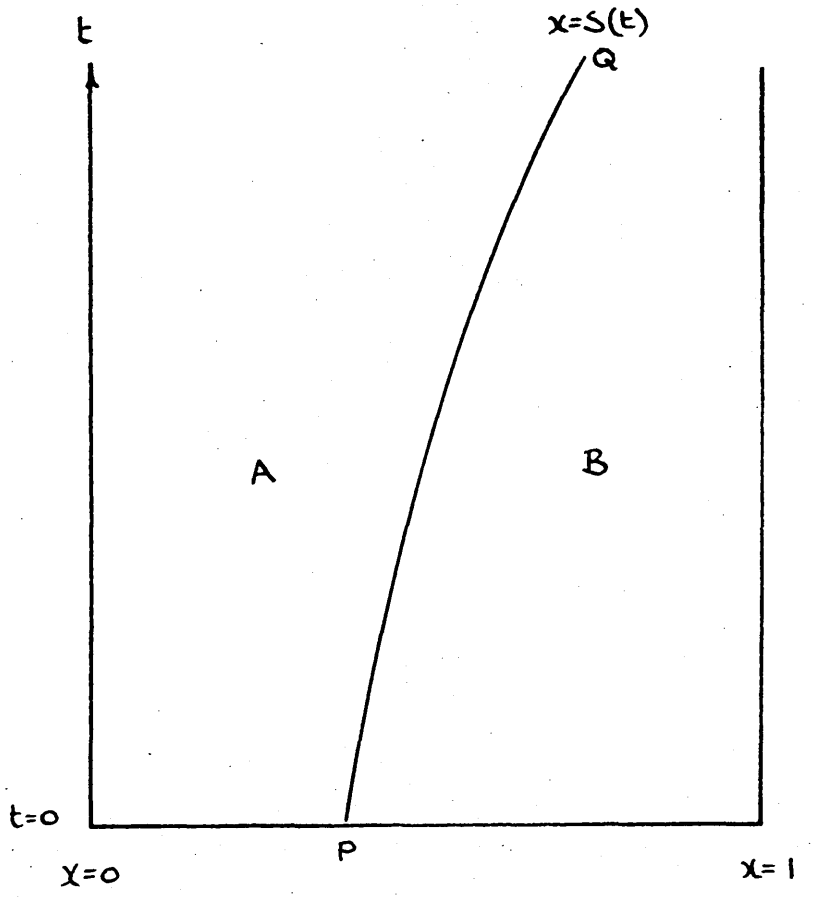

Figure 23

A Moving Boundary Problem

APPENDIX 1

Analytic Solution to Case Study 1.1

Here the analytic solution to the wave equation (6.2.1) is derived by separating the variables. Letting u=XT in (6.2.1) and dividing by XT we have

$$\frac{T''}{T} = \frac{X''}{X} = -k^2 . \qquad \text{(AP1.1)}$$

Rearranging (AP1.1) gives

$$T'' + k^2T = 0 \quad \text{and} \quad X'' + k^2X = 0 \qquad \text{(AP1.2)}$$

which have the solutions

$$T = A\text{Sin}kt + B\text{Cos}kt \quad \text{and} \quad X = C\text{Sin}kx + D\text{Cos}kx \qquad \text{(AP1.3)}$$

respectively. The general solution to (6.2.1) thus has the form

$$u(x,t) = (A\text{Sin}kt + B\text{Cos}kt)(C\text{Sin}kx + D\text{Cos}kx) \qquad \text{(AP1.4)}$$

The constants, A, B, C, D and k are now evaluated using the imposed boundary and initial conditions (6.2.2) - (6.2.4). From the left-hand boundary condition of (6.2.2) we have

$$0 = (A\text{Sin}kt + B\text{Cos}kt)D \qquad \text{(Ap.1.5)}$$

implying D=0. Similarly the right-hand boundary condition of (6.2.2) gives

$$\text{CSin}k = -\text{DCos}k \qquad \text{(AP.1.6)}$$

and thus $k = \pi$. Substituting the initial condition (6.2.3) into (AP1.4) yields

$$\text{Sin}\pi x = B(\text{CSin}kx + \text{DCos}kx). \qquad \text{(AP1.7)}$$

Since D=0 and $k=\pi$ then (AP1.7) suggest that BC=1. Finally, from the derivative initial condition (6.2.4) the following is derived

$$0 = Ak(\text{CSin}kx + \text{DCos}kx) \qquad \text{(AP1.8)}$$

giving A=0. The general solution (AP1.4) thus becomes

$$u(x,t) = \text{Sin}\pi x\text{Cos}\pi t. \qquad \text{(AP1.9)}$$

APPENDIX 2.

Analytic Solution to Case Study 1.2

The fourier series analytic solution to the wave equation (6.2.1) is given by

$$u(x,t) = \sum_{n=1}^{\infty} a_n \, \mathrm{Sinn}\pi x \, \mathrm{Cosn}\pi t \qquad \text{(AP2.1)}$$

where

$$a_n = 2 \int_o^1 u(x,o) \mathrm{Sinn}\pi x \, dx. \qquad \text{(AP2.2)}$$

In case study 1.2 the expression (AP2.2) becomes

$$a_n = 2 \int_o^1 (x^4 - x^5) \, \mathrm{Sinn}\pi x \, dx \qquad \text{(AP2.3)}$$

which after successive integration by parts gives the relationship

$$a_n = 2 \left[\frac{24}{(n\pi)^5} - \left(\frac{-8}{(n\pi)^3} + \frac{96}{(n\pi)^5} \right) \mathrm{cosn}\pi \right]. \qquad \text{(AP2.4)}$$

The analytic solution to (6.2.1) subject to (6.2.2), (6.3.1) and (6.3.2) thus has the form

$$u(x,t) = \sum_{n=1}^{\infty} 2 \left[\frac{24}{(n\pi)^5} - \left(\frac{-8}{(n\pi)^3} + \frac{96}{(n\pi)^5} \right) \mathrm{cosn}\pi \right] \mathrm{sinn}\pi x \, \mathrm{Cosn}\pi t. \qquad \text{(AP2.5)}$$

APPENDIX 3.

Analytic Solution to Case Study 1.3

The analytic solution to (6.4.1) is easily derived by the method of separation of variables employed in Appendix 1. However, for illustrative purposes, the method of Laplace Transforms is used here.

Taking Laplace Transforms of (6.4.1) we have

$$s^2 U(x,s) - su(x,0) - \frac{\partial u}{\partial t}(x,0) = \frac{d^2U}{dx^2} + cU \qquad \text{(AP3.1)}$$

which after substitution of the initial conditions (6.2.3) and (6.2.4) becomes

$$\frac{d^2U}{dx^2} - (s^2 - c)U = - s\text{Sin}\pi x. \qquad \text{(AP3.2)}$$

It is easily shown that the general solution of this differential equation has the form

$$U(x,s) = Ae^{\sqrt{s^2-c}\,x} + Be^{-\sqrt{s^2-c}\,x} + \frac{s\text{Sin}\pi x}{\pi^2+s^2-c}. \qquad \text{(AP3.3)}$$

By taking Laplace Transforms of the boundary conditions (6.2.2) we find that the constants A and B are both zero and thus (AP3.2) has the solution

$$U(x,s) = \frac{s\text{Sin}\pi x}{\pi^2+s^2-c}. \qquad \text{(AP3.4)}$$

Using inverse Laplace Transforms we therefore find that the analytic solution to (6.4.1) subject to (6.2.2), (6.2.3) and (6.2.4) is given by

$$u(x,t) = \text{Sin}\pi x \ \text{Cos}(\pi^2 - c)^{\frac{1}{2}} t. \qquad \text{(AP3.5)}$$

APPENDIX 4

Analytic Solution to Case Study 1.4

Using the method of separation of variables, (6.5.1) becomes by letting $u = XT$

$$\frac{T'}{T} = \frac{X''}{X} = -k^2 \qquad \text{(AP4.1)}$$

and thus

$$T = Ae^{-k^2 t} \qquad \text{(AP4.2)}$$

and

$$X = B\sin kx + C\cos kx \ . \qquad \text{(AP4.3)}$$

The general solution to (6.5.1) therefore has the form

$$u(x,t) = Ae^{-k^2 t}(B\sin kx + C\cos kx). \qquad \text{(AP4.4)}$$

From the boundary conditions (6.5.3) the general solution (AP4.4) becomes

$$0 = ACe^{-k^2 t} \qquad \text{(AP4.5)}$$

on $x=0$ and

$$0 = Ae^{-k^2 t}(B\sin k + C\cos k) \qquad \text{(AP4.6)}$$

on $x=1$. Since $A \neq 0$, (AP4.5) gives $C=0$ and thus (AP4.6) becomes

$$B\sin k = 0 \ . \qquad \text{(AP4.7)}$$

If $C=0$ then $B \neq 0$ or $u(x,t)=0$ and hence (AP4.7) gives $k=\pi$.

Similarly, from the initial condition (6.5.2) the equation (AP4.4) yields

$$\sin\pi x = A(B\text{Sin}kx + C\text{cos}kx) \qquad \text{(AP4.8)}$$

and AB=1.

The general solution to the parabolic partial differential (6.5.1) therefore has the form

$$u(x,t) = e^{-\pi^2 t}\,\text{Sin}\pi x. \qquad \text{(AP4.9)}$$

APPENDIX 5

Analytic Solution to Case Study 1.5

The steady-state solution to the equation (6.6.1) is when $\frac{\partial u}{\partial t} = 0$, that is when $\frac{\partial^2 u}{\partial x^2} = 0$, and thus $u = A + Bx$. From the boundary conditions (6.6.2) and (6.6.3) the constants A and B are found to be A=1 and $B=e^{-a} -1$. Denoting the steady-state solution by $u_o(x)$ we thus have

$$u_o(x) = 1 + (e^{-a}-1)x \quad . \tag{AP5.1}$$

The solutions to case study 1.5 are now defined by

$$u(x,t) = u_o(x) + v(x,t) \tag{AP5.2}$$

where v(x,t) are solutions to the problem

$$\frac{\partial v}{\partial t} = \frac{\partial^2 v}{\partial x^2} \tag{AP5.3}$$

subject to

$$v(0,t) = v(1,t) = 0 \tag{AP5.4}$$

and $$v(x,0) = u(x,0) - u_o(x) = e^{-ax} - 1 + (1-e^{-a})x. \tag{AP5.5}$$

The above problem is now in the more usual form for which the fourier series solution is

$$v(x,t) = \sum_{n=1}^{\infty} b_n \mathrm{Sin} n\pi x \; e^{-n^2\pi^2 t} \tag{AP5.6}$$

where

$$b_n = 2\int_0^1 v(x,0)\mathrm{Sin}n\pi x\,dx. \qquad \text{(AP5.7)}$$

using (AP5.5) the integral(AP5.7) becomes

$$b_n = 2\int_0^1 (e^{-ax} - 1 + (1-e^{-a})x)\mathrm{Sin}n\pi x\,dx. \qquad \text{(AP5.8)}$$

which can be shown to have the solution

$$b_n = \frac{2}{n\pi}(e^{-a}\mathrm{cos}n\pi - 1)\left(\frac{a^2}{(n\pi)^2 + a^2}\right). \qquad \text{(AP5.9)}$$

The analytic solution to (6.5.1) subject to (6.6.1), (6.6.2) and (6.6.3) is therefore given by the expression

$$u(x,t) = 1 + (e^{-a} - 1)x + \sum_{n=o}^{\infty} \frac{2}{n\pi}\left(e^{-a}\mathrm{cos}n\pi - 1\right)\left(\frac{a^2}{(n\pi)^2 + a^2}\right)\mathrm{Sin}n\pi x\, e^{-n^2\pi^2 t} \qquad \text{(AP5.10)}$$

The numerical evaluation of (AP5.10) is complicated by the presence of the $\mathrm{Sin}n\pi x$ term. In evaluating the summation it is usual to sum terms until a particular term is less than a specified magnitude. This is difficult in this case, since $\mathrm{Sin}n\pi x = 0$ for certain values of n and x, and thus significant terms for larger n will be ignored. In our computations this problem has been overcome by examining terms after those in which $\mathrm{Sin}n\pi x=0$.

An additional danger is also encountered when n is large since in such cases $e^{-n^2\pi^2 t}$ becomes too small for computer arithmetic operations.

REFERENCES

J H AHLBERG, E N NILSON and J L WALSH, The Theory of Splines and their Application, Academic Press, London (1967)

E L ALBASINY and W D HOSKINS, Cubic Spline Solutions to Two-Point Boundary Value Problems, Comput.J.12(1969)151-153

W F AMES, Numerical Methods for Partial Differential Equations, Nelson and Sons (1977)

G H BEHFOROOZ and N PAPAMICHAEL, End Conditions for Cubic Spline Interpolation, J.Inst.Maths.Applics. 23(1979)355-366

W G BICKLEY, Piecewise Cubic Interpolation and Two-Point Boundary Value Problems, Comput.J.11(1968)206-208

G BIRKHOFF and C DE BOOR, Piecewise Polynomial Interpolation and Approximation, In Approximation of Functions edited by H L Garabedian, Elsevier, Amsterdam (1965)164-190

F G BLOTTNER, Non-Uniform Grid Methods for Turbulent Boundary Layers, Proc.Fourth Int.Conf.on Numerical Methods in Fluid Dynamics, Lecture Notes in Physics 35, Springer-Verlag (1975)

H G BURCHARD, Splines (with optimal knots) are better, J.Applicable Analysis 3(1974)309-319

I CHRISTIE, D F GRIFFITHS, A R MITCHELL and O C ZIENKIEWICZ, Finite Element Methods for Second Order Differential Equations with Significant First Derivatives, Int.J. Numer.Meth.Eng. 10(1976)1389-1396

R COURANT, K FRIEDRICHS and H LEWY, Uber die partiellen Differenzengleichungen der Mathematischen Physik, Math. Ann.100(1928)32-74, English translation by Phyllis Fox, On the partial difference equations of Mathematical Physics, IBM Journal 11(1967)215-234

M G COX, An Algorithm for Spline Interpolation, J.Inst.Maths. Applics. 15(1975)95-108

S H CRANDELL, An Optimum Implicit Recurrence Formula for the Heat Conduction Equation, Qtly.Apl.Maths. 13(1955)318-320

J CRANK and R S GUPTA, A Moving Boundary Problem Arising from the Diffusion of Oxygen in Absorbing Tissue, J.Inst.Maths.Applics. 10(1972a)19-33

J CRANK and R S GUPTA, A Method for Solving Moving Boundary Problems in Heat Flow Using Cubic Splines or Polynomials, J.Inst.Maths.Applics. 10(1972b)296-304

J CRANK and P NICOLSON, A Practical Method for the Numerical Evaluation of Solutions of Partial Differential Equations of the Heat Conduction Type, Proc.Camb.Phil.Soc. 43(1947)50-67

A R CURTIS, The Approximation of a Function of One Variable by Cubic Splines, in Numerical Approximations to Functions and Data edited by J G Hayes, Athlone Press, London (1970)28-42

A R CURTIS and M J D POWELL, Using Cubic Splines to Approximate Functions of One Variable to Prescribed Accuracy, AERE Harwell Report No. AERE-R5602, HMSO(1967)

H J CROWDER and C DALTON, Errors in the Use of Nonuniform Mesh Systems, J.Comp.Physics 7(1971)32-45

C DE BOOR, Good Approximation by Splines with Variable Knots, In Spline Functions and Approximation Theory edited by A Meir and A Sharma, Birkhäuser Verlag, Basel (1973)57-72

C DE BOOR, Good Approximation by Splines with Variable Knots II, In Numerical Solution of Differential Equations edited by G A Watson, Lecture Notes in Math.No.363, Springer-Verlag (1974) 12-20

C DE BOOR, A Practical Guide to Splines, Springer-Verlag, New York (1978)

C DE BOOR and J R RICE, Least-Squares Cubic Spline Approximation II - Variable Knots, Computer Science Department Technical Report 21, Purdue University (1968)

C DE BOOR and B SWARTZ, Collocation at Gaussian Points, SIAM J. Numer.Anal.10(1973)582-606

D S DOBSON, Optimal Order Approximation by Polynomial Spline Functions, PhD Thesis, Purdue Univ. Lafayette, Ind. (1972)

J DOUGLAS, The Solution of the Diffusion Equation by a High Order Correct Difference Equation, J.Math.Phys. 35(1956)145-151

J DOUGLAS and T M GALLIE, Variable Time Steps in the Solution of the Heat Flow Equation by a Difference Equation, Proc.Amer.Soc. 6(1955)787-793

M E A EL-TOM, Spline Function Approximations to the Solution of Singular Volterra Integral Equations of the Second Kind, J.Inst.Maths.Applics. 14(1974)303-309

M E A EL-TOM, Application of Spline Functions to Systems of Volterra Integral Equations of the First and Second Kinds, J.Inst.Maths.Applics. 17(1976)295-310

R E ESCH and W L EASTMAN, Computational Methods for Best Spline Function Approximation, J.Approx.Theory 2(1969) 85-96

L FOX, Numerical Solution of Ordinary and Partial Differential Equations, Pergamon Press, London (1962)

D J FYFE, The Use of Cubic Splines in the Solution of Two-Point Boundary Value Problems, Comput.J.12(1969)188-192

T N E GREVILLE, Introduction to Spline Functions, In Theory and Applications of Spline Functions edited by T N E Greville, Academic Press, New York (1969)1-35

D F GRIFFITHS, The Stability of Finite Difference Approximations to Nonlinear Partial Differential Equations, Bull.IMA 18(1982)210-215

J G HAYES and J HALLIDAY, The Least-Squares Fitting of Cubic Spline Surfaces to General Data Sets, J.Inst.Maths.Applics. 14(1974)89-103

M K JAIN and T AZIZ, Spline Function Approximation for Differential Equations, Comp.Meth.Appl.Mech.and Eng. 26(1981) 129-143

P C JAIN and D N HOLLA, General Finite Difference Approximation for the Wave Equation with Variable Coefficients using a Cubic Spline Technique, Comp.Meth.Appl.Mech.and Eng. 15 (1978)175-180

I P JONES and C P THOMPSON, On the Use of Nonuniform Grids in Finite Difference Calculations, AERE Harwell Report No. AERE-R9765, HMSO(1980)

E KÀLNAY DE RIVAS, On the Use of Nonuniform Grids in Finite Difference Equations, J.Comp.Physics 10(1972) 202-210

D KERSHAW, Two Interpolatory Cubic Splines, J.Inst.Maths. Applics. 11(1973)329-333

A K A KHALIFA and J C EILBECK, Collocation with Quadratic and Cubic Splines, IMA J.Numer.Anal. 2(1982)111-121

F R LOSCALZO, An Introduction to the Application of Spline Functions to Initial Value Problems, in Theory and Application of Spline Functions edited by T N E Greville Academic Press, New York (1969)

F R LOSCALZO and T D TALBOT, Spline Function Approximation for Solution of Ordinary Differential Equations, SIAM J.Numer.Anal. 4(1967)433-445

M LOTKIN, The Calculation of Heat Flow in Melting Solids, Q.Appl.Math.18(1960)79-85

D E McCLURE, Feature Selection for the Analysis of Line Patterns, Ph.D.,Thesis, Brown Univ., Providence, R.I. (1970)

S McKEE, High Accuracy A.D.I. Methods for Hyperbolic Equations with Variable Coefficients, J.Inst.Maths.Applics. 11 (1973)105-109

G H MEYER, The Numerical Solution of Stefan Problems with Front-Tracking and Smoothing Methods, Brunel University Report TR/62(1976)

G MICULA, Approximate Solution of the Differential Equation $y'' = f(x,y)$ with Spline Functions, Maths of Comp. 27(1973) 807-816

A R MITCHELL, Computational Methods in Partial Differential Equations, Wiley, Aberdeen (1969)

A R MITCHELL and D F GRIFFITHS, The Finite Difference Method in Partial Differential Equations, Wiley, Chichester, New York (1980)

W D MURRAY and F LANDIS, Numerical and Machine Solutions of Transient Heat-Conduction Problems involving Melting or Freezing, J.Heat Transfer 81(1959)106-112

G G O'BRIEN, M A HYMAN and S KAPLAN, A Study of the Numerical Solution of Partial Differential Equations, J.Math.Phys. 29(1951)223-251

J R OCKENDON and W R HODGKINS (Eds), Moving Boundary Problems in Heat Flow and Diffusion, Clarendon Press, Oxford (1975)

M M PALA and P SPANO, A Cubic Spline Technique for a Parabolic Equation of Higher than the Second Order, Bollettino U.M.I. 15(1978)560-570

N PAPAMICHAEL and J R WHITEMAN, A Cubic Spline Technique for the One-Dimensional Heat Conduction Equation, J.Inst.Maths.Applics. 11(1973)111-113

N PAPAMICHAEL and A J WORSEY, End Conditions for Improved Cubic Spline Derivative Approximations, J.Comp. Appl.Maths. 7(1981)101-109

F PATRICIO, Cubic Spline Functions and Initial Value Problems, BIT 18(1978)342-347

C E PEARSON, On a Differential Equation of Boundary Layer Type, J.Math.and Phys. 47(1968)134-154

G M PHILLIPS, Error Estimates for Best Polynomial Approximation, In Approximation Theory edited by A Talbot, Academic Press, London (1970)1-6

H S PRICE, J C CAVENDISH and R S VARGA, Numerical Methods of Higher-Order Accuracy for Diffusion-Convection Equations, Soc.Pet.Eng.J. 8(1968)293-303

G F RAGGETT, On the Solution of Hyperbolic Partial Differential Equations Using Cubic Splines, Paper presented at the International Congress of Mathematicians, Vancouver, Canada (1974)

G F RAGGETT, J A R STONE and S J WISHER, The Cubic Spline Solution of Hyperbolic Partial Differential Equations with Variable Coefficients and Generalised Boundary Conditions, Research Report MS/01, Sheffield City Polytechnic (1975)

G F RAGGETT, J A R STONE and S J WISHER, The Cubic Spline Solution of Practical Problems Modelled by Hyperbolic Partial Differential Equations, Comp.Meth.Appl.Mech.and Eng. 8(1976)139-151

G F RAGGETT and P D WILSON, A Fully Implicit Finite Difference Approximation to the One-Dimensional Wave Equation Using a Cubic Spline Technique, J.Inst.Maths.Applics.14(1974) 75-77

G F RAGGETT and S J WISHER, Variable Knot Placement in the Cubic Spline Solution of Hyperbolic Partial Differential Equations - A Local Method, Research Report MS/04, Sheffield City Polytechnic (1979a)

G F RAGGETT and S J WISHER, Variable Knot Placement in the Cubic Spline Solution of Hyperbolic Partial Differential Equations - A Global Method, Research Report MS/05, Sheffield City Polytechnic (1979b)

J R RICE, On the Degree of Convergence on Non-Linear Spline Approximation, In Approximations with Special Emphasis on Spline Functions edited by I J Schoenberg, Academic Press, New York (1969)349-365

L F RICHARDSON, The Approximate Arithmetical Solution by Finite Differences of Physical Problems Involving Differential Equations, Phil.Trans.Roy.Soc.London, Series A, 210(1910)307-357

R D RICHTMYER and K W MORTON, Difference Methods for Initial-Value Problems, Interscience, New York (1967)

S G RUBIN and R A GRAVES, Viscous Flow Solutions with a Cubic Spline Approximation, Computers and Fluids 3(1975)1-36

S G RUBIN and P KHOSLA, Higher-Order Numerical Solutions Using Cubic Splines, AIAA Journal 14(1976)851-858

V K SAUL'YEV, Integration of Equations of Parabolic Type by the Method of Nets, Pergamon Press, London (1964)

S S SASTRY, Finite Difference Approximations to One-Dimensional Parabolic Equations using a Cubic Spline Technique, J.Comp. Appl.Maths 2(1976)23-26

I J SCHOENBERG, Contributions to the Problem of Approximation of Equidistant Data by Analytic Functions, Quart. Appl.Math.4(1946), Part A 45-99, Part B 112-141

M H SCHULTZ, Spline Analysis, Prentice-Hall (1973)

L L SCHUMAKER, Some Algorithms for the Computation of Interpolating and Approximating Spline Functions, In Theory and Applications of Spline Functions edited by T N E Greville, Academic Press, New York (1969) 87-102

J L SIEMIENIUCH and I GLADWELL, Analysis of Explicit Difference Methods for a Diffusion-Convection Equation, Int.J.Numer. Meth.Eng. 12(1978)899-916

D E SPALDING, A Novel Finite Difference Formulation for Differential Expressions involving both First and Second Derivatives, Int.J.Numer.Meth.Eng. 4(1972)551-559

O B WIDLUND, Stability of Parabolic Difference Schemes in the Maximum Norm, Numer.Math. 8(1966)186-202

S J WISHER, On the Use of Splines in the Numerical Solution of Hyperbolic Partial Differential Equations, M.Phil. Thesis, Sheffield City Polytechnic (1977)

G WOODFORD, Finite Difference Methods with Application to the Cavity Problem, PhD Thesis, Australian National University (1975)